PREDICTIONS OF LOADS IN GRAIN STORAGE BINS USING MICROSTRUCTURAL MECHANICS AND ENDOCHRONIC THEORIES

BY

SHAOHONG XU

A Thesis

Submitted to the Faculty of Graduate Studies
in Partial Fulfilment of the Requirements
for the Degree of

DOCTOR OF PHILOSOPHY

Department of Biosystems Engineering
University of Manitoba
Winnipeg, Manitoba

ISBN 0-612-16376-8

Name _____

Dissertation Abstracts International and *Masters Abstracts International* are arranged by broad, general subject categories. Please select the one subject which most nearly describes the content of your dissertation or thesis. Enter the corresponding four-digit code in the spaces provided.

Agricultural Engineering

SUBJECT TERM

0539 UMI

SUBJECT CODE

Subject Categories

THE HUMANITIES AND SOCIAL SCIENCES

COMMUNICATIONS AND THE ARTS

Architecture 0729
Art History 0377
Cinema 0900
Dance 0378
Fine Arts 0357
Information Science 0723
Journalism 0391
Library Science 0399
Mass Communications 0708
Music 0413
Speech Communication 0459
Theater 0465

EDUCATION

General 0515
Administration 0514
Adult and Continuing 0516
Agricultural 0517
Art 0273
Bilingual and Multicultural 0282
Business 0688
Community College 0275
Curriculum and Instruction 0727
Early Childhood 0518
Elementary 0524
Finance 0277
Guidance and Counseling 0519
Health 0680
Higher 0745
History of 0520
Home Economics 0278
Industrial 0521
Language and Literature 0279
Mathematics 0280
Music 0522
Philosophy of 0998
Physical 0523
Psychology 0525
Reading 0535
Religious 0527
Sciences 0714
Secondary 0533
Social Sciences 0534
Sociology of 0340
Special 0529
Teacher Training 0530
Technology 0710
Tests and Measurements 0288
Vocational 0747

LANGUAGE, LITERATURE AND LINGUISTICS

Language
- General 0679
- Ancient 0289
- Linguistics 0290
- Modern 0291

Literature
- General 0401
- Classical 0294
- Comparative 0295
- Medieval 0297
- Modern 0298
- African 0316
- American 0591
- Asian 0305
- Canadian (English) 0352
- Canadian (French) 0355
- English 0593
- Germanic 0311
- Latin American 0312
- Middle Eastern 0315
- Romance 0313
- Slavic and East European 0314

PHILOSOPHY, RELIGION AND THEOLOGY

Philosophy 0422
Religion
- General 0318
- Biblical Studies 0321
- Clergy 0319
- History of 0320
- Philosophy of 0322

Theology 0469

SOCIAL SCIENCES

American Studies 0323
Anthropology
- Archaeology 0324
- Cultural 0326
- Physical 0327

Business Administration
- General 0310
- Accounting 0272
- Banking 0770
- Management 0454
- Marketing 0338

Canadian Studies 0385
Economics
- General 0501
- Agricultural 0503
- Commerce-Business 0505
- Finance 0508
- History 0509
- Labor 0510
- Theory 0511

Folklore 0358
Geography 0366
Gerontology 0351
History
- General 0578
- Ancient 0579
- Medieval 0581
- Modern 0582
- Black 0328
- African 0331
- Asia, Australia and Oceania 0332
- Canadian 0334
- European 0335
- Latin American 0336
- Middle Eastern 0333
- United States 0337

History of Science 0585
Law 0398
Political Science
- General 0615
- International Law and Relations 0616
- Public Administration 0617

Recreation 0814
Social Work 0452
Sociology
- General 0626
- Criminology and Penology 0627
- Demography 0938
- Ethnic and Racial Studies 0631
- Individual and Family Studies 0628
- Industrial and Labor Relations 0629
- Public and Social Welfare 0630
- Social Structure and Development 0700
- Theory and Methods 0344

Transportation 0709
Urban and Regional Planning 0999
Women's Studies 0453

THE SCIENCES AND ENGINEERING

BIOLOGICAL SCIENCES

Agriculture
- General 0473
- Agronomy 0285
- Animal Culture and Nutrition 0475
- Animal Pathology 0476
- Food Science and Technology 0359
- Forestry and Wildlife 0478
- Plant Culture 0479
- Plant Pathology 0480
- Plant Physiology 0817
- Range Management 0777
- Wood Technology 0746

Biology
- General 0306
- Anatomy 0287
- Biostatistics 0308
- Botany 0309
- Cell 0379
- Ecology 0329
- Entomology 0353
- Genetics 0369
- Limnology 0793
- Microbiology 0410
- Molecular 0307
- Neuroscience 0317
- Oceanography 0416
- Physiology 0433
- Radiation 0821
- Veterinary Science 0778
- Zoology 0472

Biophysics
- General 0786
- Medical 0760

EARTH SCIENCES

Biogeochemistry 0425
Geochemistry 0996
Geodesy 0370
Geology 0372
Geophysics 0373
Hydrology 0388
Mineralogy 0411
Paleobotany 0345
Paleoecology 0426
Paleontology 0418
Paleozoology 0985
Palynology 0427
Physical Geography 0368
Physical Oceanography 0415

HEALTH AND ENVIRONMENTAL SCIENCES

Environmental Sciences 0768
Health Sciences
- General 0566
- Audiology 0300
- Chemotherapy 0992
- Dentistry 0567
- Education 0350
- Hospital Management 0769
- Human Development 0758
- Immunology 0982
- Medicine and Surgery 0564
- Mental Health 0347
- Nursing 0569
- Nutrition 0570
- Obstetrics and Gynecology 0380
- Occupational Health and Therapy 0354
- Ophthalmology 0381
- Pathology 0571
- Pharmacology 0419
- Pharmacy 0572
- Physical Therapy 0382
- Public Health 0573
- Radiology 0574
- Recreation 0575
- Speech Pathology 0460
- Toxicology 0383

Home Economics 0386

PHYSICAL SCIENCES

Pure Sciences

Chemistry
- General 0485
- Agricultural 0749
- Analytical 0486
- Biochemistry 0487
- Inorganic 0488
- Nuclear 0738
- Organic 0490
- Pharmaceutical 0491
- Physical 0494
- Polymer 0495
- Radiation 0754

Mathematics 0405
Physics
- General 0605
- Acoustics 0986
- Astronomy and Astrophysics 0606
- Atmospheric Science 0608
- Atomic 0748
- Electronics and Electricity 0607
- Elementary Particles and High Energy 0798
- Fluid and Plasma 0759
- Molecular 0609
- Nuclear 0610
- Optics 0752
- Radiation 0756
- Solid State 0611

Statistics 0463

Applied Sciences

Applied Mechanics 0346
Computer Science 0984
Engineering
- General 0537
- Aerospace 0538
- Agricultural 0539
- Automotive 0540
- Biomedical 0541
- Chemical 0542
- Civil 0543
- Electronics and Electrical 0544
- Heat and Thermodynamics 0348
- Hydraulic 0545
- Industrial 0546
- Marine 0547
- Materials Science 0794
- Mechanical 0548
- Metallurgy 0743
- Mining 0551
- Nuclear 0552
- Packaging 0549
- Petroleum 0765
- Sanitary and Municipal 0554
- System Science 0790

Geotechnology 0428
Operations Research 0796
Plastics Technology 0795
Textile Technology 0994

PSYCHOLOGY

General 0621
Behavioral 0384
Clinical 0622
Developmental 0620
Experimental 0623
Industrial 0624
Personality 0625
Physiological 0989
Psychobiology 0349
Psychometrics 0632
Social 0451

THE UNIVERSITY OF MANITOBA

FACULTY OF GRADUATE STUDIES

COPYRIGHT PERMISSION

PREDICTIONS OF LOADS IN GRAIN STORAGE BINS USING USING MICROSTRUCTURAL MECHANICS AND ENDOCHRONIC THEORIES

BY

SHAOHONG XU

A Thesis/Practicum submitted to the Faculty of Graduate Studies of the University of Manitoba in partial fulfillment of the requirements for the degree of

DOCTOR OF PHILOSOPHY

TABLE OF CONTENTS

ABSTRACT

A microscopic model and a finite element model have been developed for predicting loads in grain storage structures. In the micromechanical model, analytic equations for predicting bin loads were derived without the assumption of a constant lateral to vertical pressures ratio (k value). Janssen's equation, recommended by most design Standards and Codes, was found to be a special case of the microscopic model for rigid particles. The constant k value in most existing theories was shown only valid in the case of frictionless walls or rigid particles. The microscopic model was also extended for predicting hygroscopic and discharge loads in grain storage bins. Model predictions of static, hygroscopic, and discharge loads are all within standard deviations or 95% confidence intervals of reported experimental data.

In the finite element model, the behaviour of grain en masse was modelled by endochronic constitutive theories. Four types of mechanical models were constructed for describing the behaviour of grain en masse. These models were named as relaxation-type, creep-type, first mixed-type, and second mixed-type models, respectively. Endochronic constitutive equations were formulated directly from the analysis of stresses and strains of mechanical models (classical approach), and from the considerations of energy dissipations in the mechanism (energy approach). The model parameters were determined for wheat en masse using triaxial test data. The predictive finite element model was validated against experimental data from model bin tests. The maximum difference between predicted and measured lateral pressures was 9.6 % and the average difference 5.8%.

DEDICATION

To my wife, Shaoli Shi, and my sons, Chu Xu and Michael Xu,

for the happiness and fulness of my life.

ACKNOWLEDGEMENTS

I sincerely thank my dissertation advisor, Dr. Q. Zhang, for his guidance and encouragement throughout the course of this research.

I am also grateful to other members of my advisory committee, Dr. M.G. Britton, Dr. N.R. Bulley, Dr. Nimal Rajapakse, and Dr. V.M. Puri for their critical evaluations and suggestions toward my dissertation.

The acknowledgements are given to Graduate Studies at the University of Manitoba for awarding me the Fellowship throughout my Ph.D. program, and to Natural Science and Engineering Research Council of Canada for the financial support of our research project.

LIST OF FIGURES

LIST OF TABLES

LIST OF SYMBOLS

This list contains all symbols with their definitions in this study. These symbols are defined when they are first used in the text.

A	cross-sectional area of the bin
A_r	material constant
$a_1^{(r)}$	positive intermediate variables (viscosity-like shear coefficient)
$a_2^{(r)}$	positive intermediate variables (viscosity-like hydrostatic coefficient)
$a_{21}^{(r)}$	positive intermediate variable (viscosity-like coupling coefficient)
B_r	material constant
$b_1^{(r)}$	intermediate (viscosity-like) shear coefficient
$b_2^{(r)}$	intermediate (viscosity-like) hydrostatic coefficient
$b_{21}^{(r)}$	intermediate (viscosity-like) coupling coefficient
C_0	$1/a_1^{(0)}$
C_0	material parameter
C_1	material parameter
C_r	$1/k^{(r)}$
c	cohesion
$C^{(r)}$	$1/k^{(r)}$, material constants
$D^{(r)}$	material constants
D_1	horizontal deformation caused by vertical stress component
d_1	$\lambda E_i(1-\nu_i)/[(1+\nu_i)(1-2\nu_i)]$
d_2	$\lambda E_i\nu_i/[(1+\nu_i)(1-2\nu_i)]$
d_{max}	maximum dilatancy shear displacement
dZ	increment of intrinsic time scale
dz_d	deviatoric component of intrinsic time
dz_h	hydrostatic component of intrinsic time
de_{ij}	increment of total deviatoric strain
$d\sigma_h$	hydrostatic stress increment
$d\epsilon_h$	volumetric strain increment
dz_d	deviatoric intrinsic time component
dz_h	hydrostatic intrinsic time component
ds_{ij}	deviatoric stress increment tensor
E	elastic modulus of particle
E'	tangent modulus during wetting or discharging
E_i	elastic modulus of interface in compression
E_w	elastic modulus of bin wall material
e	natural log base
e^p_{ij}	plastic deviatoric strain tensor
F	vertical resultant frictional force, kN/m
F_0	static frictional force, kN/m
F_h	hydrostatic hardening function

F_d deviatoric hardening function
f moisture factor, or ratio of elastic moduli of unwetted grain to wetted grain in a rigid container
f_d discharge overpressure factor
G elastic shear modulus
G_i shear modulus of interface element
G(.) Gibbs free energy density
G_d deviatoric components of Gibbs free energy
G_h hydrostatic components of free energy
$G_d^{(r)}$ deviatoric components of Gibbs free energy in r-th unit
g gravitational acceleration constant, m/s^2
H_d deviatoric components of Helmholtz free energy
H_h hydrostatic components of Helmholtz free energy
J hydrostatic kernel function
J_0 $1/a_2^{(0)}$, model parameter for simplified hydrostatic kernel function
K_h elastic bulk modulus
K hydrostatic bulk modulus
K_r $(\zeta_r b_{21}^{(r)})/(\kappa F_h)$, material constant
K_i initial bulk modulus, kPa
K_t tangent bulk modulus, kPa
K_r $K^{(r)}$
$k^{(r)}$ spring constants in r-th spring element
k ratio of lateral to vertical stress
L lateral bin pressure during loading, or wetting, or discharging, kPa
L_0 initial lateral pressure (before wetting), kPa
L_d discharge load
$l_{\alpha i}$ direction cosine of p_α
MC_0 initial grain moisture content, %db
N displacement modulus
P_{ijkl} material property tensor
p_α microstresses, α=1,2,3
$Q^{(r)}$ internal variables (hydrostatic stress) in r-th slip element
$Q_{ij}^{(r)}$ internal variables (stresses) in r-th slip element
q_{ij} deviatoric internal strain tensor
q_h hydrostatic internal strain
$q_{ij}^{(r)}$ internal deviatoric strains in r-th slip element
$q^{(r)}$ internal hydrostatic strain in r-th slip element
R hydraulic radius (A/S) of the bin, m
r radius of particle
S bin perimeter
s deviatoric stress under triaxial loading
s relative displacement
s_{ij} deviatoric stress tensor

s_∞	deviatoric stress at failure (at $z_d=\infty$) under triaxial loading
s_0	deviatoric stress at yield (at $z_d=0$) under triaxial loading
T_{ij}	internal stress tensor
TOL	prescribed small tolerance
t	thickness of the interface element
U_{ij}	internal strain tensor
V	vertical bin pressure, kPa
V_0	initial vertical pressure (before wetting), kPa
y	depth of grains, m
z'	dummy variable
[B]	gradient matrix
[D]	elastic coefficient matrix
$[D_w]$	the stress-strain matrix for the wall
$[D_i]$	stress-strain matrix for the interface
{dH}	plastic stress vector
$\{d\sigma\}$	$[d\sigma_r\ d\sigma_z\ d\sigma_\theta\ d\sigma_{rz}]^T$, stress vector
$\{d\epsilon\}$	$[d\epsilon_r\ d\epsilon_z\ d\epsilon_\theta\ d\epsilon_{rz}]^T$, strain vector
[N]	matrix of shape (interpolation) functions
{T}	surface traction force vector
{X}	unit volume body force vector
ϕ	macroscopic (overall) angle of internal friction
ϕ_μ	microscopic (true) angle of friction
Φ_d	deviatoric kernel function
ϵ_{ij}	macrostrains
ϵ_α	microstrains, α=1,2,3
ϵ_v	volumetric strain of wetted kernel, m^3/m^3
$\epsilon_{v,ult}$	asymptotic value of volumetric strain, m^3/m^3
ϵ^p_{ij}	plastic strain tensor
ϵ^p_h	plastic hydrostatic strain
γ	micro-structural angle
γ	shear strain (s/t) in interface element
μ	friction coefficient of grain on wall
ΔMC	increase in moisture content, %db
ρ_{k0}	initial kernel density, kg/m^3
ρ_w	density of water, kg/m^3
ρ	bulk density of stored materials, kg/m^3
σ_{ij}	stress tensor, kPa
σ_h	hydrostatic stress, kPa
σ_∞	hydrostatic stress at $z_h=\infty$, kPa
σ_0	confining pressure in triaxial test (at $z_h=0$), kPa
σ_n	normal stress
β_r	$k^{(r)}/a_1^{(r)}$
$\beta^{(r)}$	$1/(a_1^{(r)}C^{(r)})$, intermediate variable

β_1	material parameter
Γ	coupling kernel function
Γ_0	$b^{(0)}/a_2^{(0)}$, model parameter for simplified coupling kernel function
λ_r	$K^{(r)}/a_2^{(r)}$, model parameter
$\lambda^{(r)}$	$1/(a_2^{(r)}D^{(r)})$
λ_p	participation factor
ν	Poisson's ratio of particles
ν_w	Poisson's ratio of bin wall material
ν_i	Poisson's ratio of interface element
α_r	$A_r/b_1^{(r)}$, material constant
α	material constant
ζ_r	$B_r/b_2^{(r)}$, material constant
τ	shear stress
θ	dilatancy angle
θ_{max}	maximum dilatancy angle
$^{(r)}$	in *r*-th element
$\| \|$	norm ("length") of tensor or vector
$\| \|$	absolute value

1. INTRODUCTION

In design and analysis of grain storage and handling systems, predictions of loads exerted by stored materials on the structures are critical (Britton and Zhang 1989). Excessive design loads increase the cost, whereas insufficient design loads may lead to structural failures. Loads in grain bins are categorized as either static loads or dynamic loads. Static loads are exerted by grains on structures under at-rest conditions. Changes in environmental or operational conditions cause bin loads to increase. These increased loads are known as dynamic loads. Because some dynamic loads are not unique to grain-bin systems and may be covered in other engineering practice, those loads such as snow, wind, and earthquake loads are excluded in this study. Two most significant conditions of dynamic loadings in grain-bin systems occur during grain wetting and discharging. Bin loads dramatically increase during wetting as hygroscopic grain expansion occurs. At the onset of discharging, bin loads tend to increase instantly, resulting in dynamic discharge loads. In this study, the term "dynamic loads" is reserved for representing discharge loads or hygroscopic loads.

One hundred years ago, Janssen (1895) provided the first set of analytical equations to calculate the static stresses within a granular mass contained in a deep bin by considering the equilibrium of vertical forces acting on a small element of the stored material. His formula is still widely used in predicting static loads in grain bins. Airy (1897) used a sliding wedge theory to compute lateral pressures in silos. Both Janssen's and Airy's theories assumed that the ratio of lateral to vertical pressures (k value) is constant. Reimbert and Reimbert (1956) first considered k values as a function of the height of the stored material and proposed a set of predictive equations

for static loads. All of these theories are continuum theories. They were all founded on some basic assumptions, i.e., rigid bin walls, constant k value, or constant friction coefficient between wall and grain. In reality, few bins have rigid walls. Increases in wall stiffness result in higher bin wall pressures (Ooi and Rotter 1990). The k value is not a constant material property parameter (Cowin 1979). The friction coefficient may vary with the moisture content. If Janssen's equation is used, a higher k value may result in a higher bin wall pressure. As the coefficient of wall friction decreases, the vertical force on the wall decreases but the bin wall pressure increases. It is critical for designers to select an adequate combination of variables when using those classical theories (Britton and Zhang 1989).

Compared to static loads, dynamic loads are still poorly understood. Although dynamic loads have been identified to be the major cause of structural failures of bulk solids storage systems (Jenike and Johanson 1969, Smith and Lohnes 1980), to date no adequate predictive theories are available for bin designers. In most modern design standards and codes (DIN 1987, ACI 1983, ASAE 1995), discharge loads are simply estimated by multiplying static loads by overpressure factors, but no recommendations are given for hygroscopic loads. For discharge loads, many researchers observed overpressures, but few rationalized the cause. Jenike and Johanson (1969) explained that discharge loads were due to the switch of the stress state in the stored materials from an active pressure field to a passive pressure field. Smith and Lohnes (1980) hypothesized that dilation (increase in volume due to shearing) of the stored material is the main cause of the overpressure of grain on bin walls during discharge. Kmita (1991) observed that discharge loads were a result of impact loads. Among these hypothetical explanations, dilation hypothesis is the only one which considers the key unique characteristics (volumetric behaviour)

of granular materials. For hygroscopic loads, Dale and Robinson (1954) observed that lateral pressures on the wall adjacent to the bin bottom increased from 2.1 kPa to 13.5 kPa for a moisture increase of 4% (w.b.). To date, no adequate theories are available for designers to predict the hygroscopic loads.

Discharge loads are attributed to the internal shearing of the grain with a shear-volumetric expansion restricted by the structure. During discharge, grain in different parts of the bin moves at different velocities, thus shearing occurs within the grain mass. This internal shearing causes the grain bulk to dilate laterally. The dilation, however, is restricted by the bin wall, thus an increase in the wall pressure occurs (Xu et al. 1993a). For hygroscopic loads, swelling of grain particles is responsible for the overpressure on bin walls during wetting. Grain particles swell when their moisture contents increase. Thus, the grain bulk tends to expand. This expansion, however, is restricted by bin walls, and consequently, additional pressures, termed hygroscopic pressures, are imposed on the bin walls (Zhang et al. 1995). Because of the importance of volumetric expansion in analysis of discharge and hygroscopic loads, the key step in developing models for predicting dynamic loads is the modelling of the volumetric constitutive behaviour of the granular materials.

Both theories of micromechanics and macromechanics may be used to develop the constitutive laws for granular materials. Micromechanics is based on the study of individual particles' interactions. Although some micromechanics theories have been developed for granular materials (e.g., Prat and Bazant 1991, Granik and Ferrari 1993), no theories have been applied to predictions of bin loads. In the macromechanics category, earlier models were based on the classical plasticity postulate (e.g., Coulomb 1773, Lade 1977), which were formulated on the criteria of material yielding and unloading-reloading. Shear-induced volumetric expansion was not

taken into consideration. Therefore, classical plasticity theories are limited in predicting dynamic loads.

Endochronic theory was founded on the irreversibility principle of thermodynamics (Valanis 1971). The theory provided a unified approach to describe the plastic behaviour of materials (Watanabe and Atluri 1986). The theory has been applied to many kinds of materials such as metals, concretes, soils, and sands. The latest advance for granular materials was an endochronic model (Valanis and Peters 1991) which accounts for the grain dilatancy. To date, no systematic studies of endochronic theories for grain en masse can be found in the literature.

The finite element method (FEM) provides a powerful tool in solving complicated structural problems. Mahmoud (1979) used the method to predict wall pressures for bins with flexible corrugated walls. He employed a nonlinear elastic hyperbolic model to describe the stress-strain behaviour of the stored material in the primary loading conditions. Zhang (1987), using an elastoplastic constitutive model, proposed a finite element algorithm for predicting static and thermal-induced loads in grain storage bins. Schmidt and Wu (1989) developed a finite element model based on Lade's (1977) elastoplastic constitutive equation for calculating dynamic loads during discharge. Xu et al. (1993b) developed a finite element predictive model using endochronic constitutive equation of Valanis and Peters (1991). Much research has shown that the finite element method has a great potential in predicting loads in bulk solids storage structures. It should be noted that the predictive capacity of the FEM is to a large extent dependent on model's capability of capturing the constitutive behaviour of the stored bulk solids.

The research done to date has enhanced our understanding of the loads exerted by the stored materials on the structure. However, no adequate theories have been developed for

predicting bin loads, especially dynamic loads. Micromechanics may be used to develop the microscopic theory of bin loads. The investigation of discharge and hygroscopic mechanisms may throw a new light on developing the theories of dynamic loads. Systematic studies of endochronic theory may lead to a new class of endochronic theories (macromechanics models) for constitutive modelling of granular materials. Based on these constitutive theories, finite element models may be developed for the analysis of grain storage structures.

2. OBJECTIVES

The goal of this research is to develop predictive models for bin loads with an emphasis on modelling of the fundamental behaviour of granular materials.

The specific objectives are:

1) To investigate the deformation mechanism of granular materials, microscopically and macroscopically.

2) To develop and verify microscopical theories for predicting static, hygroscopic, and discharge loads in grain bins.

3) To investigate the physical basis of endochronic theory for granular materials.

4) To develop stress-based endochronic models for grain en masse by using the Gibbs free energy formulation to account for shear-volumetric coupling.

5) To implement the endochronic models in finite element algorithms to predict loads in grain storage structures.

6) To validate the predictive finite element algorithms against published experimental data obtained from model bin tests.

3. LITERATURE REVIEW

In this chapter, classical theories of bin loads are briefly reviewed first. Then current advances in predicting discharge and hygroscopic loads are discussed. Loads in grain bins depend on constitutive behaviour of grain, therefore, reviews are extended to the constitutive theories for grains and the finite element predictions of bin loads as well.

3.1 Bin Load Theories

3.1.1 Static bin loads

Historically, bins are categorized into deep bins and shallow bins depending on their dimensions and properties of stored materials. One accepted definition is according to the rupture plane. A bin is a deep bin if the rupture plane of grain intercepts the bin wall, otherwise, it is a shallow bin. Rankine's (1857) theory is used for predicting static loads in shallow bins, and Janssen's (1895) theory for deep bins.

Rankine's theory

Rankine's (1857) theory assumes that bin walls are frictionless. Lateral and vertical pressures on bin walls are determined as:

$$L = \rho g y \tan^2(45^0 - \frac{\phi}{2}) \qquad \textbf{(3.1)}$$

$$V = \rho g y \qquad \textbf{(3.2)}$$

Where:

V = vertical pressure, kPa

L = lateral pressure, kPa

ϕ = angle of internal friction of stored materials, degree

ρ = bulk density of stored materials, kg/m^3

g = gravitational acceleration constant, m/s^2

y = grain depth, m

Equations (3.1) and (3.2) indicate that the lateral to vertical pressure ratio, k value, is a constant which may be calculated as:

$$k = \frac{L}{V} = \tan^2(45^0 - \frac{\phi}{2}) \qquad \textbf{(3.3)}$$

where:

k = ratio of lateral to vertical pressure

Rankine's theory is not applicable to bins with rough or corrugated walls because of the assumption of frictionless walls.

Janssen's theory

For deep bins, bin wall friction plays an important role in calculating loads. By assuming a constant k value, the lateral pressure is calculated as:

$$L = kV \qquad \textbf{(3.4)}$$

Vertical pressure is then determined from the vertical force equilibrium on a slice of grain over the cross-section as follows:

$$V=\frac{\rho g R}{k\mu}[1-e^{-\frac{k\mu y}{R}}] \tag{3.5}$$

where:

μ = friction coefficient of grain on the wall

R = hydraulic radius of the bin, m

e = natural log base

The friction load on the wall is calculated as:

$$F=\int_0^y \mu L\, dy \tag{3.6}$$

where

F = vertical friction load, kN/m

Janssen's equation has been recommended by most design Standards and Codes (ASAE Standards 1995, DIN 1987, ACI 1991, CFBC 1990).

There are other approaches to predicting static loads. Airy (1897) used the sliding wedge theory to calculate lateral pressures in silos. The theory assumed a constant k value. Reimbert and Reimbert (1956) first considered the k value as a function of the height of the stored material and proposed a set of prediction equations for static loads. But they did not consider the direct effect of the stress state on the k value. More details may be found in Manbeck et al. (1995).

Of all the theories mentioned above, bin walls are assumed to be rigid and wall friction is assumed to be constant. In reality, few bins have rigid walls and friction may vary along the bin

depth.

The k value and bin wall friction are not two independent material properties in Janssen's theory. In Janssen's equation (3.5), k and μ appear together as one parameter, and the effect of selecting friction coefficient on predicted bin loads could be cancelled by selecting the "right" k values. If we lower the value of the friction coefficient in Janssen's theory, the wall friction force will decrease. A decreased friction force on the wall means that less of the grain mass is supported by the bin wall and a higher vertical pressure within the grain mass. If the k value is constant, this higher vertical pressure will result in a higher lateral pressure which will yield a higher wall friction force. Thompson et al. (1995) measured lateral pressures of a full-scale bin, and tried to use Janssen's equation to fit the data and determine the μ value. They found that two different values of μ (0.4 and 0.6) could have been used to obtain almost identical results for their 11.0 m-diameter bin. This raises a question as how for a designer to select the "right" μ and k value for predicting the design loads.

3.1.2. Discharge loads

At the onset of discharge of grain from bins, lateral pressure increases instantly. This increased lateral pressure is called discharge load. Discharge loads are, usually, much higher than static loads. To date, no adequate predictive theories are available for bin designers.

In design practice, discharge loads are estimated from static loads by using an overpressure factor (f_d) (DIN 1987, ACI 1990, ASAE 1995):

$$L_d = f_d L \tag{3.7}$$

where:

L_d = lateral pressure during discharge, k Pa

f_d = overpressure (dynamic load) factor

Values of overpressure factors in the range from 1.4 to 2.1 are recommended by various design Standards and Codes, but values up to 5 have been reported in the literature. This implies that the discharge load actually experienced by a bin may be twice the design load, which partially explains why most bin failures have occurred during discharging of stored materials.

Although much research has been carried out in the past 30 years on discharge loads, the mechanism of the formation of discharge loads is still not clear. Jenike and Johanson (1969) explained that discharge loads were due to the switch of the stress state in the stored materials from an active pressure field to a passive pressure field. Kmita (1991) observed that discharge loads were a result of impact loads. Impact loads can be distinguished from static loads by the speed of application. If an object is put on a structure slowly, the force exerted by the object on the structure (the applied load) equals the weight of the object (static load). If the object is put on the structure suddenly, a load twice the static load is exerted on the structure (impact load). In a storage bin when the discharge gate is opened suddenly, the material above the gate suddenly acts on the remaining material, thus impact loads are induced. Smith and Lohnes (1980) hypothesized that dilation (increase in volume due to shearing) of the stored material is the main cause of the overpressure of grain on bin walls during discharge, but they did not advance their hypothesis to prediction equations. Discharge of grain from a bin causes the grain in the different parts of the bin to move at different velocities. Thus, shearing occurs within the grain mass. This internal shearing causes the grain bulk to dilate. Dilation, however, is restricted by the bin wall, thus an

increase in the wall pressure occurs. Based on this hypothesis, Xu et al. (1993a) and Zhang et al. (1994a, 1994b) developed mechanical models to predict dynamic loads during discharge. The overpressure factor was shown to be related to the dilatancy angle of the stored materials.

3.1.3 Hygroscopic loads

Little can be found in the literature on the prediction of the hygroscopic loads. Grain particles swell when absorbing moisture, thus the grain bulk expands. This expansion, however, is restricted by bin walls. Consequently, additional pressures, termed hygroscopic pressures, are imposed on the bin walls. It is the swollen of grain particles that exerts the hygroscopic loads (overpressure) of grain on bin walls during wetting.

Dale and Robinson (1954) observed more than sixfold increases of lateral pressure for a moisture increase of 4% (w.b.) in the grains. Blight (1986) measured fourfold increases of lateral pressure for grain sorghum in simulating the ingress of rain. Britton et al. (1993) monitored vertical forces during the wetting processes. The swelling force lifted the bin wall from the bin bottom for a moisture increase of 6% (w.b.) in the grains. These experiments indicate that grain wetting may cause extremely high loads in grain storage bins. Zhang et al. (1995) rationalized the hygroscopic loads from macroscopic mechanics. No theory has been developed from microscopic mechanics.

3.2 Constitutive Models for Granular Materials

Generally, constitutive models for granular materials may be classified into two categories: macromechanics (or continuum) models (e.g., Lade 1977, Valanis and Peter 1991) and

micromechnics (or particulate) models (e.g., Prat and Bazant 1991, Granik and Ferrari 1993). Micromechnics models are based on the analysis of stresses and strains within the microstructure of granular materials. By contrast, macromechanics models describe the macroscopic phenomenological behaviour.

3.2.1 Micromechanics

Fundamentally, a granular medium is a collection of individual particles. Micro-scale interactions between particles control the macro-scale behaviour (Chang 1993). Therefore, constitutive behaviour of granular media depends on their microstructures (or fabric). An assembly of individual particles usually has a random microstructure (Bideau and Hansen 1993). The disorder of the microstructure makes it very difficult to model. Much effort has been made on description of granular fabric (Oda 1977, Nemat-Nasser 1982, Subhash et al. 1991), but few theories are adequate for solving engineering problems. The idealisation of the microstructure provided a way to cope the problem of random assembly. Balendran and Nemat-Nasser (1993) used the concept of double-sliding plane to model viscoplastic flow of planar granular materials. Granik and Ferrari (1993) treated the granular media as a Bravais lattice and developed a complete set of constitutive equations. The details of this model will be discussed in Section 5.1. Generally, discrete element method may be used to solve microscopic constitutive models (Rong 1994).

3.2.2 Macromechanics

To model the inelastic behaviour of granular materials, macromechanics requires a

measurement to define the inelastic state of materials. Stresses and strains are the two fundamental sets of variables. Therefore, either stresses or strains can be used to construct a measurement for describing the state of the materials. By using stresses, a yielding surface can be constructed (e.g., Lade 1977). By using strains, an intrinsic time can be defined (e.g., Valanis and Peters 1991). Yielding surface and intrinsic time are the two alternative ways of describing the state of materials. The concept of yielding surfaces is the foundation of the classical plasticity theory which has more than two centuries of development. Intrinsic time is the key concept of endochronic theory which initially developed by Valanis (1971). Endochronic theory is considered to be more general than the classical plasticity (Wanabe and Atluri 1979, Dafalis and Popov 1975). It provides a unified way of describing material behaviour without using the concept of yielding which is difficult to define for most granular materials (Valanis and Fang 1984).

Classical plasticity models

Classical plasticity is based on the concepts of yielding surface and unloading-reloading criteria. It is assumed that an initial yielding surface governs the initial yield of the material. This surface changes as the material deforms. The changed yielding surfaces are called "subsequent yielding surfaces". The evolution of subsequent yielding surfaces is described by hardening rules. A flow rule specifies the stress-strain relationship (Fung 1965).

Coulomb in 1773 first considered the effect of the hydrostatic pressure on the strength of granular materials (Chen and Mizuno 1990). The yield criterion in the Coulomb model states that failure occurs when the shear stress (τ) and normal stress (σ) satisfy the following linear equation (Chen and Mizuno 1990):

$$|\tau| + \sigma \tan\phi - c = 0 \qquad \textbf{(3.8)}$$

where:

c = cohesion, kPa

ϕ = internal friction angle, degree

The absolute value means that the shear may occur in the opposite direction. If the material is frictionless (ϕ=0), the criterion reduces to the Tresca criterion (the maximum shear stress criterion), and the cohesion c becomes the yield stress. Shield (1955) showed that the yielding surface of Coulomb's model is an irregular hexagonal pyramid in the principal stress space, whose corners cause some difficulties in numerical analysis. Coulomb's model neglects the effects of intermediate principal stress on yielding. Lade and Duncan (1973) investigated the effects of intermediate principal stress on the failure strength of granular materials. They developed an isotropic elastic-plastic work-hardening model which contained subsequent yield surfaces and a failure surface (Lade and Duncan 1975). Lade (1977) modified the model by introducing a curved yield surface which is suitable for numerical analysis. To get a more realistic description of the material yielding, more complex yielding surfaces must be used, such as nested yield surfaces (Mróz 1967), bounding surfaces (Dafalias and Popov 1975), and cap surfaces (Katona and Mulert 1984). However, the greatest difficulty encountered in the application of the classical theory of plasticity to granular materials remains the lack of knowledge of the configuration of subsequent yield surfaces (Valanis and Fan 1984).

Endochronic plasticity

Endochronic plasticity describes the behaviour of materials by the measurement of intrinsic

time. The constitutive laws are derived from the thermodynamic principle and evolution equations of internal variables.

Intrinsic time is a "time-like" parameter of the material, which increases monotonically. In the original version of the endochronic theory, the theory was developed for metal, in which volumetric response is considered elastic. Valanis (1971) initially defined intrinsic time to be an equivalent length of the total strain path (from the initial (zero) strain to the final state on the stress-strain curve):

$$dz^2 = de_{ij} P_{ijkl} de_{kl} \tag{3.9}$$

where:

dz = increment of intrinsic time scale

de_{ij} = increment of total deviatoric strain

P_{ijkl} = material property tensor

I=1,2,3; j=1,2,3 for three-dimensional problems.

The repetition of an index (subscription) in a term denotes a summation with respect to that index over its range.

Valanis (1980) subsequently found this definition too limiting (valid for small strains only) and introduced a new definition of intrinsic time as the equivalent length of the plastic deviatoric strain path:

$$dz^2 = de_{ij}^p P_{ijkl} de_{kl}^p \tag{3.10}$$

where de_{ij}^p is the plastic deviatoric strain increment tensor given as:

$$de_{ij}^{p} = de_{ij} - \frac{ds_{ij}}{2G} \tag{3.11}$$

where:

ds_{ij} = deviatoric stress increment tensor, kPa

G = elastic shear modulus, kPa

Based on this definition of intrinsic time, various classical plasticity theories have been shown to be the asymptotic cases of the endochronic theory (Valanis 1980).

For granular materials, the volumetric behaviour is unlikely to be elastic and may be coupled with deviatoric behaviour. Valanis and Peters (1991) investigated the coupling between deviatoric and hydrostatic behaviour, which led to dilatant deformation of the material. They used a coupling parameter (κ) to introduce the plastic volumetric strain $d\epsilon_h^p$ into the intrinsic time:

$$dz^2 = de_{ij}^{p} de_{ij}^{p} + \kappa^2 (d\varepsilon_h^p)^2 \tag{3.12}$$

where the plastic volumetric strain increment ($d\epsilon^p_h$) was given as:

$$d\varepsilon_h^p = d\varepsilon_h - \frac{d\sigma_h}{K_h} \tag{3.13}$$

where:

$d\sigma_h$ = hydrostatic stress increment, kPa

$d\epsilon_h$ = volumetric strain increment

K_h = elastic bulk modulus, kPa

The constitutive behaviour of granular materials is characterised by both deviatoric behaviour and hydrostatic behaviour. Deviatoric behaviour is measured by deviatoric intrinsic time

dz_d, and volumetric by hydrostatic intrinsic time dz_h. These two intrinsic time components are related to the total intrinsic time through a hydrostatic hardening function (F_h) and a deviatoric hardening function (F_d):

$$dz_d = \frac{dz}{F_d} \quad and \quad dz_h = \frac{dz}{\kappa F_h} \tag{3.14}$$

where:

dz_d = deviatoric intrinsic time component

dz_h = hydrostatic intrinsic time component

F_h = hydrostatic hardening function

F_d = deviatoric hardening function

Using these definitions of intrinsic time, constitutive models can be developed for granular materials. A model can be either a relaxation-type, which relates the load (stress) response to applied deformation (strain), or a creep-type, which relates deformation (strain) response to applied load (stress). Relaxation-type models are formulated from the Helmholtz energy representation (strain-based theory), whereas creep-type models from the Gibbs energy representation (stress-based theory). Within the elastic limit, stress-based and strain-based models are identical. Beyond the elastic limit, they are complementary. A Helmholtz formulation was developed for granular materials by Valanis and Peters (1991), and applied to wheat en masse by Xu (1992). With the original definition of intrinsic time (total strain path), Wu and Wang (1983) derived a Gibbs formulation for sand. No work has been reported in the literature on Gibbs formulation using the new definition of intrinsic time.

For non-viscous granular materials, Darve et al. (1988) classified all continuum

constitutive models according to the number of their tensorial zones, which are defined as domains, separated by either the plastic potentials or the loading-unloading criteria, in the stress space. A constitutive model has 2^n tensorial zones if the model has n plastic potentials or loading-unloading criteria. For example, elastic models have only one tensorial zone, Lade's (1977) elastoplastic model with two plastic potentials has four tensorial zones, and endochronic models have an infinite number of tensorial zones. The number of tensorial zones characterizes the structure of the model, which strongly influences the predictive capability of the model (Darve et al. 1988). In theory, endochronic models, with an infinite number of tensorial zones, have the strongest predictive capacity (Darve et al. 1988).

3.3 Finite Element Analysis of Grain Storage Structures

The finite element method (FEM) provides a powerful tool of solving complex engineering problems. It has been applied to the study of loads in grain bins. It gives an integrated analysis of behaviour of stored grain, storage structure, and their interactions.

Mahmoud (1979) used the finite element method to predict wall pressures for bins with flexible corrugated walls. He employed a nonlinear elastic hyperbolic model to describe the stress-strain behaviour of the stored material in the primary loading conditions. Zhang et al. (1987), using an elastoplastic constitutive model, proposed a finite element algorithm which adequately predicted static and thermal-induced loads in grain storage bins. Rotter and Zhang (1989) investigated the stability of silos using FEM. Schmidt and Wu (1989) developed a finite element model based on Lade's (1977) elastoplastic constitutive equation for predicting dynamic loads during discharge. Puri and Manbeck (1991) studied the potential of finite element method in

modelling load response of particulate materials. Xu et al. (1993b) developed a finite element predictive model using endochronic constitutive equation of Valanis and Peters (1991).

It should be noted that most existing FEM models were formulated using potential energy principles. The primary variables in these models are displacements, although forces (pressures) are of primary interest in bin design, the predictive capacity of the FEM is to a large extent dependent on model's capability of capturing the constitutive behaviour of the stored bulk solids and their interactions with the storage structures.

4. MICROSTRUCTURE AND BEHAVIOURS OF GRANULAR MEDIA

A granular medium is an assembly of individual particles (grains). The microstructure within particles is stable in comparison with the microstructure of particles' assembly. Therefore, the discussion in this chapter is focused on the microstructure of particles' assembly instead of microstructure within particles. Granular media of different microstructure may behave differently. The real microstructure of a granular medium is unique, because the medium is packed somewhat randomly. It is very difficult to treat each medium individually. When a granular medium is tested, it is unlikely to identify the real microstructure. This implies that the real microstructure is traditionally treated equally as an idealised one. It is important to understand the deviation of the material response and the effects of microstructure changes on behaviours of granular media. In this Chapter, factors affecting microstructure are analyzed, triaxial tests of two kinds of microstructure are conducted, and the relationship between microstructure and behaviours of granular media is discussed on the basis of test results.

4.1 Factors Affecting Microstructure

Microstructure of granular media depends on the type, quantity and quality of particle contacts, as well as the shape, size, and surface condition of the individual particles. There are many factors affecting microstructure of grains stored in a bin. Filling of grains into a bin gives an initial microstructure of granular materials. Different filling methods will yield different initial microstructures. During the storage, environmental changes have impacts on the microstructure. A temperature (or moisture content) increment in a particle will induce a thermal (or hygroscopic)

expansion in the particle which will interact with the neighbouring particles. Consequently, change the microstructure. Vibration is another important factor which tends to consolidate the bulk materials significantly resulting in a higher bulk density. Therefore, microstructure during storage could be affected by temperature fluctuation, moisture fluctuation, foundation (or storage structure) vibration, particles' creep and relaxation, biological and chemical reactions, etc. Some factors (e.g., filling method and vibration) mainly affect particles' contacts, other factors (e.g., moisture and temperature fluctuations) may affect not only the contacts but also the properties of individual particles. To investigate all these effects is beyond the scope of this study. Therefore, only vibration effects will be investigated for the purpose of a better understanding of the effect of changes in microstructure on the behaviour of granular media.

4.2 Experimental Investigation of Vibration Effects

Vibration has been used to improve the handling of bulk solids. During vibrating, bulk solids are likely to exhibit lower strength and better flowability than in the static state (Roberts 1991). Vibration also reduces friction between structures and grain. When discharging bulk solids from bins, vibration may convert a funnel-flow bin to a mass-flow bin. A vibrated granular medium is likely to behave differently from a non-vibrated one, because vibration causes changes in the microstructure (fabric) of the grain bulk. The visible change in fabric is expected to be the reorientation of grain particles which may result in an increase in bulk density. Invisible changes may be the modes of contact between grain particles. These changes affect the physical and mechanical properties of grain en masse. Because forces applied to a grain bulk are transmitted through inter-particle contacts, quantity and quality of contact points between particles may

dictate behaviour of the grain bulk. One of most important variables is the total number of contacts in the assembly of grain particles. If no force is being transmitted through a contact, the contact is a pseudo-contact, which should be excluded from the total number of effective contacts. A contact may be characterized by the contact normal (normal to the contact surface) and contact area. All these aspects of interests will be briefly discussed in this Chapter through examining triaxial test results on vibrated grain samples.

4.3 Triaxial Test

Grain bulk changes its volume during deformation. Therefore, strength (resistance to microstructure changes) and dilation are the key macroscopic characteristics in responses of grain en masse. Conventional triaxial tests were conducted to measure the axial forces and volumetric changes when the samples were subjected to axial deformation.

Preparation of Test Samples

Grain used in all tests was Katepwa wheat. The moisture content of the wheat was determined as 13.2 % (d.b.) by oven method (ASAE 1995), and particle specific gravity was 1.42 by comparison pycnometer. Samples were prepared using a latex membrane sleeve held inside an aluminium jacket. A vacuum was applied between the membrane and the inside surface of the jacket to ensure the shape and dimensions of the sample. Wheat was centrally filled into the membrane sleeve. The jacket was 260 mm in height and 106 mm in diameter, which produced cylindrical specimens 215 mm in height and 100 mm in diameter. After the jacket was filled with wheat, it was fixed on the top of a vibratory device (Eriez Magnetics, Eriez Manufactory Co., Erie, PA, USA), and vibrated at a frequency of 50 Hz and an amplitude of 0.3 mm for 10 min. A

vacuum was applied from the bottom of the specimen to hold the sample when the jacket was removed. The sample was then placed in a sealed chamber and subjected to a constant confining pressure of 41.4 kPa regulated by an air pressure regulator (Fig. 4.1).

Test Procedures

All tests were performed using a Chatillon ET 1100 universal testing machine. The triaxial test apparatus was placed between the loading frames of the universal machine, and an axial force was applied to the grain samples through a loading rim (Fig. 4.1). The universal testing machine was controlled by a microcomputer. The axial displacement rate was set at 10 mm/min. The axial forces and displacements were recorded automatically by a data acquisition system. Pore pressure of the grain sample was recorded manually, using an H_2O differential pressure monometer, for every 1 mm of axial displacement. Volumetric strains were calculated from the measured pore pressure data using the perfect gas law. The experiments were replicated three times for both vibrated and non-vibrated samples.

4.4 Visual Observation of Vibration-induced Fabric Changes

Fabric changes in wheat en masse during the vibration were observed by vibrating a wheat sample in a transparent plexiglass container (152 mm in diameter and 238 mm in height) using the same vibratory device as described in the triaxial test. The observed fabric changes provided a better understanding of the macroscopic behaviour of vibrated microstructure of wheat en masse.

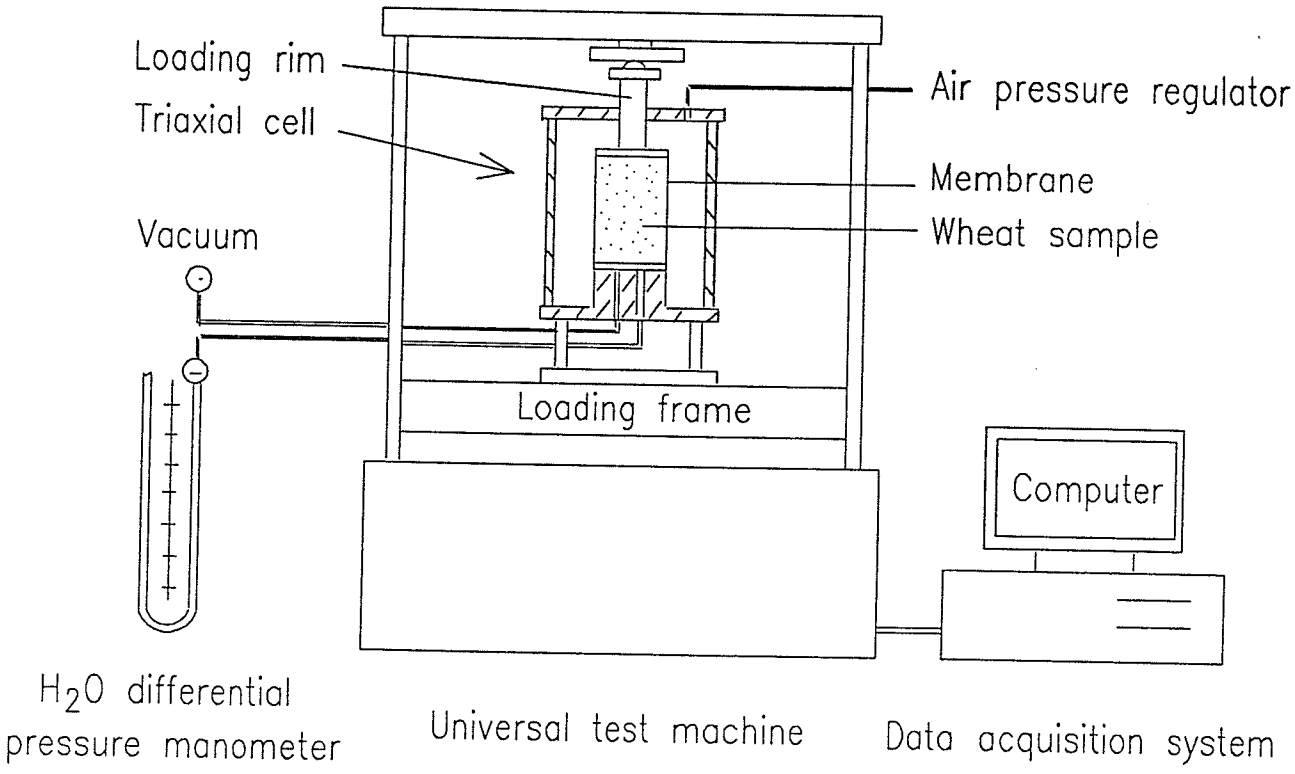

Figure 4.1 Triaxial test apparatus

4.5 Test Results and Discussion

Behaviour in Triaxial Tests

Following the sign convention of soil mechanics, compressive stresses and strains are considered to be positive in this thesis. The data averaged from three tests are shown in Fig. 4.2. The standard deviations of deviatoric stress and volumetric strain from the mean values are summarized in Table 4.1. There were some variations (within 2 %) between tests in the initial bulk density (IBD). The mean IBDs are 906.8 and 857.7 kg/m^3 for vibrated and non-vibrated samples, respectively.

The stress-strain-dilatancy behaviour of vibrated wheat samples was compared with that of non-vibrated samples (Fig. 4.2). The deviatoric stresses of vibrated samples were higher than that of non-vibrated ones, but they approached similar values at large axial strains. The average difference in the mean measured deviatoric stresses between vibrated and non-vibrated samples was 4.5 kPa. The maximum difference was 25.8 kPa at an axial strain of $6x10^{-3}$. The peak stress of vibrated samples was 67.2 kPa, slightly higher than the 63.7 kPa stress for non-vibrated samples for a difference of 3.5 kPa.

Vibration increased the dilatancy of wheat samples. The average difference in the measured mean volumetric strains was $8.1x10^{-3}$ mm^3/mm^3. At an axial strain of $200x10^{-3}$, the volumetric strain of vibrated samples was $14.1x10^{-3}$ mm^3/mm^3, five times the volumetric strain for non-vibrated samples $2.8x10^{-3}$ mm^3/mm^3. Vibrated samples dilated throughout most of the loading process, whereas non-vibrated samples first consolidated and then dilated (Fig. 4.2).

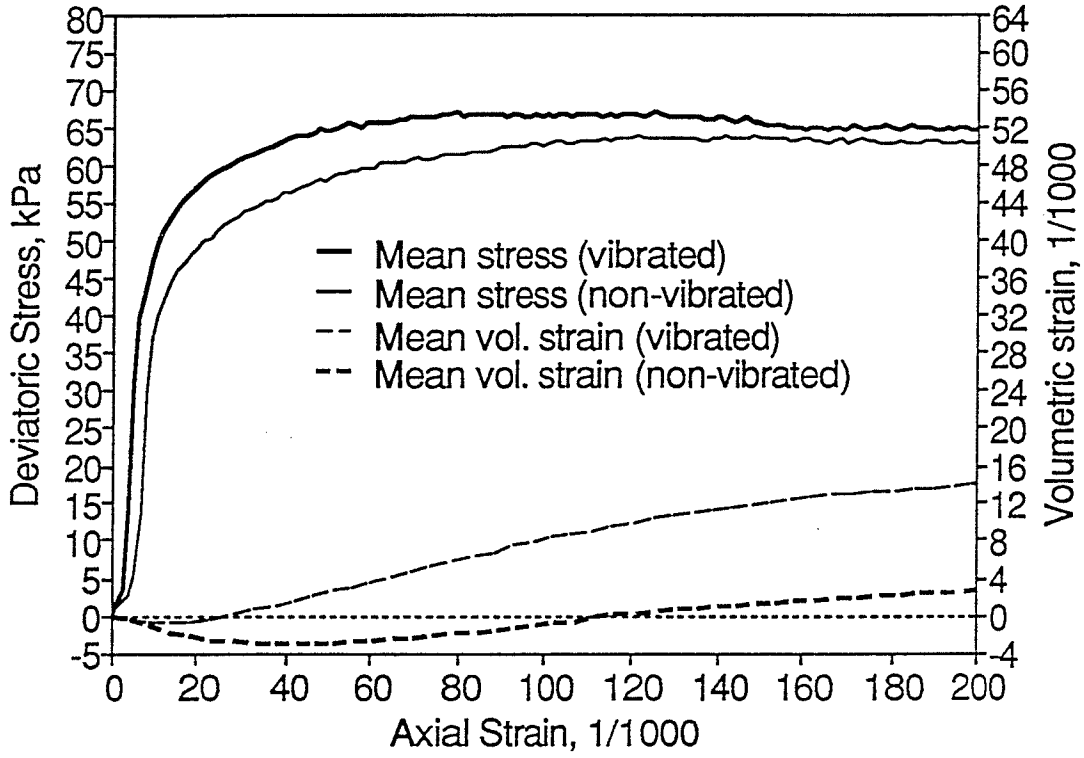

Figure 4.2 Comparison of the stress-strain behaviour between vibrated and non-vibrated wheat samples (m.c.=13.2%d.b.) at a confining pressure of 41.4 kPa.

Table 4.1 Standard deviations for measured stresses and strains

Tests	Vibrated			Non-vibrated		
	$\Delta D\%$	$S(\sigma_d)$	$S(\epsilon_v)$	$\Delta D\%$	$S(\sigma_d)$	$S(\epsilon_v)$
1	-1.8	6.33	1.87	0.6	3.33	0.63
2	0.1	2.89	0.53	-1.0	4.88	0.18
3	1.6	3.56	1.66	0.4	2.02	0.64

$\Delta D\%$: Relative difference of measured IBD from the mean value

$S(\sigma_d)$: Standard deviation of measured deviatoric stresses, kPa

$S(\epsilon_v)$: Standard deviation of measured volumetric strains, 1/1000

Observations of Microstructural Changes

From observations of a wheat sample in a plexiglass container, the response of the grain bulk to vibration was found to occur in two stages. When wheat was initially filled into the container, there was some unstable micro-structure in the assembly, and most particles were deposited with the long-axis more or less parallel to the horizontal because of gravity effects during filling. Contact normals tend to concentrate toward the vertical direction (Oda 1993), which coincides with the direction of the applied compression force in conventional triaxial tests. At the very beginning of vibration, wheat particles mainly translated into voids, resulting in

consolidation of the grain bulk, i.e., a higher bulk density. At this stage, most particles were sliding over one another, and the number of effective contacts for each grain particle increased. Most increased contacts had their normals in the horizontal direction, which is important for the stability of the fabric (Oda 1993). Further vibration seemed to have fluidized the grain bulk, and produced less than 20 percent of the total change in bulk density, estimated from the surface movement of top grains. During this stage, wheat particles adjacent to the wall moved downward, whereas those located in the central region were forced to move upward. Particles travelled in such a way that their long-axes were consistent with the moving path to minimize the resistance to the motion, thus some particles were reoriented with their long-axes in the vertical direction.

Macroscopically, the wheat bulk gains more strength through increasing the number of contacts, therefore, vibrated samples exhibit higher strength. Especially, an increase in number of horizontal contact normals stabilises the fabric and results in higher resistance to vertical loads. As the vibrated wheat bulk dilates, contact points in the medium decrease which lowered the strength of the medium. For non-vibrated samples, the initial shear strength is much lower because of fewer contacts in the medium, the consolidation increases the number of contacts and the shear strength is also increasing. Lee and Seed's (1967) observed that, for a constant confining pressure, volume changes which accompany the shearing deformations tend to produce samples with the same void ratio at failure. This implies that contact points in vibrated samples are comparable to those in non-vibrated samples at failure. Therefore, the stress response of vibrated samples approached that of non-vibrated samples at larger deformation (Fig. 4.2).

Microstructural Stability

For the purpose of illustrating dilation microscopically, four particles in contact are

considered (Fig. 4.3). Figure 4.3a shows an unstable microstructure (Fabric I) with Particles A and B in an unstable position. There are four contacts, two vertical and two horizontal ones. If only gravitational force exists, Points 1 and 3 (horizontal contacts) are pseudo-contacts because no force is transmitted across these two points. Figure 4.3b shows a stable microstructure (Fabric II), Particles A and B are now in a stable position. There are five contacts, none of them are in vertical contact. Fabric II has less void than Fabric I. If both fabrics are now subject to a simple shear, say, Particles A and B move leftwards. Fabric I will show a lower shear strength with consolidation, whereas Fabric II will show a higher shear strength with dilation. A grain bulk consists of many Fabrics I and II aggregations. Vibration tends to convert Fabric I aggregations to Fabric II type in the grain bulk, thus a vibrated grain bulk exhibits higher shear strength and dilates more.

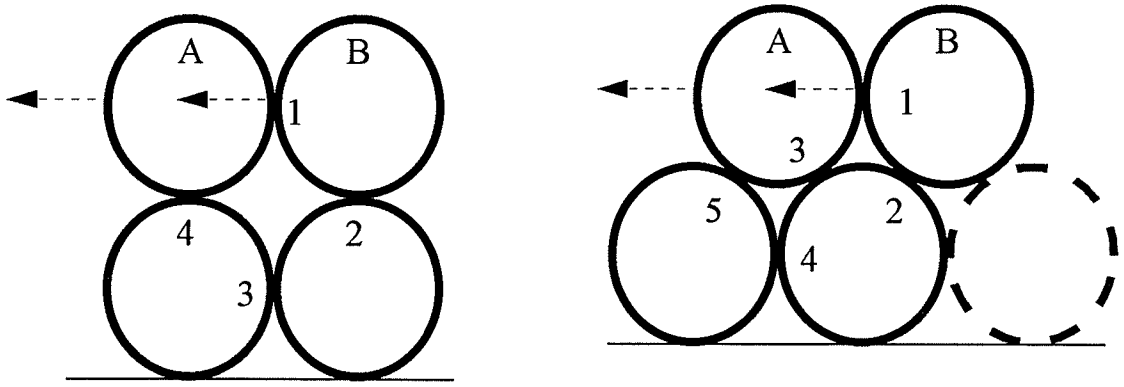

a) b)

Figure 4.3 Illustration of grain particle assemblies: a) Fabric I, unstable; and b) Fabric II, stable.

5. MICROSCOPIC THEORY OF BIN LOADS

Analytic theories for predicting loads exerted by granular material on storage structures have been traditionally derived from macroscopic approach (Janssen 1895, Reimbert and Reimbert 1987). An underlining assumption in macroscopic theories is that granular materials behave like continua. These continuum theories predict loads in storage structures with reasonable accuracy if appropriate model parameters are used. Unfortunately, some of these model parameters often cannot be clearly defined because of the inherent discontinuous nature of granular materials. For example, predictions of the Janssen theory rely on the ratio of lateral to vertical pressures (k value), but many researchers have shown that the lateral to vertical pressure ratio is not a constant material property parameter (Cowin 1979, Atewologun and Riskowski 1991).

Discontinuity is a fundamental characteristic of granular media. When external stresses are imposed on a granular medium, they are carried by the contacts between particles. Macroscopic deformations of the medium result from inter-particle movements (slip and rotation) and particle deformation. Therefore, to accurately characterize granular systems, parameters relating to individual particles (granules) and inter-particle interactions should be considered. These fundamental microscopic property parameters cannot be directly included in continuum theories. In this chapter, an analytic predictive model is developed for loads in granular material storage structures (bins and silos) from a micromechanics theory. Some important particle properties are considered in the model development. Because most storage bins (silos) are axial symmetry, stresses are approximated as being two-dimensional, and so discussion is limited to this condition in the following sections.

5.1 Microstructural Mechanics

The predictive model is developed from a theory of microstructural mechanics for granular media (Granik and Ferrari 1993). In their theory, a pair of particles (doublet) is considered as a basic structural unit. When a granular medium is subject to loads macroscopically, strains develop within the doublet because of deformations, rotation and slipping of particles. These strains are termed microstrains. Corresponding to microstrains, microstresses also develop within the doublet. These microstresses are: elongation (compression) microstress corresponding to separation (convergence) of the particles; torsional microstress corresponding to rotation of particles about the doublet axis; and shear microstress corresponds to slip between particles. The relationship between microstrains (or microstresses) and macrostrains (or macrostresses) depends on the structure of the granular medium. For a granular medium consisting of equal-sized spheres, two basic types of idealized structures may exist in two-dimensional conditions: square packing and packing hexagonal (Fig. 5.1) (Granik and Ferrari 1993). Square packing seldom exists in real granular media because of its instability. The present theory assumes that a granular medium consists of hexagonally packed elastic spheres. In such a structure, an individual particle is involved in six doublets which are separated by a structural angle γ=60° (Fig.5.2). For non-sphere particles, it is a good approximation if the media are packed isotropically. Otherwise, the structural angle should be adjusted to reflect the non-isotropic microstructure. Under static conditions, rotation and slip of particles are negligible in a granular medium. It follows that the two corresponding microstresses, torsional and shear stresses, may be assumed to be negligible. Therefore, microstresses acting on a particle may be expressed by three components, p_1, p_2 and p_3 , in three directions (Fig. 5.2). It should be noted that these microstresses are conceptually different from contact stresses between particles. Contact stresses in

doublets are local and discrete. However, by averaging contact stresses over projected area of particles, discrete contact stresses may be approximated by continuous microstresses (Granik and Ferrari 1993). In a doublet, microstress acting on each particle represents a fictitious stress uniformly distributed over the projected area of the particle, in the direction of the line connecting the centres of the particles (Fig.5.2). Microstresses can be transformed to macroscopic stresses in a rectangular Cartesian coordinate system as follows (Granik and Ferrari 1993):

$$\sigma_{ji} = \sum_{\alpha=1}^{3} \ell_{\alpha j} \ell_{\alpha i} p_{\alpha} \qquad \textbf{(5.1)}$$

where:

$\ell_{\alpha i}$ = directional cosine of p_{α}, α =1, 2, 3

σ_{ji} = macrostress tensor, i=1, 2; j=1,2

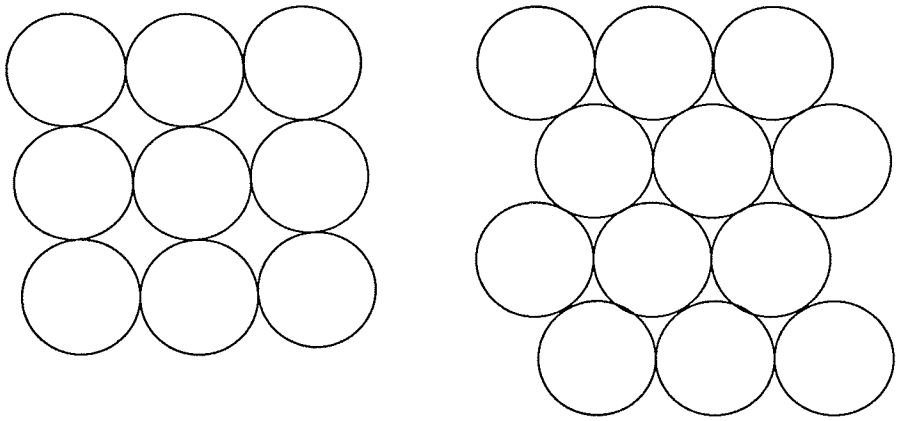

(a) (b)

Figure 5.1 Idealized structures of equal sized spheres in two-dimensions: a) square packing, and b) hexagonal packing.

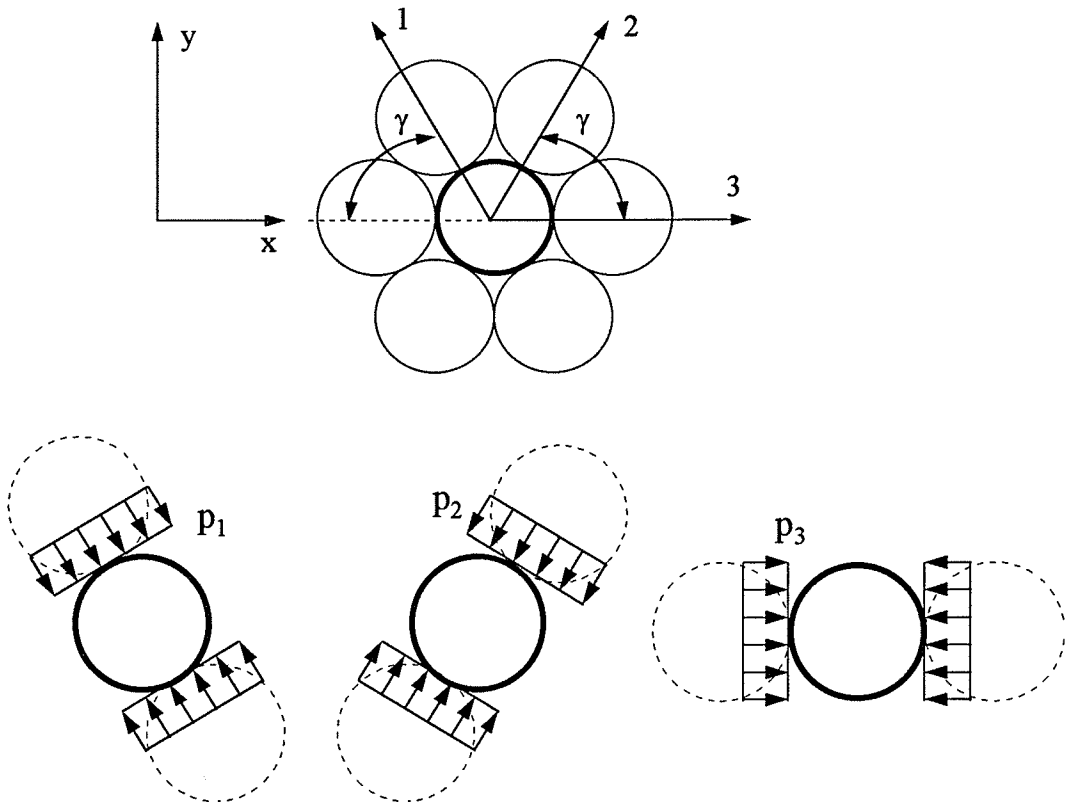

Figure 5.2 A basic unit of hexagonal structure and microstresses on a particle.

Since $(\ell_{11}, \ell_{21}, \ell_{31}) = (-\cos\gamma, \cos\gamma, 1)$ and $(\ell_{12}, \ell_{22}, \ell_{32}) = (-\sin\gamma, \sin\gamma, 0)$, equation (5.1) can be expanded as:

$$\sigma_x = \sigma_{11} = (p_1 + p_2)\cos^2\gamma + p_3 \qquad \textbf{(5.2)}$$

$$\sigma_y = \sigma_{22} = (p_1 + p_2)\sin^2\gamma \qquad \textbf{(5.3)}$$

$$\tau_{xy} = \sigma_{12} = (p_1 - p_2)\cos\gamma \sin\gamma \quad \textbf{(5.4)}$$

where:

σ_x = normal stress in x direction

σ_y = normal stress in y direction

τ_{xy} = shear stress on xy plane

Corresponding to the three microstress components, there are three microstrain components, ε_1, ε_2, and ε_3. Physically, microstrain represents the rate of change in distance between particle centres in a doublet. If particles are elastic, the relationship between microstresses and microstrains takes the simple form of (Granik and Ferrari 1993):

$$p_\alpha = E\varepsilon_\alpha \quad \textbf{(5.5)}$$

where:

p_α = microstress, $\alpha = 1, 2, 3$

ε_α = microstrain, $\alpha = 1, 2, 3$

E = elastic modulus of the particle

The kinematic relations relate the macrostrains to microstrains as (Granik and Ferrari 1993):

$$\varepsilon_\alpha = \ell_{\alpha i}\ \ell_{\alpha j}\varepsilon_{ij} \quad \textbf{(5.6)}$$

where:

ε_{ij} = macrostrains

By noting that repeating subscripts i and j imply summations (except the Greek letter α), equation (5.6) may be written as:

$$\varepsilon_1 = \varepsilon_x \cos^2\gamma + 2\varepsilon_{xy} \sin\gamma \cos\gamma + \varepsilon_y \sin^2\gamma \tag{5.7}$$

$$\varepsilon_2 = \varepsilon_x \cos^2\gamma - 2\varepsilon_{xy} \sin\gamma \cos\gamma + \varepsilon_y \sin^2\gamma \tag{5.8}$$

$$\varepsilon_3 = \varepsilon_x \tag{5.9}$$

where:

ε_x = strain (ε_{11}) in x direction

ε_y = strain (ε_{22}) in y direction

ε_{xy} = shear strain (ε_{12}) on x-y plane

From continuum mechanics, equations governing the equilibrium of macrostresses and the compatibility of the macrostrains (Fung 1965):

$$\frac{\partial \sigma_{ji}}{\partial x_j} + X_i = 0 \tag{5.10}$$

$$2\frac{\partial^2 \varepsilon_{xy}}{\partial x \partial y} = \frac{\partial^2 \varepsilon_x}{\partial^2 y} + \frac{\partial^2 \varepsilon_y}{\partial x^2} \tag{5.11}$$

where:

X_i = body force, i=1, 2

Substitution of Eqs. (5.2) to (5.4) into Eq. (5.10) gives:

$$\frac{\partial(p_1+p_2)}{\partial x}+\frac{\partial(p_1-p_2)}{\partial y}\tan\gamma+\frac{\partial p_3}{\partial x}\cos^{-2}\gamma=0 \qquad \textbf{(5.13)}$$

$$\frac{\partial(p_1-p_2)}{\partial x}+\frac{\partial(p_1+p_2)}{\partial y}\tan\gamma-\frac{\rho g}{\cos\gamma\sin\gamma}=0 \qquad \textbf{(5.12)}$$

where:

γ = micro-structural angle

ρ = bulk density

g = gravitational acceleration constant

Equations (5.13) and (5.14) alone are not sufficient to determine three microstresses. Therefore, the compatibility equation (5.11) must be used. Substituting Eqs. (5.5) into (5.7), (5.8) and (5.9), then into (5.11) yields:

$$\frac{\partial^2(p_1+p_2)}{\partial x^2}-\frac{\partial^2(p_1-p_2)}{\partial x\partial y}\tan\gamma-2\frac{\partial^2 p_3}{\partial x^2}\cos^2\gamma+2\frac{\partial^2 p_3}{\partial y^2}\sin^2\gamma=0 \qquad \textbf{(5.14)}$$

Equations (5.13), (5.14), and (5.15) are the three governing equations which can be solved simultaneously for the three unknown p_1, p_2 and p_3. It should be noted that compression stresses are considered to be positive in the above equations.

5.2 Static loads

5.2.1 Pressures in bins with frictionless walls

Consider a hypothetical bin with frictionless walls to develop some understanding of the relationship between microstresses and macroscopic pressures in storage bins. If no friction exists between the granular material and its containing structures, shear stress τ_{xy} should be zero and microstresses do not vary across the bin cross-section (x direction). Therefore, from equation (5.4), we have:

$$p_1 = p_2 = p(y) \tag{5.15}$$

where $p(y)$ is a microstress which is determined by substituting Eq. (5.15) into Eq.(5.13):

$$p(y) = \frac{\rho g y}{2\sin^2\gamma} \tag{5.16}$$

Substituting Eqs.(5.15) and (5.16) into Eq.(5.12) yields:

$$\frac{\partial p_3}{\partial x} = 0 \tag{5.17}$$

Equation (5.17) indicates that p_3 is a function of y only, i.e., $p_3 = p_3(y)$. Using this condition and Eqs. (5.15) and (5.16), Eq. (5.14) is simplified as:

$$\frac{\partial^2 p_3}{\partial y^2} = 0 \tag{5.18}$$

By integrating equation (5.18) and applying the boundary condition of $p_3=0$ at $y=0$, we obtain:

$$p_3 = \lambda y \tag{5.19}$$

where λ is an integration constant. This constant (λ) can be determined by examining the horizontal microstrain ε_3. If particles in the granular medium are perfectly rigid (Poisson's ratio is zero), microstrain ε_3 is zero for symmetric structures like hexagonal packing, and therefore, microstress p_3 is zero as indicated by Eq.(5.5) with $\varepsilon_3 = 0$. Consequently, λ is zero as indicated by Eq.(5.19). However, particles are deformable for most real granular media. Therefore , microstresses p_1 and p_2 will cause the particle to deform in the horizontal direction, resulting in microstrain ε_3. To determine the magnitude of ε_3, microstresses p_1 and p_2 are resolved into horizontal (p_x) and vertical components (p_y) (Fig. 5.3). The magnitudes of horizontal components are ($p_1 cos^2\gamma = pcos^2\gamma$) and ($p_2 cos^2\gamma = pcos^2\gamma$) for p_1 and p_2, respectively. The two respective vertical components are ($p_1 sin^2\gamma = psin^2\gamma$) and ($p_1 sin^2\gamma = psin^2\gamma$). If the particle has a modulus of elasticity of E and Poisson's ratio of ν, the horizontal deformations due to the horizontal and vertical stress components are:

$$D_1 = -\left(\frac{P_x}{E}\right)(2r\cos\gamma) = -\left(\frac{p\cos^2\gamma}{E}\right)(2r\cos\gamma) \tag{5.20}$$

$$D_2 = \left(\frac{p_y}{E}\right)(\nu)(2r) = \left(\frac{p\sin^2\gamma}{E}\right)(\nu)(2r) \tag{5.21}$$

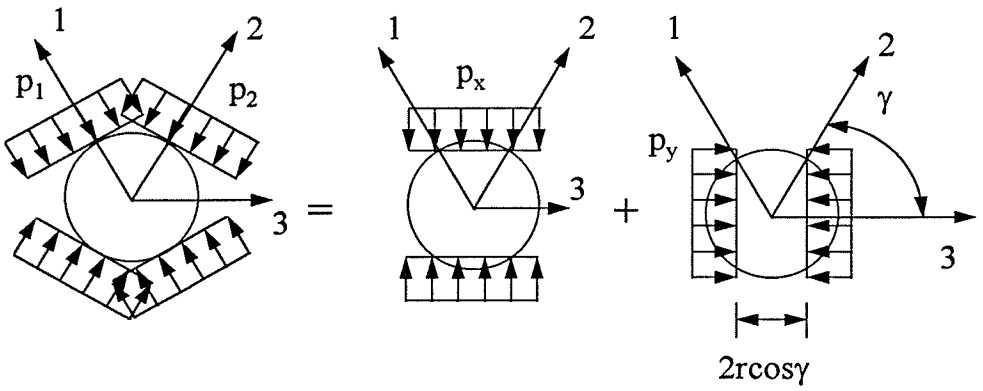

Figure 5.3 Decomposition of microstresses p_1 and p_2 into horizontal and vertical components p_x and p_y.

where:

D_1 = horizontal deformation caused by the horizontal stress component

D_2 = horizontal deformation caused by the vertical stress component

r = radius of the particle

It should be noted that only a portion of the particle ($2r\ cos\gamma$) is considered to be subject to deformation when calculating D_1 (Fig.5.3). The total change in the particle diameter in the horizontal direction is $(D_1 + D_2)$. Therefore, the horizontal strain ε_3 is determined as $(D_1+D_2)/2r$. By using Eq. (5.5), the horizontal microstress is calculated as:

$$p_3 = E\varepsilon_3 = E\left(\frac{D_1 + D_2}{2r}\right) = p(\nu\sin^2\gamma - \cos^3\gamma) \qquad \textbf{(5.22)}$$

Combining equations (5.16), (5.19) and (5.22) gives:

$$\lambda = \left(\frac{\rho g}{2\sin^2\gamma} \right) (\nu \sin^2\gamma - \cos^3\gamma) \tag{5.23}$$

Macrostresses can now be calculated from microstresses by using Eqs. (5.2)-(5.4), (5.16), and (5.19):

$$\sigma_x = (\rho g \cot^2\gamma + \lambda) y \tag{5.24}$$

$$\sigma_y = \rho g y \tag{5.25}$$

$$\tau_{xy} = 0 \tag{5.26}$$

From equations (5.24) and (5.25), the lateral to vertical pressure ratio (k value) is determined as:

$$k = \frac{\sigma_x}{\sigma_y} = \begin{cases} \cot^2\gamma & for\ \lambda = 0 \\ \dfrac{\nu}{2} + \cot^2\gamma \left(1 - \dfrac{\cos\gamma}{2} \right) & for\ \lambda \neq 0 \end{cases} \tag{5.27}$$

Equations (5.24) to (5.27) may be used to predict pressures in shallow bins where wall friction can generally be ignored.

5.2.2 Pressures in bins with frictional walls

The frictional force between grain and the bin wall transfers a portion of the grain weight to the bin wall. For a slice of grain (Fig.5.4), the total grain weight is ($g\rho A\Delta y$), where A is the cross-sectional area of the bin and Δy is the height of the slice. The portion of grain weight that is transferred to the bin wall is ($\mu\sigma_x S\Delta y$), where μ is the coefficient of friction between granular material and wall and S is the bin perimeter. The grain weight (b) that is actually supported by the grain mass itself is the total weight less that transferred to the wall:

$$b = \rho g A\Delta y - \mu\sigma_x S\Delta y \tag{5.28}$$

Therefore, the equivalent body force is calculated as the effective grain weight (b) per volume:

$$Y = \frac{b}{A\Delta y} = \rho g - \mu\sigma_x \frac{S}{A} = \rho g - \frac{\mu\sigma_x}{R} \tag{5.29}$$

where:

Y = equivalent body force

S = bin perimeter

A = cross-sectional area of the bin

R = hydraulic radius (A/S) of the bin

μ = coefficient of friction between granular material and wall

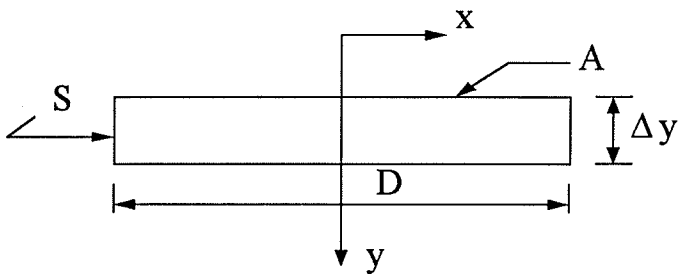

Figure 5.4 A slice of grain over the bin cross-section.

By using this equivalent body force in Eq.(5.13), the frictional force is included in the equilibrium equation :

$$\frac{\partial(p_1-p_2)}{\partial x}+\frac{\partial(p_1+p_2)}{\partial y}\tan\gamma-\left(\rho g-\frac{\mu\sigma_x}{R}\right)\frac{1}{\cos\gamma\sin\gamma}=0 \qquad \textbf{(5.30)}$$

Since the force equilibrium is considered for a slice of grain over the bin cross-section, it is implied that stresses are uniform across the bin cross-section. In essence, stresses considered here are "mean" stresses and microstresses p_1 and p_2 are equal across the cross-section. This suggests that equation (5.15) remains valid for bins with frictional walls. Substituting Eqs. (5.2), (5.15), and (5.19) into Eq. (5.30) and solving the resulting equation yields:

$$\frac{d(2p)}{dy}\sin^2\gamma-\rho g+\frac{\mu}{R}(2p\cos^2\gamma+\lambda y)=0 \qquad \textbf{(5.31)}$$

Microstress p can now be determined by solving Eq. (5.31) with proper boundary conditions, e.g., $p=0$ *at* $y=0$. Equation (5.31) is a first order differential equation with constant coefficients. It has a

particular solution of:

$$p(y) = \frac{R}{\mu\cos^2\gamma}(\rho g + \lambda\tan^2\gamma - \frac{\mu\lambda y}{R}) \tag{5.32}$$

and a complementary solution of:

$$2p(y) = Ce^{-\frac{\mu\cot^2\gamma}{R}y} \tag{5.33}$$

Combining Eqs. (5.32) and (5.33) gives the general solution to Eq. (5.31):

$$2p(y) = \frac{R}{\mu\cos^2\gamma}(\rho g + \lambda\tan^2\gamma - \frac{\mu\lambda y}{R}) + Ce^{-\frac{\mu\cot^2\gamma}{R}y} \tag{5.34}$$

where C is the integration constant, which is determined by substituting the boundary condition $p=0$ at $y=0$ into the above equation:

$$C = -\frac{R}{\mu\cos^2\gamma}(\rho g + \lambda\tan^2\gamma) \tag{5.35}$$

Substitution of Eq.(5.35) into Eq.(5.34) gives:

$$2p(y) = \frac{(\rho g + \lambda\tan^2\gamma)R}{\mu\cos^2\gamma}(1 - e^{-\frac{\mu\cot^2\gamma}{R}y}) - \frac{\lambda y}{\cos^2\gamma} \tag{5.36}$$

The horizontal stress can now be determined by substituting Eqs.(5.36) and (5.19) into Eq. (5.4):

$$\sigma_x = \frac{(\rho g + \lambda \tan^2\gamma)R}{\mu}\left(1 - e^{-\frac{\mu y}{R\tan^2\gamma}}\right) \quad \textbf{(5.37)}$$

From Eqs.(5.2), (5.3) and (5.19), vertical pressure can be calculated as:

$$\sigma_y = (\sigma_x - \lambda y)\tan^2\gamma \quad \textbf{(5.38)}$$

From equation (5.38), the lateral to vertical pressure ratio is determined as:

$$k = \cot^2\gamma + \frac{\lambda y}{\sigma_y} \quad \textbf{(5.39)}$$

Equation (5.39) indicates that for bins with frictional walls, the lateral to vertical stress ratio is not a constant, instead it varies with the depth and stress level. A constant k value exists only if particles are rigid ($\lambda = 0$) or the vertical stress is linearly proportional to depth like in shallow bins where wall friction is ignored. Therefore, k value can no longer be viewed as a material parameter in load predictions of deep bins. It should be noted that Equations (5.37) to (5.39) are reduced to the well-known Janssen's equation if $\lambda = 0$. This means that the Janssen's equation is a special case of the present theory with assumption of a constant pressure ratio (k) or rigid particles (λ=0). Apparently, equation (5.39) cannot be solved directly for the k value, but the k value is not needed when using equations (5.37) and (5.38) to predict lateral and vertical pressures.

5.3 Hygroscopic Loads

Hygroscopic pressures are induced in grain storage bins when grain moisture changes. Several

researchers have reported that hygroscopic pressures may be considerably higher than static pressures (Dale and Robinson 1954; Blight 1986; Britton et al. 1993). Unfortunately, hygroscopic loads have not been included in most design standards and codes because of the lack of information on predictive theories for hygroscopic loads. Only the ASAE EP433 (ASAE 1995) cautions that increases in grain moisture content should be maintained within one or two percent during storage to prevent high hygroscopic loads from occurring.

The difficulty of predicting hygroscopic loads arises from the complex nature of grain en masse and interactions between grain and containing structures. Zhang and Britton (1995) developed a predictive model for hygroscopic loads by assuming that grain bulk moves like a continuum during hygroscopic expansion. But grain en masse is of inherent discontinuous. Therefore, predicting hygroscopic loads should be based on the behaviour of individual grain particles and interactions among particles. In this section, the behaviour of wetted grain is examined from the point of view of microscopic mechanics, and a model is developed for predicting loads induced by increased moisture of grain in bins.

5.3.1 Hygroscopic expansion of grain particles

When a grain particle absorbs moisture, its volume increases. The volumetric strain of swollen grain particles may be estimated from grain moisture changes as follows (Zhang and Britton 1995):

$$\varepsilon_v = \left(\frac{\Delta MC}{1 + MC_0} \right) \left(\frac{\rho_{k0}}{\rho_w} \right) \tag{5.40}$$

where:

ϵ_v = volumetric strain of a wetted particle, m^3/m^3

ΔMC = increase in moisture content, %db

MC_0 = initial grain moisture content, %db

ρ_{k0} = initial particle density, kg/m^3

ρ_w = density of water, kg/m^3

If assuming that particles expand uniformly, the hygroscopic microstrain can be calculated as:

$$\varepsilon_\alpha = \frac{\varepsilon_v}{3} = \frac{1}{3}\left(\frac{\Delta MC}{1 + MC_0}\right)\left(\frac{\rho_{k0}}{\rho_w}\right) \quad \textbf{(5.41)}$$

5.3.2 Hygroscopic pressures

Volumetric increases of individual grain particles cause the grain bulk to expand. If the expansion is not restrained, the grain bulk should not undergo a significant stress increment. If the grain bulk is restrained, a hygroscopic pressure will be induced as a result of the restriction of grain expansion. In other words, there would be no hygroscopic pressures induced if the grain is allowed to expand freely (like in a completely flexible container), and hygroscopic pressures would reach the maximum (for a certain moisture change) if the grain is stored in rigid containers.

To determine the maximum hygroscopic pressure (in a rigid container), the moisture-induced expansion may be viewed in analogue to thermal expansion between two bodies of exactly the same shape, one subject to heating and the other one not. Following the theorem of Duhamel-Neumann analogy in thermoplasticity (Fung 1965), the hygroscopic pressures of swelling grain bulk confined in a perfectly rigid container are calculated as:

$$L = \sigma_x = L_0 + (p_1 + p_2)\cos^2\gamma + p_3 \quad \textbf{(5.42)}$$

$$V = \sigma_y = V_0 + (p_1 + p_2)\sin^2\gamma \quad \textbf{(5.43)}$$

where:

L = lateral pressure (during wetting), kPa

V = vertical pressure (during wetting), kPa

L_0 = initial lateral pressure (before wetting), kPa

V_0 = initial vertical pressure (before wetting), kPa

The L_0 and V_0 are static pressures, and the p_1, p_2 and p_3 are the moisture-induced microstresses, which may be calculated by a modified Eq. (5.5): $p_\alpha = E'\varepsilon_\alpha$, where E′ is the modulus of elasticity for wetting grain in rigid containers. Equations (5.42) and (5.43) predict hygroscopic pressures in perfect rigid containers. However, grain storage bins are usually not perfectly rigid. Bin walls and floors deform and grain is free to move at the bin top when grain expands. Zhang and Britton (1995) indicated that structural deformations are negligible comparing with the upward movement of grain. In the process of wetting, hygroscopic stresses initially reduce the static frictional force (F_0) between the bin wall and grain, further wetting reverses the direction of frictional force, and grain starts moving upward until the frictional force reaches its maximum value. Before grain starts to move upwards, the bin could be treated as in a rigid container if wall and floor deflections are ignored. When upward movement occurs, the microstresses p_1 and p_2 should be calculated from the vertical force equilibrium of grain at a given depth (y). Vertical force equilibrium conditions, before wetting

and after wetting, may be approximated as follows:

$$V_0 = \rho g y - \frac{F_0}{R} \tag{5.44}$$

$$V = \rho g y + \frac{F}{R} \tag{5.45}$$

where:

ρ = bulk density, kg/m^3

g = gravitational acceleration constant, m/s^2

y = depth of grain, m

F_0 = initial (static) frictional force, kN/m

F = frictional force during wetting, kN/m

R = hydraulic radius of bin, m

Combining Eqs. (5.43) - (5.45) gives:

$$p_1 + p_2 = \frac{F_0 + F}{R \sin^2 \gamma} \tag{5.46}$$

Since ε_3 is restricted by the bin wall, microstress may still be calculated as $p_3 = E' \varepsilon_3$. However, wetted grain may become softer, therefore, the modulus of elasticity during wetting should be modified when calculating p_3.

$$p_3 = (fE')\frac{\varepsilon_v}{3} \tag{5.47}$$

where:

E′ = modulus of elasticity for wetted grain, kPa

f = moisture reduction factor due to softening of wetted grain

To estimate the modulus of elasticity E′ for wetting grain in equation (5.47), an empirical correlation proposed by Smith and Lohnes (1983) for bulk moduli for maize (shelled corn), wheat, barley and oats is used:

$$K_t = \left[\frac{\sigma_h}{K_i \varepsilon_{v,ult}} + 1\right]^2 K_i \tag{5.48}$$

where:

K_t = tangent bulk modulus, kPa

σ_h = hydrostatic stress, kPa

$\epsilon_{v,ult}$ = asymptotic value of volumetric strain, m^3/m^3

K_i = initial bulk modulus, kPa

Because the granular medium is approximated as being isotropic and homogenous, E′ may be determined from Eq.(5.48) as:

$$E' = 3(1-2\nu)K_t = 3(1-2\nu)\left[\frac{\sigma_h}{K_i \varepsilon_{v,ult}} + 1\right]^2 K_i \tag{5.49}$$

where:

ν = Poisson's ratio of wetting grain.

Equation (5.49) is used to evaluate the initial tangent modulus for wetting grain. During wetting, the modulus may fluctuate due to stress change and grain softening. So, the moisture reduction factor f may be defined as the ratio of initial modulus to that of wetted grain in a rigid container. Physically, the modified modulus (fE′) represents a segment modulus for wetting grain. It should be noted that the modulus of elasticity (E) in Eq.(5.5) represents the modulus of an idealised granular medium (Fig. 5.1) subject to static loading, and that the modulus of elasticity (E′) in Eq.(5.49) represents the modulus of a deformed granular medium subject to hygroscopic loading.

5.4 Discharge Loads

5.4.1 Patterns of shear deformation

The mechanism of shear deformation of granular media may be best illustrated by the simple (direct) shear test (Fig.5.5). When a sample is sheared horizontally, a macroscopic shear plane (SS-plane) develops. The actual motion of particles, however, occurs along a wavy S'S' plane because of the discontinuity of granular materials. This wavy plane is termed the slip plane (Nemat-Nasser, 1980). The slip plane divides the sample into two portions, namely an upper portion and a lower portion. Each portion behaves like a rigid block at a given instance (Horne 1964, Nemat-Nasser 1980). Therefore, the shear deformation is explained as sliding between the two serrated faces of rigid blocks (Fig.5.5) (Rowe 1962). When shearing occurs horizontally, upper block moves upwards, and thus dilation takes place vertically.

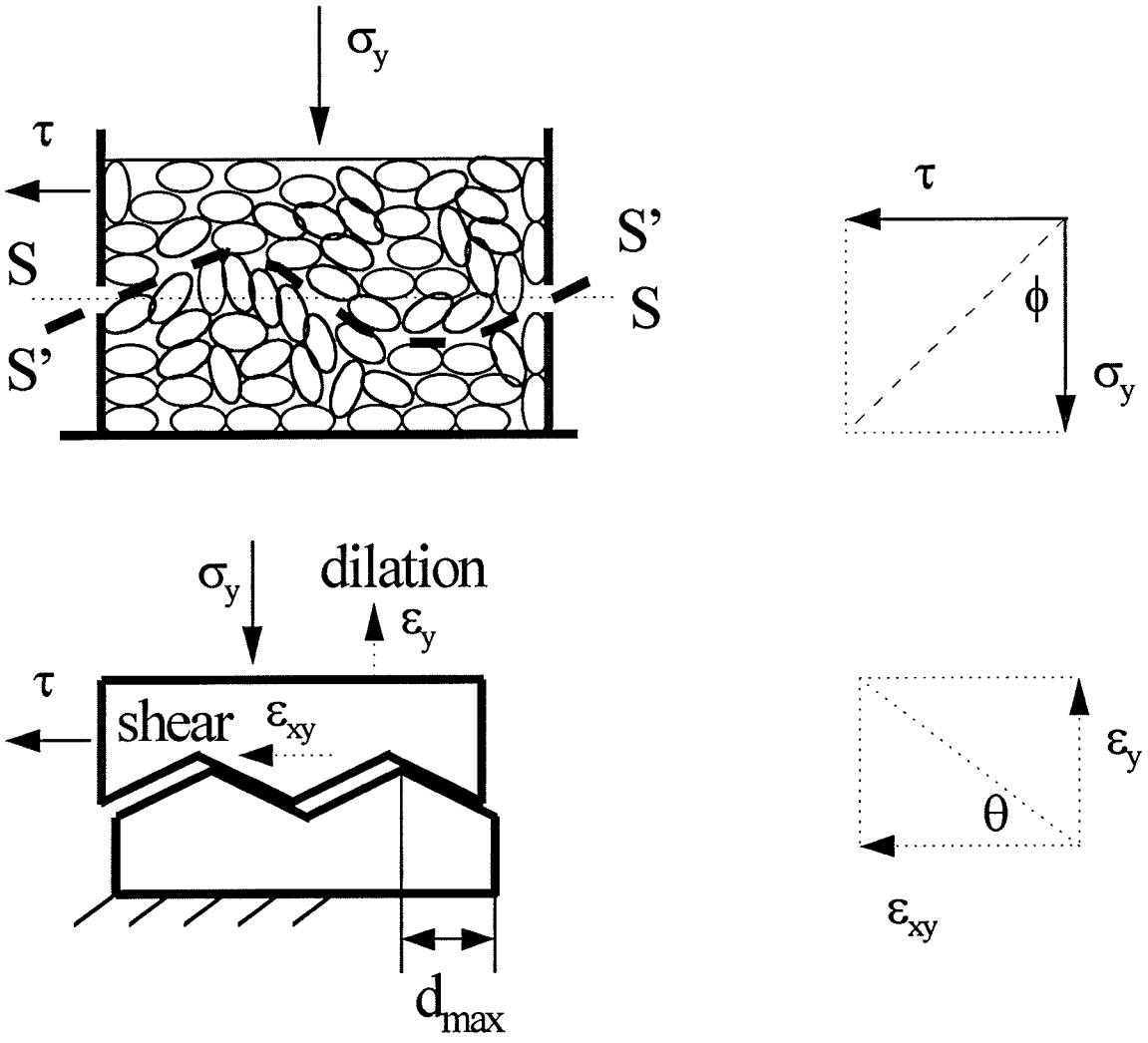

Figure 5.5 Simple shear test and shear-induced dilation mechanism.

Dilatancy Angle

Dilatancy angle θ is often used to characterize the dilation mechanism (Fig.5.5). This angle is related to friction angles of granular materials as follows (Rowe 1962, Nemat-Nasser 1980, Moroto 1987):

$$\theta = \phi - \phi_\mu \qquad \textbf{(5.50)}$$

where:

θ = dilatancy angle

ϕ = macroscopic (overall) angle of internal friction

ϕ_μ = microscopic (true) angle of friction

It should be noted that the shear stress is related to normal stress by the angle of internal friction, and volumetric expansion strain is related to the shear strain by the dilatancy angle. For example, in simple shear test (Fig.5.5), $\tau_{xy} = (\sigma_y \tan\phi)$, and $\varepsilon_y = (\varepsilon_{xy} \tan\theta)$. Under biaxial loading condition, the slip plane is represented by a shear band with an inclination angle of minimum value of $(45^\circ+\theta/2)$ with respect to the minor principal stress (Han and Drescher 1993) or $(45^\circ-\theta/2)$ with respect to the major principal strain increment (Bard 1990). Dilatancy angle θ can be calculated from the rate of plastic volume strain ($\dot{\varepsilon}_v^p$) and the rate of plastic shear strain ($\dot{\varepsilon}_s^p$) (Ord et al. 1991):

$$\sin(\theta) = -\frac{\dot{\varepsilon}_v^p}{\dot{\varepsilon}_s^p} \qquad \textbf{(5.51)}$$

The above equation indicates that the dilatancy angle is not a constant but a function of the deformation process.

5.4.2 Discharge loads

Similar to the hygroscopic loads, discharge loads may be calculated as:

$$L = \sigma_x = L_0 + (p_1 + p_2)\cos^2\gamma + p_3 \tag{5.52}$$

$$V = \sigma_y = V_0 + (p_1 + p_2)\sin^2\gamma \tag{5.53}$$

where:

L = lateral pressure (during discharging), kPa

V = vertical pressure (during discharging), kPa

L_0 = static lateral pressure, kPa

V_0 = static vertical pressure, kPa

The microstresses p_1, p_2 and p_3 are now representing the shear-induced stresses. These stresses are unlikely to be obtained exactly because of the complexity of the discharging problem. An approximation may be obtained from the analysis of the shearing.

For a layer of grain to slide over another layer of grain, internal friction must be overcome. At the onset of discharge, internal shearing is initiated. Fast-moving grains overcome the friction on slow moving (or dead) grains, in other words, a frictional load is applied to the slow-moving grains which interact with the structure. Shear-induced vertical stress (the second term on the right side of Eq. 5.53) is approximated by this frictional load, which is estimated as (L $\tan\phi$) by using Coulomb's criterion:

$$p_1 + p_2)\sin^2\gamma = L\tan\phi \tag{5.54}$$

i.e.,

$$p_1 + p_2 = \frac{L\tan\phi}{\sin^2\gamma} \tag{5.55}$$

The vertical shearing causes a horizontal expansion of the grain en masse. This expansion is restricted by the bin wall and an additional lateral load (p_3) is induced. It seems reasonable to assume that the maximum expansion corresponds the maximum lateral pressure. By the relationship of dilatancy, the maximum lateral expansion displacement may be approximated as ($d_{max}\tan\theta_{max}$), where d_{max} is the maximum length of dilatancy shear (Fig.5.5). Since the horizontal expansion is restricted by the bin wall, the lateral expansion per unit diameter gives an average microstrain ε_3:

$$\varepsilon_3 = \frac{d_{max}\tan\theta_{max}}{2r} \tag{5.56}$$

where:

r = radius of the bin, m

d_{max} = maximum length of dilatancy shear

θ_{max} = maximum dilatancy angle

By assuming that $p_3 = E'\varepsilon_3$ and using Eqs (5.55), (5.56), and (5.49), the maximum lateral pressure is obtained by solving Eq.(5.52):

$$L = \frac{1}{1 - \tan\phi \cot^2\gamma}\left(L_0 + 3(1-2\nu)\frac{d_{max}\tan\theta_{max}}{2r}\left(\frac{\sigma_h}{K_l\varepsilon_{v,ult}}+1\right)^2 K_i \right) \quad \textbf{(5.57)}$$

By definition, the overpressure factor may be calculated as:

$$f_d = \frac{L}{L_0} = \frac{1}{1 - \tan\phi \cot^2\gamma}\left(1 + 3(1-2\nu)\frac{d_{max}\tan\theta_{max}}{2r}\left(\frac{\sigma_h}{K_l\varepsilon_{v,ult}}+1\right)^2 \frac{K_i}{L_0} \right) \quad \textbf{(5.58)}$$

If no dilatancy ($\theta_{max} = 0$), equation (5.58) is reduced to:

$$f_d = \frac{1}{1 - \tan\phi \cot^2\gamma} \quad \textbf{(5.59)}$$

Equation (5.59) implies that overpressure factor is a function of structural angle and internal frictional angle of the granular medium even if neglecting the dilatancy effects. If further no internal friction (ϕ=0), equation (5.59) gives that $f_d = 1$. Therefore, the overpressure may be attributed to the internal friction and dilatancy of the granular medium.

5.5 Model Validation

5.5.1 Static Loads

Model predictions are compared with experimental data reported by (1) Dale and Robinson (1954) for shelled maize in a smooth walled model bin, (2) Thompson et al. (1995) for maize in a full-

size corrugated bin, and (3) Zhang et al. (1987) for wheat in a smooth walled model bin. There is a large volume of data in the literature on loads in bulk solids storage structures. These three were selected as being representative of agricultural products. Dale and Robinson (1954) conducted five tests, loads (vertical, lateral, and friction) were only reported for Tests 2 and 3, which are used in the following comparisons. Model predictions are also compered with the Janssen theory for the model bin of Dale and Robinson (1954). Three values (0.4, 0.5 and 0.7) of the lateral to vertical stress ratio are selected to cover the range of k values recommended by design codes and standards for agricultural materials (e.g., DIN 1987). Bin dimensions and material property parameters used in model predictions are summarized in Table 5.1. It is assumed that the maize has a Poisson's ratio of 0.40 (ASAE 1995) and the coefficient of friction 0.34 (Mohsenin 1986) for smooth steel of Dale and Robinson's model bin. Applying the Janssen equation to data reported by Thompson et al. (1995), the coefficient of friction was estimated to be 0.55 for the full-size corrugated bin of Thompson et al. (1995). Parameters for Zhang et al.'s wheat bin are taken from their paper (Zhang et al. 1987).

Lateral and vertical stresses are predicted by Eqs. (5.37) and (5.38), respectively, and the resultant friction force on the bin wall is calculated from Eq. (3.6). Predicted bin loads are in close agreement with the experimental data for all three cases (Tables 5.2 and 5.3). It is noted that differences between the model predictions and Janssen's theory are dependent on the k value selected. Janssen's equation predicts too high vertical pressures if a lower k value is used, and too low vertical pressures if a high k value is used (Table 5.2).

Table 5.1 Parameters used in microscopic theoretical predictions

Parameters	Model bin of maize*	Model bin of wheat✪	Full-size bin of maize†
Bin height, y_{max}	1.524 m	1.2 m	14 m
Bin radius, r	0.2286 m	0.45 m	5.5 m
Hydraulic radius, R	0.1143 m	0.225 m	2.75 m
Bulk density, ρ	780 kg/m^3	817 kg/m^3	718 kg/m^3
Friction coefficient, μ	0.34	0.19	0.55
Poisson's ratio	0.4	0.29	0.4

*: Data from Dale and Robinson (1954)

✪: Data from Zhang et al. (1987)

†: Data from Thompson et al. (1995)

Table 5.2 Comparisons of theoretical predictions with test data for a model bin (Dale and Robinson 1954)

Loads	Predicted	Data†	Janssen's		
			k=0.4	k=0.5	k=0.7
Lateral (kPa)	2.70	2.86 ±0.73	2.15	2.30	2.46
Vertical (kPa)	4.02	3.93 ±0.06	5.38	4.61	3.52
Friction (kN/m)	0.87	0.88±0.01	0.72	0.80	0.93

† average of data from tests: #2 and #3 reported by Dale and Robinson (1954).

Table 5.3 Comparisons of theoretical predictions of lateral pressure (kPa) with test data for a full-size bin of maize (Thompson et al. 1995) and a model bin of wheat (Zhang et al. 1987)

Full-size bin of maize			Model bin of wheat		
Depth (m)	Predicted	Data	Depth (m)	Predicted	Mean data
3.1	8.9	10.2±1.8	1.08	2.95	2.91
6.1	15.9	17.1±2.1	0.825	2.33	2.59
9.1	21.9	24.1±3.1	0.57	1.67	1.67
11.9	26.0	26.9±4.0			

5.5.2 Hygroscopic Loads

To validate the proposed model, predicted hygroscopic pressures are compared with experimental results reported by Dale and Robinson (1954). Only the data from their Test No.'s 2 and 4 are used in the following comparisons because the exact grain moisture changes were reported for these two tests. In Test No.2, Dale and Robinson observed an increase in lateral pressure from 2.1 to 13.5 kPa and an increase in vertical pressure from 3.98 to 15.2 kPa at the bin bottom, while the grain moisture changed from 13.0% to 16.9%wb. These represent an overpressure of 11.4 kPa and 11.2 kPa in the lateral and vertical directions, respectively, for a moisture increase of 4%wb. In Test No.4, ten minutes of flooding was applied to the grain bulk, and the maximum lateral pressure of 21.93 kPa and vertical pressure of 20.34 kPa were observed in approximately two hours with the change of moisture content about 10%(wb) from 12.5% to 22.4%.

Material parameters reported by Smith and Lohnes (1983) for maize (shelled corn) (Table 5.4) are used in equation (5.49) to calculate the modulus of elasticity E′. For a small increment of moisture content, the moisture factor is taken a value of 1 due to the limitation of available data. The moisture factor is estimated to be 0.75 from maize data reported by Blight (1986) for flooding situation. Static pressures L_0 and V_0 are taken from the test data of Dale and Robinson (1954). The hydrostatic stress in equation (5.49) is replaced by the average of static vertical and lateral pressures $((2L_0+V_0)/3)$ for a cylindrical bin. Since the resultant friction force during wetting was not recorded in the test and no equation can be found to predict it, it is assumed that the friction is the same as static condition, i.e., $F=F_0$, where F_0 was also taken from the test data of Dale and Robinson (1954). Other model parameters are listed in Table 5.5.

An overpressure of 10.9 kPa is predicted both laterally and vertically for an increase of 4%wb

Table 5.4 Measured initial bulk moduli and asymptotic volumetric strains for maize (shelled corn) at 15% moisture content, and for wheat at 10.3% moisture content (Smith and Lohnes 1983).

	Maize	Wheat
Bulk Density ρ, kg/m^3	771	779
Initial Modulus K_i, kPa	591.3	645
Asymptotic Strain $\epsilon_{v,ult}$, x10^{-3}	41.03	73.12

Table 5.5 Material property parameters used in model predictions

Initial Particle Density (ρ_{k0}), kg/m^3	1400
Initial Bulk Density (ρ), kg/m^3	774*
Initial Moisture Content (MC_0), %db	13
Poisson's Ratio (ν)	0.4

* reported by Dale and Robinson (1954)

in grain moisture, which gives a hygroscopic lateral pressure of 13.0 kPa and vertical pressure of 14.9 kPa. The relative differences between predictions and data in Test No.2 are 3.7% and 2.1% for lateral and vertical pressures, respectively. For the flood situation in Test No.4, the initial static pressures were not reported, and it was assumed to be the same as in Test No.2. The predicted vertical pressure was 19.38 kPa and lateral pressure 20.9 kPa at the bin bottom for a moisture increase of 10%. The relative differences between predicted hygroscopic pressures and data in Test No.4 are 4.7% for both lateral and vertical pressures.

Table 5.6 Comparison of predicted hygroscopic pressures with measured data.

Hygroscopic pressure	Moisture content increment	Predicted (kPa)	Measured (kPa)	%Difference
Lateral	4.0%	13.0	13.5	3.7%
Vertical	4.0%	14.9	15.2	2.1%
Lateral	10.0%	20.9	21.9	4.7%
Vertical	10.0%	19.4	20.3	4.7%

5.5.3 Discharge Loads

To validate the model of discharge loads, the overpressure factor predicted by Eq. (5.58) is compared with experimental data reported by Zhang et al. (1993) for wheat in a smooth and a

corrugated-walled model bin. Table 5.7 lists the reported bin dimensions, wheat properties and discharge operations. Table 5.8 collects reported ranges of dilatancy angles for some granular materials in the literature. The maximum dilatancy angle was reported as 19.3 degrees for wheat (Zhang et al. 1994). There is no theory available to calculate the maximum length of dilatancy shear. The d_{max} is estimated as the shear rate times the peak time of lateral pressure from the discharge operation (Table 5.7). The shear rate may be estimated from the discharge rate and the height of the measurement. When the orifice is opened, the mass loss of support starts moving downward whereas those supported by the bin bottom forms a dead zone with an inclined angle of $(\pi/4+\theta/2)$ with respect to the bottom. It should be noted that this angle (during discharge) is different from the angle of repose which is measured from the materials left in the bin after discharge. At the height of 0.38m, the radius of the central moving zone is calculated as the sum of orifice radius (0.03) and (0.38 $\cot(\pi/4+\theta/2)$), i.e., 0.3 m. Therefore, the discharge rate divided by the moving area gives an approximated shear (flow) rate, which is calculated as $(4.79 m^3/3600s)/(\pi\ 0.3^2\ m^2) = 0.0047$ m/s. The parameters used to calculate the discharge expansion modulus are taken from the test data reported for wheat by Smith and Lohnes (1983) (Table 5.4). The hydrostatic stress is taken as the average of static vertical and lateral pressures $((2L_0+V_0)/3)$ for a cylindrical bin. By using Eq. (5.58) with these parameters, the overpressure factor was estimated as 1.55 for the smooth wall and 1.44 for the corrugated wall (Table 5.9). From Eq. (5.59) if no dilatancy, the overpressure factor was calculated as 1.19 for the effect of internal friction only, therefore, the dilatancy contribution may be estimated as 1.36 for the smooth wall and 1.25 for the corrugated wall. The relative differences between predicted and measured overpressure factors were less than 1% (Table 5.9).

Table 5.7. Bin dimensions, physical properties of wheat, and discharge operations

Bin dimensions:	Bin height, y_{max}	1.5 m
	Bin diameter, 2r	1.0 m
	Orifice diameter	0.06 m
	Measuring height	0.38 m
Wheat properties:	Bulk density, ρ	779 kg/m^3
	Poisson's ratio	0.29
	Angle of internal friction	25.6^0
	Moisture content	11.3 %
Discharge operation:	Discharge rate	4.79 m^3/h
	Time of peak lateral pressure	0.6 s (smooth wall)
		0.4 s (corrugated wall)

Table 5.8 Summary of reported dilatancy angles.

materials	ranges (degree)	source
gravel	0 to 12	Jacobsen (1990)
sand	3.5 to 18.7	Vardoulakis (1980)
coarse sand	-9 to 19	Han & Drescher (1993)
sandstone	-19.3 to 27	Ord et al. (1991)
soil	-10 to 30	Bardet (1990)
wheat	0.7 to 19.3	Zhang et al. (1994)

Table 5.9 Comparison of predicted discharge overpressure factor with measured data.

Overpressure factor	Predicted	Measured	%Difference
Smooth wall	1.55	1.56	0.6%
Corrugated wall	1.44	1.45	0.7%

6. ENDOCHRONIC CONSTITUTIVE EQUATIONS

A systematic modelling of macroscopic stress-strain behaviour of granular media is necessary to develop finite element models for predicting bin loads. Two mechanical models, namely creep-type and relaxation-type, are constructed for developing a stress-based constitutive model and a strain-based model, respectively. In the creep-type model, strain responses are predicted from applied stresses, therefore, the theory is called stress-based theory. In the relaxation-type model, stress responses are predicted from applied strains, and the theory is called strain-based theory.

6.1 Mechanical Models for Grain En Masse

Grain en masse is elastoplastic, therefore, the macroscopic constitutive behaviour of grain en masse can be modelled by using different connections of spring-elements (elastic) and slip-elements (plastic), with springs storing energy whereas slip-elements dissipating energy. Traditionally, slip-elements are symbolically represented by the two parallel bars for frictional slips, where shear and volumetric deformations are not coupled. To account for the shear-volumetric coupling, the traditional slip-elements are modified to slip-dilatancy elements represented by two curved parallel bars. The physical basis of slip-dilatancy elements are shown in Fig. 5.5. With these mechanical elements, mechanical models of relaxation-type and creep-type are constructed for modelling the stress responses under deformation and strain responses under loads, respectively.

6.1.1 Relaxation-type model

A relaxation-type mechanical model consists of many spring-slip units connected in parallel. In each spring-slip unit, a spring element and a slip-dilatancy element are connected in series. Figure 6.1 shows such a relaxation model for describing deviatoric (shear) behaviour of materials. When the material is subject to a plastic deviatoric strain e_{ij}^{p}, each and every unit experiences the same strain, but the total stress is the summation of the stress spectrum of each spring-slip unit.

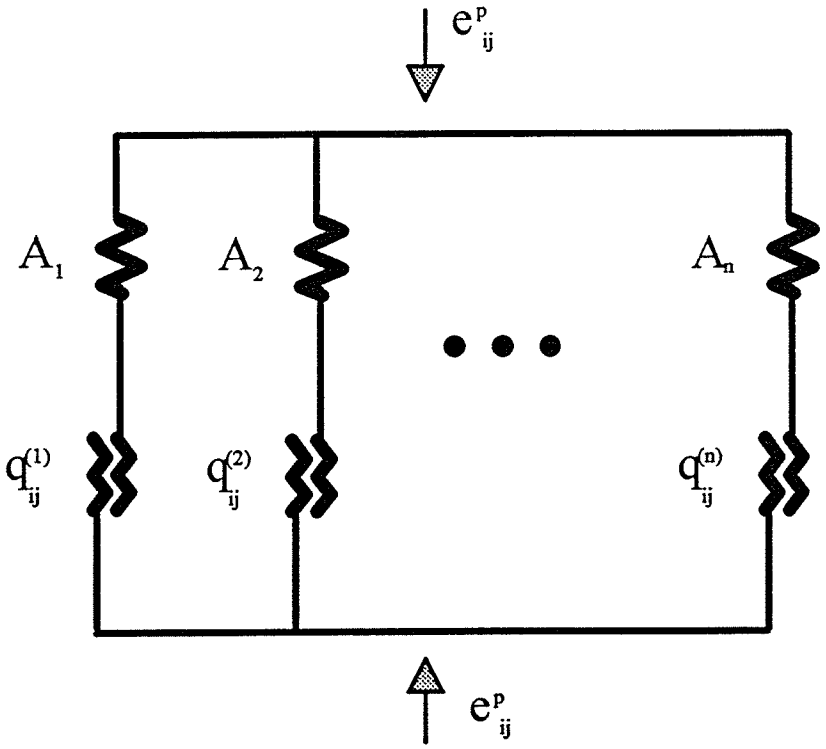

Figure 6.1 Relaxation mechanical model for shear response.

To illustrate the process of modelling the material responses using relaxation-type models, models with three spring-slip units are considered for one dimensional shear conditions (Figs.6.2). To simplify the discussion, no shear-induced volumetric deformations are considered. Therefore, slip-dilatancy elements are approximated as slip (frictional sliding) elements. To further simplify calculations, it is assumed that all the springs have the same stiffness as k_1, but each slider has a different friction limit, such that: P1<P2<P3. For describing force responses to applied plastic deformations (U^P), spring constant vanishes in one of the units. At the onset of applying U^P, the force response increases instantly until P = P1 when Slider 1 is triggered to slide. This means that the initial tangent stiffness is infinitive (Figs.6.2). The sliding of Slider 1 indicates an initial material yield, then, U^P is directly applied to Springs 1 and 2. Therefore, the tangent stiffness changes from infinity to $2k_1$. Further deformations cause the force response ($P= P1+ 2k_1U^P$)

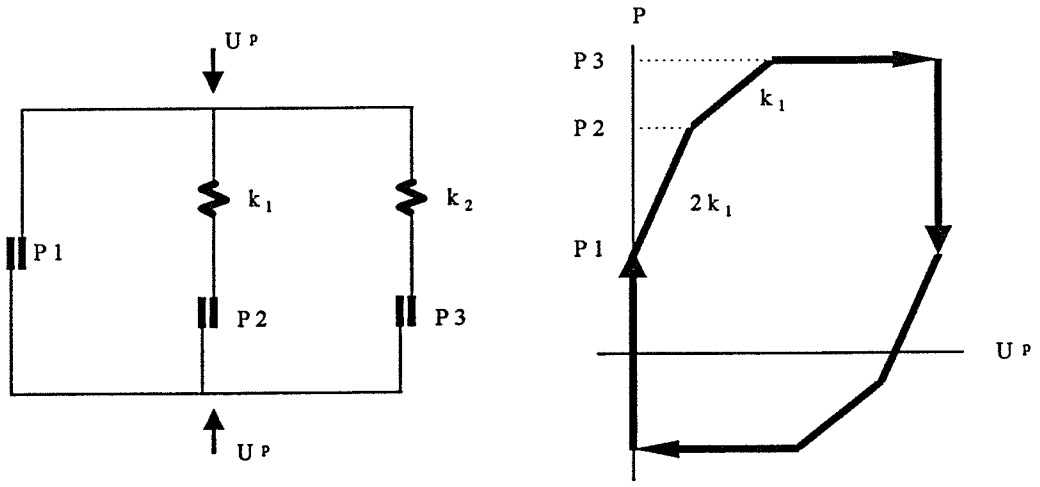

Figure 6.2 Illustration of responses of relaxation model in one-dimensional shear.

reaching P2, Slider 2 is triggered to slide. Now, the additional force can only be taken by Spring 2 and the tangent stiffness is further reduced to k_1, and $P= P1+k_1U^p$. When the increments of U^p makes P reach P3, no more forces can be taken by the materials and the plastic deformation U^p may reach infinity, i.e., the material fails. The unloading is a mirror process of loading.

A similar relaxation model can be constructed for volumetric response (Fig. 6.3). Rectangular boxes represent volumetric endochronic elements, in which volumetric slip-elements are coupled with the shear slip-dilatancy elements (Fig.6.3) for shear-induced volumetric

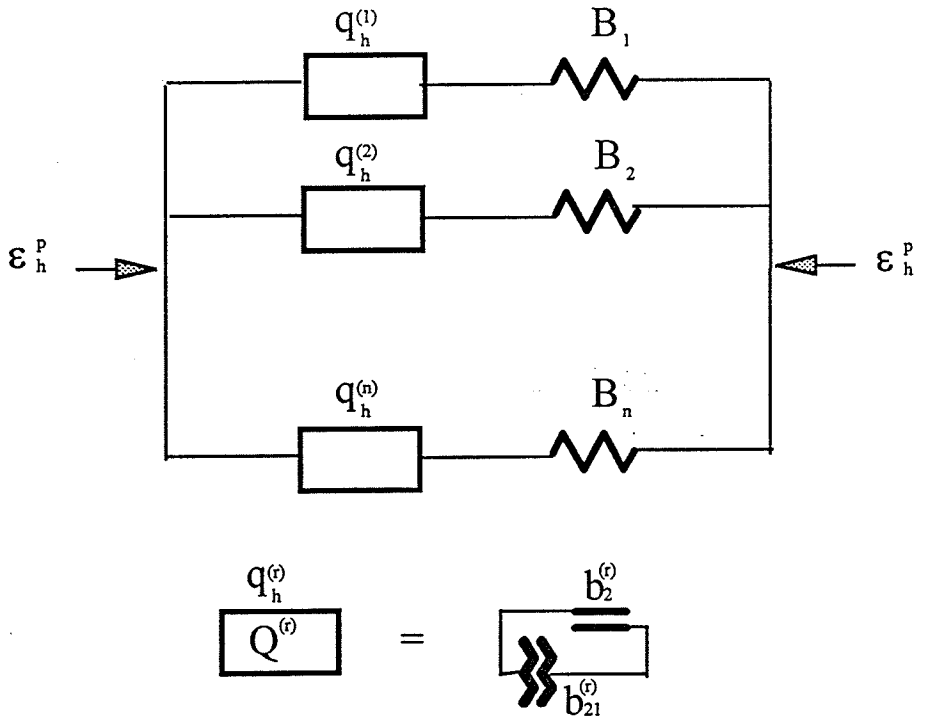

Figure 6.3 Relaxation mechanical model of volumetric response.

deformations. When the material is subject to a plastic volumetric strains ε_h^p, each and every unit experiences the same strain, and the total hydrostatic stress is the summation of the stress spectrum of each spring-slip unit.

Figure 6.4 shows the mechanism of the relaxation-type model, in which deviatoric response and volumetric response are combined together with the vertical direction for the deviatoric behaviour (solid line) and horizontal direction for the volumetric behaviour (thin solid line).

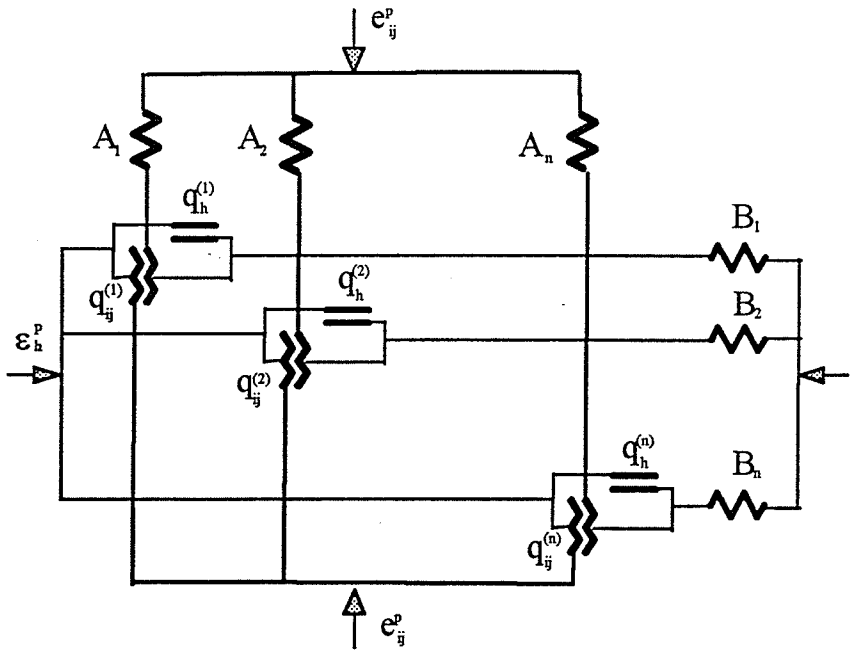

Figure 6.4 Mechanism of relaxation-type model for strain-based endochronic theory.

6.1.2 Creep-type Model

A creep-type mechanical model consists of many spring-slip units connected in series. In each spring-slip unit, a spring element is connected with a slip element in parallel. Figure 6.5 illustrates a creep model for describing deviatoric (shear) strain responses of materials to an applied shear stress S_{ij}. When applying a deviatoric stress S_{ij} to the material, the stress is applied to each and every unit, and the strain responses are the summations of the strains from all parallel-connected spring-slip units.

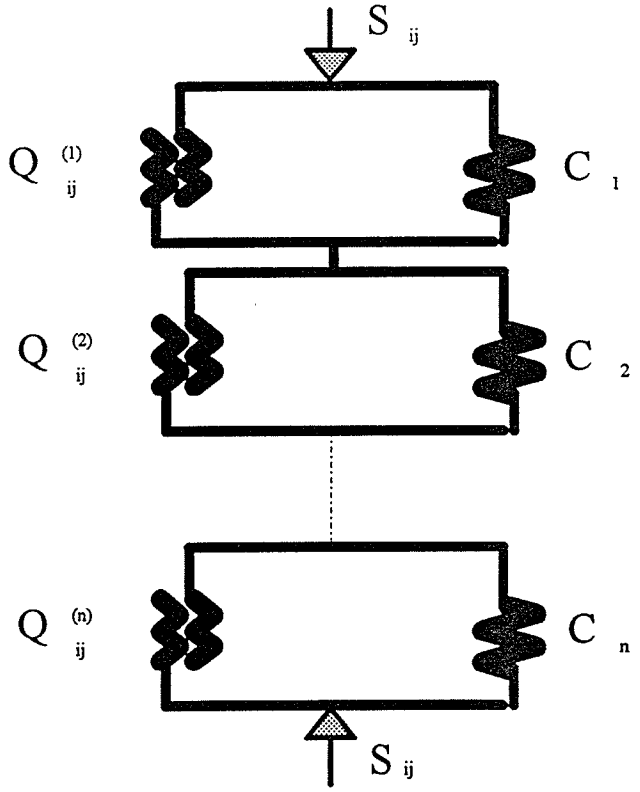

Figure 6.5 Creep mechanical model for shear response.

To illustrate the process of modelling the material responses using creep-type models, models with three spring-slip units are considered for one dimensional shear conditions (Figs.6.6). To simplify the discussion as for creep-type models, slip-dilatancy elements are approximated as slip (frictional sliding) elements, and all the springs are assumed to have the same stiffness as k_1. Consider each slider having a different friction limit, such that: P1<P2<P3. For describing the flow properties of materials (failure), spring constant vanishes in one of the units. When the applied force P is smaller than P1, Slider 1 is the controlling element, and the initial tangent stiffness is infinitive (Figs.6.6). When P is increased to P1 (an initial material yield point), Slider 1 starts to slide (yield surface expansion) and Spring 1 deforms and the tangent stiffness decreases from infinity to k_1. When P reaches P2, Slider 2 is triggered to slide, both Spring 1 and Spring 2 deform and the tangent stiffness is further reduced to $k_1/2$. When P=P3, plastic deformation U^p increases to infinity, i.e., the material fails. The unloading is a mirror process of loading.

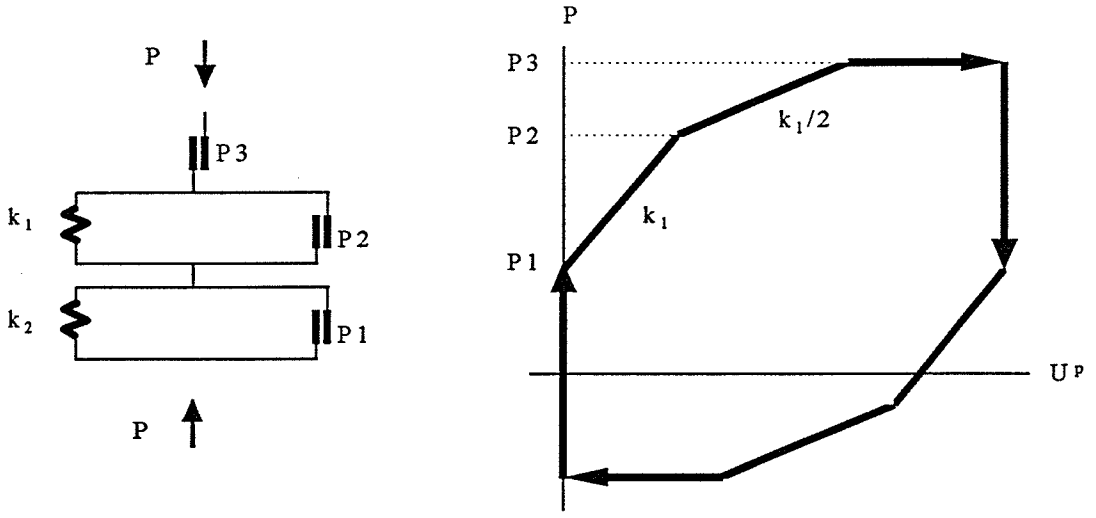

Figure 6.6 Illustration of responses of creep model in one-dimensional shear.

A similar creep model can be constructed to characterized the volumetric behaviour of materials (Fig.6.7), in which shear slip-dilatancy elements are also contributed to volumetric behaviours. When the material is subject to a hydrostatic stress σ_h, each and every unit experiences the same stress, and plastic volumetric strains ε_h^p is the summation of the strain spectrum of each spring-slip unit.

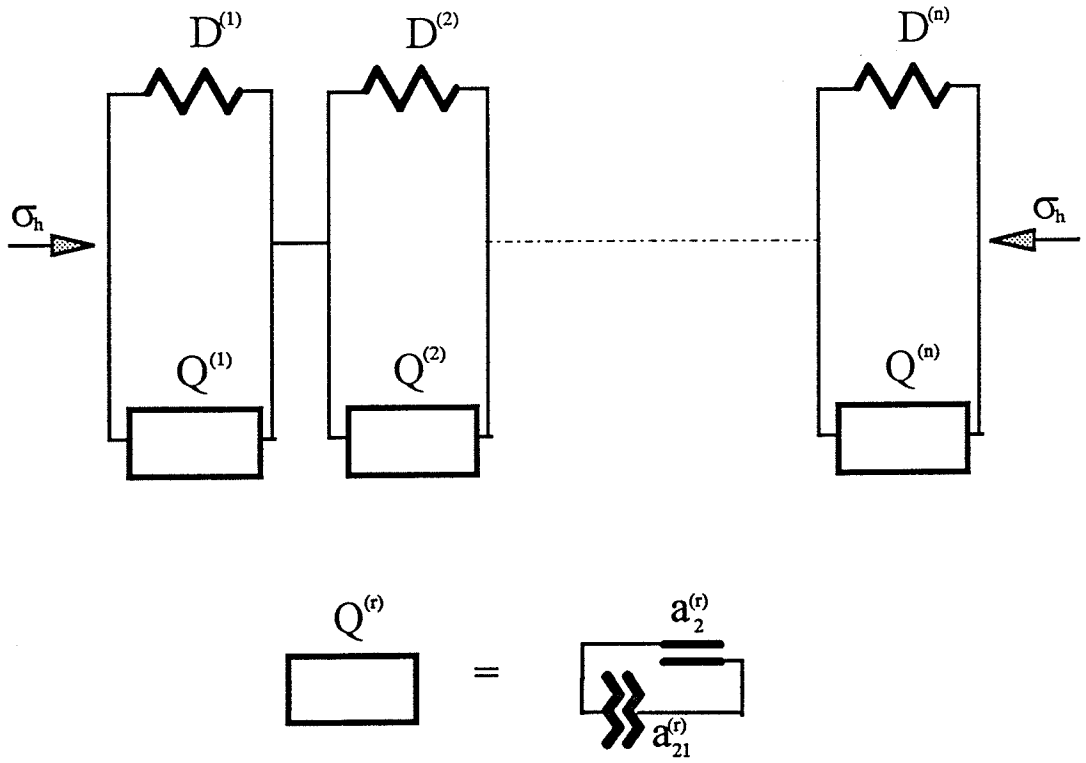

Figure 6.7 Creep mechanical model of volumetric response.

Figure 6.8 shows the mechanism of creep-type model, a combination of deviatoric (shear) and volumetric responses with the vertical direction for the deviatoric behaviour (solid line) and horizontal direction for the volumetric behaviour (thin solid line).

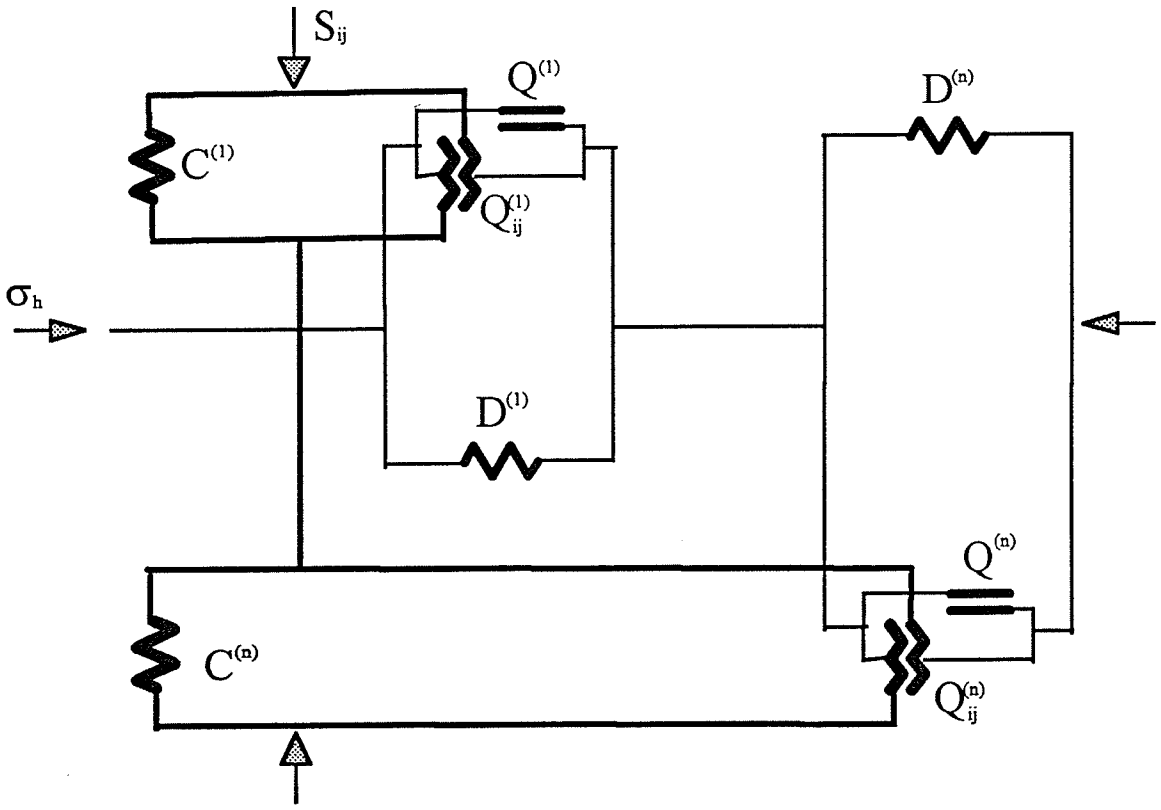

Figure 6.8 Mechanism of creep-type model for stress-based endochronic theory.

6.1.3 Mixed-type models

The previous two sections indicate that either creep-type model or relaxation-type model may be selected for describing the deviatoric behaviour or volumetric behaviour, respectively. A cross-selection of a relaxation-type model and a creep-type model, for shear and volumetric behaviours, gives alternative ways of modelling the constitutive behaviour of materials. These models are of the mixed-type of creep-type and relaxation-type models.

Figure 6.9 shows the first mixed-type model, in which shear response is of creep-type (in vertical direction) and volumetric response is of relaxation-type (in horizontal direction).

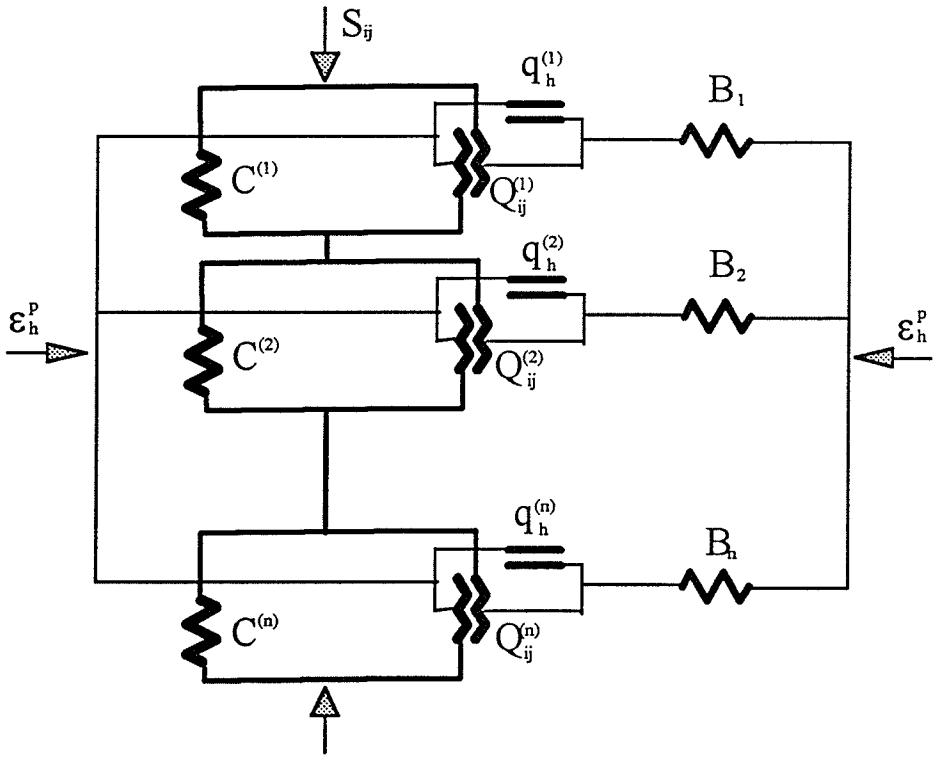

Figure 6.9 First mixed-type mechanical model.

Figure 6.10 shows the second mixed-type model, in which volumetric response is of creep-type and shear response is of relaxation-type.

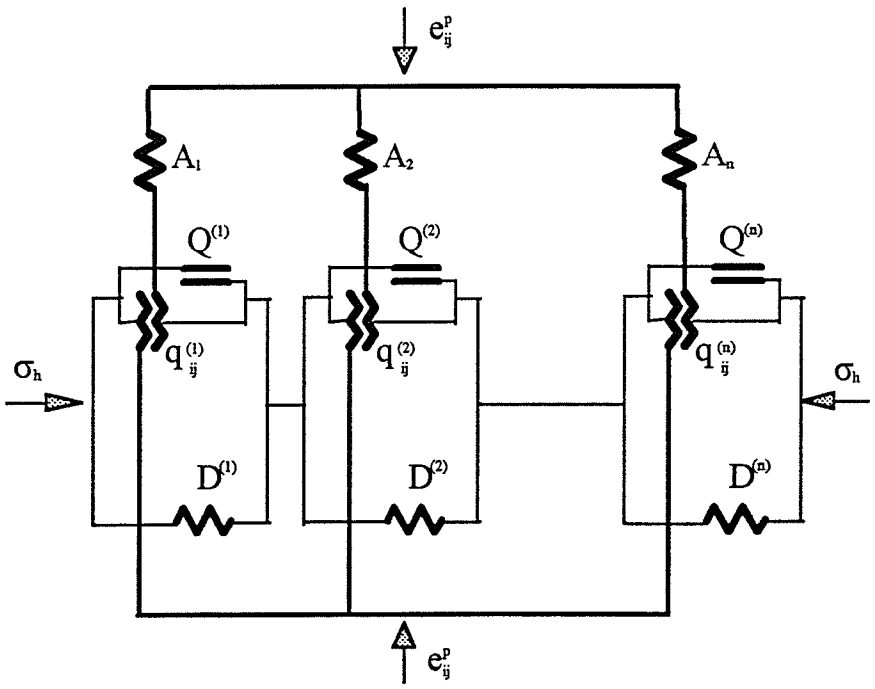

Figure 6.10 Second mixed-type mechanical model.

6.2 Formulation of Stress-based Constitutive Model

The stress-based model may be formulated by either the classical approach or energy approach. Classical approach uses the force equilibrium equations and geometry relationship, whereas the energy approach uses the principle of irreversible thermodynamics.

6.2.1 Classical Approach

We first consider a one-dimensional situation. Figure 4.2 implies that the slope of the stress-strain curve at large deformation may be zero in some situations. To capture this failure behaviour in Fig. 6.5, the spring element in the unit where maximum internal stress develops is vanished. Figure 6.11 shows such a modified creep-type model for describing the deviatoric behaviour of the material subject to a uniaxial load. The stresses and strains in frictional elements are treated as internal variables. Internal deviatoric stresses are denoted as $Q^{(0)}$, $Q^{(1)}$, $Q^{(2)}$, ..., $Q^{(n)}$, and internal plastic deviatoric strains as $q^{(0)}$, $q^{(1)}$, $q^{(2)}$, ... $q^{(n)}$, where $Q^{(0)}$ represents the maximum internal stress and the other internal stresses are arranged in sequence by their magnitude. The spring constants, which are model parameters, are assumed to be $k^{(1)}$, $k^{(2)}$, ... $k^{(n)}$ for the corresponding spring elements. When the material is loaded by a deviatoric stress S, the stress equilibrium for a typical unit is:

$$S = Q^{(r)} + k^{(r)} q^{(r)} \tag{6.1}$$

The superscription (r) represents the r-th unit (r=0,1, ..., n.). In endochronic theory, the internal stresses $Q^{(r)}$ are assumed to be proportional to the rate of internal strains as $q^{(r)}$ with respect to intrinsic time (Valanis 1981). Therefore, the constitutive equations for the *r*-th frictional element

are:

$$Q^{(r)} = a_1^{(r)} \frac{dq^{(r)}}{dz_d} \tag{6.2}$$

where:

$a_1^{(r)}$ = proportional constant

z_d = deviatoric component of intrinsic time

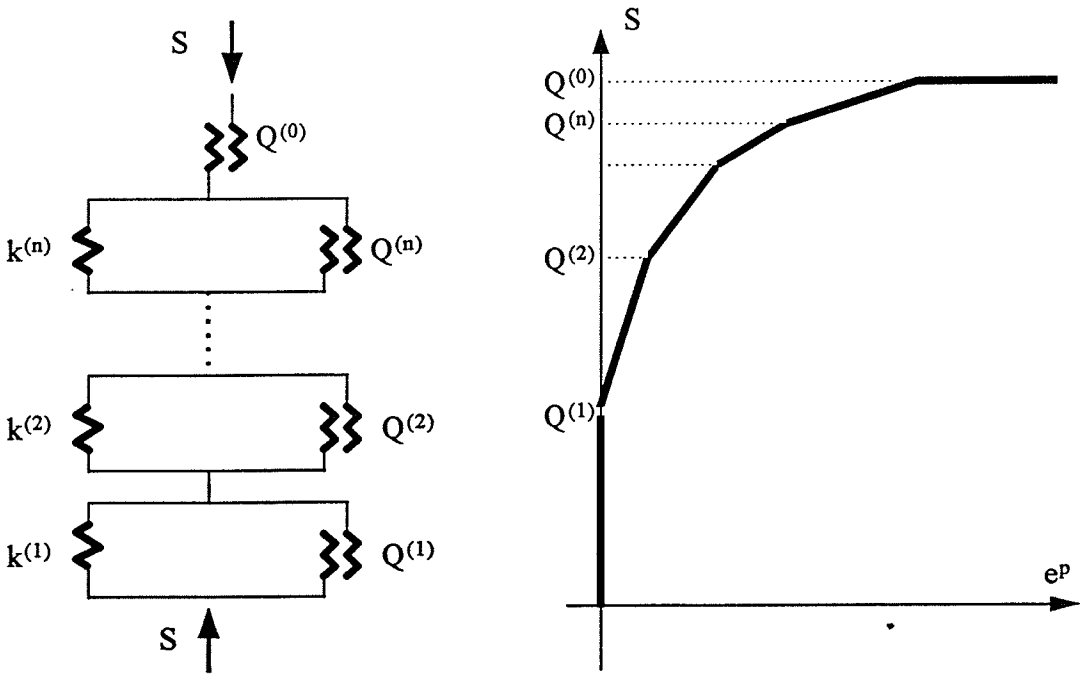

Figure 6.11 A one-dimensional mechanical model with a yield and a failure point.

Substituting of Eq. (6.2) into Eq. (6.1) gives:

$$S = a_1^{(r)} \frac{dq^{(r)}}{dz_d} + k^{(r)} q^{(r)} \tag{6.3}$$

and $q^{(r)}$ (r≠0) may be obtained by solving Eq. (6.3):

$$q^{(r)} = \int_0^{z_d} C_r (1 - e^{-\beta_r (z_d - z')}) \frac{dS}{dz'} dz' \tag{6.4}$$

where:

z′ = dummy variable

$C_r = 1/k^{(r)}$

$\beta_r = k^{(r)} / a_1^{(r)}$

and $q^{(0)}$ may also be obtained by solving Eq. (6.3) with $k^{(0)} = 0$:

$$q^{(0)} = \int_0^{z_d} C_0 (z_d - z') \frac{dS}{dz'} dz' \tag{6.5}$$

where:

$C_0 = 1/a_1^{(0)}$

Since all creep units are connected in series, the overall plastic strain can be calculated as the sum of strains of all individual frictional elements (Fig.6.11):

$$e^p = \sum_{r=0}^{n} q^{(r)} \tag{6.6}$$

Substituting Eqs. (6.4) and (6.5) into Eq. (6.6) results:

$$e^{p} = \int_{0}^{z_d} \Phi_d(z_d - z') \frac{dS}{dz'} dz' \tag{6.7}$$

where:

$$\Phi_d(z_d) = C_0 z_d + \sum_{r=1}^{n} C_r (1 - e^{-\beta_r z_d}) \tag{6.8}$$

Equation (6.7) may be generalised for three-dimensional cases by using tensor expression as follows:

$$e_{ij}^{p} = \int_{0}^{z_d} \Phi_d(z_d - z') \frac{ds_{ij}}{dz'} dz' \tag{6.9}$$

Equation (6.9) is the constitutive equation for deviatoric behaviour of grain en masse. Equation (6.8) may be viewed as the kernel function of tensorial zones. The mechanical model of volumetric behaviour is similar to that of deviatoric behaviour. Stress equilibrium in a r-th unit, similar to Eq. (6.1), may be written as:

$$\sigma_h = Q_h^{(r)} + K^{(r)} q_h^{(r)} \tag{6.10}$$

where:

σ_h = hydrostatic stress

Q_h = internal hydrostatic stress variable

q_h = internal hydrostatic strain variable

K = hydrostatic bulk modulus

$^{(r)}$ = in r-th elastic element

However, unlike deviatoric behaviour, volumetric deformation has two sources: I) hydrostatic compression, and ii) shear-induced dilation (Valanis and Peters 1991). The hydrostatic compression is proportional to the rate of internal hydrostatic strain variables, and shear-induced hydrostatic stress is proportional to the integration of complementary deviatoric plastic work:

$$Q_h^{(r)} = a_2^{(r)} \frac{dq_h^{(r)}}{dz_h} - b^{(r)} \int_0^{z_h} e_{ij}^p \frac{ds_{ij}}{dz} dz' \tag{6.11}$$

where:

$a_2^{(r)}$ = constant

$b^{(r)}$ = constant

z_h = hydrostatic component of intrinsic time

Following the similar discussion for deviatoric behaviour, the hydrostatic constitutive equation may be obtained:

$$\varepsilon_h^p = \int_0^{z_h} J(z_h - z') \frac{d\sigma_h}{dz'} dz' + \int_0^{z_h} \Gamma(z_h - z') e_{ij}^p \frac{ds_{ij}}{dz'} dz' \tag{6.12}$$

$$J = J_0 z_h + \sum_{r=1}^{n} \frac{1}{K_r} (1 - e^{-\lambda_r z_h}) \tag{6.13}$$

$$\Gamma = \frac{\Gamma_0 z_h}{\kappa F_h} + \sum_{r=1}^{n} \frac{c_r}{K_r \kappa F_h}(1 - e^{-\lambda_r z_h}) \qquad \textbf{(6.14)}$$

where:

J = hydrostatic kernel function

Γ = coupling kernel function

$\lambda_r = K^{(r)}/a_2^{(r)}$, model parameter

$J_0 = 1/a_2^{(0)}$, model parameter

$\Gamma_0 = b^{(0)}/a_2^{(0)}$, model parameter

$K_r = K^{(r)}$

For materials with an initial yield point and a failure point, the deviatoric kernel function expressed by Eq. (6.8) may be approximated by one linear term and one exponential term:

$$\Phi_d \approx C_0 z_d + C_1(1 - e^{-\beta_1 z_d}) \qquad \textbf{(6.15)}$$

where:

C_0, C_1 and β_1 = material parameters

Under one-dimensional conditions, Eq. (6.15) is a mathematical representation of a mechanical model consisting of a friction element and a friction-spring unit, as shown in Fig. 6.1 when n =1. Here $Q^{(1)}$ and $Q^{(0)}$ define the initial yield point and the failure point, respectively, and z_d represents a deviatoric plastic strain scale.

Compared with deviatoric deformation, hydrostatic deformation is small for grain en masse under most loading conditions. The linear term alone is a sufficient approximation to the hydrostatic and coupling kernel functions (Valanis and Fan 1984):

$$J \approx J_0 z_h \tag{6.16}$$

$$\Gamma \approx \Gamma_0 (\kappa F_h)^{-1} z_h \tag{6.17}$$

where:

J_0 = material parameter for simplified hydrostatic kernel function

Γ_0 = material parameter for simplified coupling kernel function

6.2.2 Energy Approach

Energy approach provides a unified way to formulate endochronic equations. When grain en masse is loaded by a stress σ_{ij}, energy is dissipated by friction elements and stored in spring elements. Internal stresses T_{ij} (stresses in friction elements) are responsible for the energy dissipation, which are governed by the principle of irreversible thermodynamics. Gibbs free energy, which is used for modelling creep-type behaviour, is stored in spring elements in terms of applied stresses and internal stresses. The strain responses of the material are calculated by taking the derivative of Gibbs free energy with respect to applied stresses:

$$\varepsilon_{ij}^{p} = \frac{\partial G(\sigma_{ij}, T_{ij})}{\partial \sigma_{ij}} \tag{6.18}$$

where:

ε^{p}_{ij} = plastic strain tensor

σ_{ij} = stress tensor

T_{ij} = internal stress tensor

G( ) = Gibbs free energy density

Similarly, internal strains may be calculated as follows:

$$U_{ij} = -\frac{\partial G(\sigma_{ij}, T_{ij})}{\partial T_{ij}} \qquad \textbf{(6.19)}$$

where:

U_{ij} = internal strain tensor

Gibbs Free Energy

The total free energy in the system is the summation of the energy stored in each spring element. It is assumed that internal stresses T_{ij} is resolved into deviatoric component Q_{ij} and hydrostatic component Q, and that Gibbs free energy is also resolved into a deviatoric component G_d and hydrostatic component G_h. For a typical spring element *r*, the deviatoric stress acting on it is $s_{ij}^{(r)}$ which is equal to the total stress s_{ij} less the internal deviatoric stress on the friction element $Q_{ij}^{(r)}$, i.e., $s_{ij}^{(r)}=(s_{ij} - Q_{ij}^{(r)})$ (Fig. 6.11), and the corresponding strain of the spring element is $e_{ij}^{(r)} = s_{ij}^{(r)}/k^{(r)}$. Therefore, the deviatoric component of Gibbs free energy stored in a single spring element $G_d^{(r)}$ is determined as:

$$G_d^{(r)} = \frac{1}{2} e_{ij}^{(r)} s_{ij}^{(r)} = \frac{1}{2}\frac{1}{k^{(r)}} \| s_{ij} - Q_{ij}^{(r)} \|^2 \qquad \textbf{(6.20)}$$

where:

$G_d^{(r)}$ = deviatoric components of Gibbs free energy in r-th unit

s_{ij} = deviatoric stress tensor

$Q_{ij}^{(r)}$ = internal deviatoric stress variables

$\| \|$ = the norm ("length") of tensor.

The total free energy stored in the system is the sum of energy stored in all spring elements:

$$G_d = \sum_{r=1}^{n} G_d^{(r)} = \frac{1}{2}\sum_{r=1}^{n} C^{(r)} \| s_{ij} - Q_{ij}^{(r)} \|^2 \qquad \textbf{(6.21)}$$

where:

G_d = deviatoric components of Gibbs free energy

$C^{(r)} = 1/k^{(r)}$, material constants

Deviatoric stress s_{ij}, together with internal deviatoric stress $Q_{ij}^{(1)} \ldots Q_{ij}^{(n)}$, defines the deviatoric state of the material. Similarly, for hydrostatic behaviours, hydrostatic component of free energy may be written as:

$$G_h = \frac{1}{2}\sum_{r=1}^{n} D^{(r)} | \sigma_h - Q^{(r)} |^2 \qquad \textbf{(6.22)}$$

where:

G_h = hydrostatic components of Gibbs free energy

$D^{(r)}$ = material constants

σ_h = hydrostatic stress

$Q^{(r)}$ = internal hydrostatic stress variables

$| \ |$ = absolute value

Evolution equations

To calculate Gibbs free energy using Eqs. (6.221) and (6.22), determinations of internal stresses are necessary. Internal stresses are governed by the energy dissipation. Following the principle of

irreversible thermodynamics, the rate of energy dissipation should be always positive for an irreversible process:

$$Q_{ij}^{(r)}\left(\frac{dq_{ij}^{(r)}}{dz_d}\right) > 0 \qquad and \qquad Q^{(r)}\left(\frac{dq^{(r)}}{dz_h}\right) > 0 \tag{6.23}$$

where:

$q_{ij}^{(r)}$ = internal deviatoric strains

$q^{(r)}$ = internal hydrostatic strain

The above inequalities can be satisfied mathematically in many possible ways. A simple way is to express $Q_{ij}^{(r)}$ and $Q^{(r)}$ as positive linear functions of internal strain rates (Valanis 1984):

$$Q_{ij}^{(r)} = a_1^{(r)}\frac{dq_{ij}^{(r)}}{dz_d} \tag{6.24}$$

$$Q^{(r)} = a_2^{(r)}\frac{dq^{(r)}}{dz_h} \tag{6.25}$$

where

$a_1^{(r)}$ = positive constant (viscosity-like shear coefficient)

$a_2^{(r)}$ = positive constant (viscosity-like hydrostatic coefficient)

These equations assume that deviatoric and hydrostatic responses are independent. For grain en masse, however, shearing may cause volume changes (dilatancy). Therefore, Eq. (6.25) is modified to account for shear-volume coupling by including shear work, which is calculated as the product of the shear strain e^{p}_{ij} and the shear stress rate (ds_{ij}/dz) integrated over the range of

hydrostatic intrinsic time:

$$Q^{(r)} = a_2^{(r)} \frac{dq^{(r)}}{dz_h} - a_{21}^{(r)} \int_0^{z_h} e_{ij}^{p} \left(\frac{ds_{ij}}{dz} \right) dz' \tag{6.26}$$

where:

$a_{21}^{(r)}$ = positive constant

By using Eq. (6.19), internal strains can be determined by differentiating Gibbs free energy densities with respect to internal stresses:

$$q_{ij}^{(r)} = -\frac{\partial G_d}{\partial Q_{ij}^{(r)}} \qquad and \qquad q^{(r)} = -\frac{\partial G_h}{\partial Q^{(r)}} \tag{6.27}$$

Substituting Eq. (6.27) into (6.24) and (6.26) yields:

$$Q_{ij}^{(r)} + a_{11}^{(r)} \frac{d}{dz_d} \left(\frac{\partial G_d}{\partial Q_{ij}^{(r)}} \right) = 0 \tag{6.28}$$

$$Q^{(r)} + a_2^{(r)} \frac{d}{dz_h} \left(\frac{\partial G_h}{\partial Q^{(r)}} \right) = -a_{21}^{(r)} \int_0^{z_h} e_{ij}^{p} \left(\frac{ds_{ij}}{dz} \right) dz' \tag{6.29}$$

Equations (6.28) and (6.29) are the evolution equations which may be used for determining the internal stresses.

Stress-based Theory

Stress-based theory is obtained by solving Eqs. (6.18) - (6.29). From Eq. (6.18), the deviatoric and hydrostatic responses are written as:

$$e_{ij}^{p} = \frac{\partial G_d}{\partial s_{ij}} \quad and \quad \varepsilon_h^p = \frac{\partial G_h}{\partial \sigma_h} \tag{6.30}$$

where:

e^p_{ij} = plastic deviatoric strain tensor

ε^p_h = plastic hydrostatic strain

Substitution of Eq.(6.21) into Eqs. (6.28) and (6.30), and performing the Laplace transformation on the resulting equations gives:

$$\bar{e}_{ij}^{p} = \sum_{r=1}^{n} C^{(r)}[\bar{s}_{ij} - \bar{Q}_{ij}^{(r)}] \tag{6.31}$$

$$\bar{Q}_{ij}^{(r)} - a_1^{(r)} C^{(r)} t(\bar{s}_{ij} - \bar{Q}_{ij}^{(r)}) = 0 \tag{6.32}$$

where t is a transformation parameter; and an overhead bar ($\bar{}$) indicates that the variable is in the transformed domain. Solving Eq. (6.32) for $\bar{Q}_{ij}^{(r)}$ and substituting it into Eq.(6.31) yields:

$$\bar{e}_{ij}^{p} = \sum_{r=1}^{n} C^{(r)} \left[\frac{1}{1 + a_1^{(r)} C^{(r)} t} \right] \frac{1}{t}\, t\, \bar{s}_{ij} \tag{6.33}$$

Using the convolution theorem of Laplace transformation expressed by Eq. (6.34) (Hirsch 1985):

$$L\left\{ \int_0^{z_d} f_1(z_d - z')f_2(z')dz' \right\} = L\{f_1(z_d)\}\ L\{f_2(z_d)\} \tag{6.34}$$

where:

L{ } = Laplace transformation

the inverse Laplace transformation of Eq.(6.33) gives:

$$e_{ij}^{p} = \int_{0}^{z_d} \Phi_d(z_d - z') \frac{ds_{ij}}{dz'} dz' \qquad \textbf{(6.36)}$$

$$\Phi_d = \sum_{r=1}^{n} C^{(r)} \left[1 - e^{-\beta^{(r)} z_d}\right] \qquad \textbf{(6.35)}$$

where:

Φ_d = the deviatoric kernel function

$\beta^{(r)} = 1/(a_1^{(r)} C^{(r)})$, intermediate variable

Equation (6.35) may be viewed as the summation of an incremental constitutive equation $de_{ij}^{p} = \Phi_d ds_{ij}$ over the entire intrinsic time history, where Φ_d is equivalent to a tangent compliance.

By noting that $C^{(r)} = C_r$ and $\beta^{(r)} = \beta_r$, Equations (6.35) and (6.36) are basically identical to Eqs.(6.7) and (6.8). Therefore, for materials with an initial yield point and a failure point, the deviatoric kernel function expressed by Eq. (6.36) may be approximated by one linear term and one exponential term, as stated in Eq.(6.15).

Following a similar procedure, a constitutive equation similar to Eq. (6.35) is obtained for the hydrostatic response:

$$\varepsilon_h^{p} = \int_{0}^{z_h} J(z_h - z') \frac{d\sigma_h}{dz'} dz' + \int_{0}^{z_h} \Gamma(z_h - z') e_{ij}^{p} \frac{ds_{ij}}{dz'} dz' \qquad \textbf{(6.37)}$$

$$J = \sum_{r=1}^{n} D^{(r)} \left[1 - e^{-\lambda^{(r)} z_h}\right] \qquad \textbf{(6.38)}$$

$$\Gamma = \sum_{r=1}^{n} \frac{a_{21}^{(r)}}{a_2^{(r)} \kappa F_h} \left[1 - e^{-\lambda^{(r)} z_h}\right] \tag{6.39}$$

where:

J = the hydrostatic kernel function

Γ = the coupling kernel function

$\lambda^{(r)} = 1/(a_2^{(r)} D^{(r)})$

For granular materials which are subject to large plastic deformations and negligible elastic deformations, Equations (6.38) and (6.39) may be simplified as Eqs. (6.16) and (6.17).

6.3 Formulation of Strain-based Model

Strain-based model may be derived by either the classical or energy approaches. Both approaches will yield to the same results, as in the case of creep-type model. Therefore, relaxation-type model is formulated by energy approach only in this section, because of its unified concept and solid physical basis of irreversible thermodynamics.

Strain-Based Theory

Helmholtz free energy is used for modelling the relaxation-type model (Valanis and Peters 1991). Following stress-based theory, Helmholtz free energy is assumed to be composed of a deviatoric component and a hydrostatic component. For a given plastic strain, the energy stored in the relaxation type mechanical models may be written as quadratic functions of applied strains and internal strains (Fig.6.3):

$$H_d = \frac{1}{2}\sum_{r=1}^{n} A_r \| e_{ij}^p - q_{ij}^{(r)} \|^2 \quad and \quad H_h = \frac{1}{2}\sum_{r=1}^{n} B_r |\varepsilon_h^p - q_h^{(r)}|^2 \tag{6.40}$$

where:

H_d = deviatoric components of Helmholtz free energy

H_h = hydrostatic components of Helmholtz free energy

q_{ij} = deviatoric internal strain tensor

q_h = hydrostatic internal strain

A_r = material constant

B_r = material constant

Following the procedure used in deriving the stress-based model, internal shear stresses are proportional to the rate of internal strains, internal hydrostatic stresses are proportional to the rate of internal volumetric strains as well as the rate of plastic deviatoric work for shear-induced volumetric deformations. Therefore, evolution equations for relaxation-type model may be expressed as:

$$Q_{ij}^{(r)} = b_1^{(r)} \frac{dq_{ij}^{(r)}}{dz_d} \tag{6.41}$$

$$Q^{(r)} = b_2^{(r)} \frac{dq^{(r)}}{dz_h} - b_{21}^{(r)} s_{ij} \frac{de_{ij}^p}{dz} \tag{6.42}$$

where:

$b_1^{(r)}$ = intermediate (viscosity-like) shear coefficient

$b_2^{(r)}$ = intermediate (viscosity-like) hydrostatic coefficient

$b_{21}^{(r)}$ = intermediate coupling coefficient

Following Eq.(6.30), internal stresses are related to internal strains as follows:

$$Q_{ij} = -\frac{\partial H_d}{\partial q_{ij}} \quad and \quad Q = -\frac{\partial H_h}{\partial q} \tag{6.43}$$

Substitution of Eq. (6.43) into Eqs. (6.41) and (6.42) yields the following evolution equations:

$$\frac{\partial H_d}{\partial q_{ij}^{(r)}} + b_1^{(r)} \frac{dq_{ij}^{(r)}}{dz_d} = 0 \tag{6.44}$$

$$\frac{\partial H_h}{\partial q^{(r)}} + b_2^{(r)} \frac{dq^{(r)}}{dz_h} = -b_{21}^{(R)} s_{ij} \frac{de_{ij}^p}{dz} \tag{6.45}$$

The stress responses to applied strains may be calculated from the derivative of Helmholtz free energy with respect to the corresponding plastic strains (Valanis and Peters 1991):

$$s_{ij} = \frac{\partial H_d}{\partial e_{ij}^p} \quad and \quad \sigma_h = \frac{\partial H_h}{\partial \varepsilon_h^p} \tag{6.46}$$

Similarly as in stress-based model, the following constitutive equations can be obtained by solving Eqs.(6.40) - (6.46):

$$s_{ij} = \int_{o}^{z_d} \Psi_d(z_d - z') \frac{de_{ij}^p}{dz'} dz' \tag{6.47}$$

$$\sigma_h = \int_{0}^{z_h} \Psi_h(z_h - z') \frac{d\varepsilon_h^p}{dz'} dz' + \int_{0}^{z_h} \Pi(z_h - z') s_{ij} \frac{de_{ij}^p}{dz'} dz' \tag{6.48}$$

where three kernel functions Ψ_d, Ψ_h and Π take the forms of:

$$\Psi_d = \sum_{r=1}^{n} A_r e^{-\alpha_r z_d} \tag{6.49}$$

$$\Psi_h = \sum_{r=1}^{n} B_r e^{-\zeta_r z_h} \tag{6.50}$$

$$\Pi = \sum_{r=1}^{n} K_r e^{-\zeta_r z_h} \tag{6.51}$$

where

$\alpha_r = A_r/b_1^{(r)}$, material constant

$\zeta_r = B_r/b_2^{(r)}$, material constant

$K_r = (\zeta_r b_{21}^{(r)})/(\kappa F_h)$, material constant

Equations (6.47) to (6.51) are consistent with those of Valanis and Peters (1991).

For the mixed-type mechanical models, constitutive equations may be selected according to the types of deviatoric and hydrostatic responses, respectively. Equations (6.35) and (6.48) are for the first mixed-type mechanical model, and equations (6.37) and (6.47) are for the second mixed-type mechanical model.

6.4 Determination of Model Parameters

Model parameters for the strain-based theory have been determined by Xu (1992) for wheat en masse. The following section discusses determination of model parameters for the stress-based theory.

Model parameters for the stress-based theory were evaluated using triaxial test data reported by Zhang et al.(1987) for wheat at a moisture content of 8.1% (w.b.) and a bulk density of 817 kg/m^3. Their data, collected from conventional cylindrical triaxial tests, include four sets of data from axial compression tests at confining pressures of 20.7, 34.5, 48.3 and 62.1 kPa, and one set from hydrostatic compression tests. Axial compression data for a confining pressure of 48.3 kPa and hydrostatic compression data were used in determining model parameters. Because the definition of intrinsic time is the same as that used by Valanis and Peters (1991) in their strain-based theory, all parameters associated with the intrinsic time remain identical to those determined by Xu et al. (1992) for the grain (Table 6.1). Detailed procedures for determining these parameters can also be found in Xu et al. (1993). Determination of parameters associated with the kernel functions are discussed in the following sections.

Under triaxial loading conditions, the deviatoric stress may be expressed as (Valanis and Peters 1991):

$$s = s_\infty + (s_0 - s_\infty) e^{-\alpha z_d} \tag{6.52}$$

where:

s = deviatoric stress under triaxial loading

s_∞ = deviatoric stress at failure (at $z_d = \infty$) under triaxial loading

s_0 = deviatoric stress at yield (at z_d =0) under triaxial loading

α = material constant

Table 6.1. Model parameters determined for wheat at a moisture content of 8.1% w.b. and a bulk density of 817 kg/m^3

Elastic bulk modulus (K), kPa		2067†
Elastic shear modulus (G), kPa		2750†
Coupling parameter (κ)		1.13†
Hydrostatic hardening function (F_h)		
	Φ_1	0.7†
	a	8.8×10^{-5} †
	c	73.2†
Simplified coupling function (Γ_1), kPa^{-1}		-7
Hydrostatic kernel function (J_1), kPa^{-1}		0.154
Deviatoric kernel function (Φ_d)		
	C_0, kPa^{-1}	2.92
	β_1	3164
	C_1, kPa^{-1}	8.0×10^{-4}

† Reported by Xu et al.(1993)

When the material is subjected to axial compression as in the conventional triaxial tests, the plastic volumetric strain increment $d\epsilon_v^p$ is negligible compared with the plastic deviatoric strain de^p, therefore $de^p/dz \approx 1$ as indicated by Eq. (3.12) ($de^p_{ij} = de^p$ under axial compression, thus $de^p_{ij}\, de^p_{ij} = (de^p)^2$). It follows from Eq. (3.14) that:

$$\frac{de^p}{dz_d} = \frac{de^p}{dz} F_d \approx F_d \tag{6.53}$$

Under axial compression, the deviatoric hardening function F_d may be expressed as (Valanis and Peters 1991):

$$F_d = \sigma_0 + bs \tag{6.54}$$

where b has a constant value of 0.408 (Valanis and Peters 1991). Combining Eqs.(6.53) and (6.54) yields:

$$de^p = (\sigma_0 + bs)dz_d \tag{6.55}$$

Substituting Eq. (6.52) into (6.55) and integrating the resulting equation gives:

$$e^p = (\sigma_0 + bs_\infty)z_d - \frac{b}{\alpha}(s_\infty - s_0)(1 - e^{-\alpha z_d}) \tag{6.56}$$

The deviatoric strain can also be calculated from Eqs. (6.7) and (6.15) as follows:

$$e^p = (C_0 z_d + C_1)(s - s_0) - \alpha(s_\infty - s_0)(I_1 + I_2) \tag{6.57}$$

where I_1 and I_2 are the integrations:

$$I_1 = \int_0^{z_d} z' e^{\alpha z'} dz' = \frac{z_d}{\alpha} e^{-\alpha z_d} - \frac{1}{\alpha^2}(e^{-\alpha z_d} - 1) \qquad \textbf{(6.58)}$$

$$I_2 = \int_0^{z_d} e^{\beta_1 z_d + (\beta_1 - \alpha) z'} dz' = \begin{cases} \dfrac{1}{\beta_1 - \alpha}(e^{-\alpha z_d} - e^{-\beta_1 z_d}) & \text{if } \beta_1 \neq \alpha \\ z_d e^{-\alpha z_d} & \text{if } \beta_1 = \alpha \end{cases} \qquad \textbf{(6.59)}$$

If assuming $\beta_1 \neq \alpha$, comparison of Eq. (6.57) with (6.56) results in:

$$e^{-\alpha z_d} = e^{-\beta_1 z_d} \qquad \textbf{(6.60)}$$

which indicates that β_1 must be equal to α. Eq. (6.52) suggests that α is the slope of $(s_\infty - s)$ vs. z_d curve plotted in a semi-log scale. The α value was determined to be 3164 by Xu (1992) for the wheat used in this study.

Substituting Eq. (6.52) into (6.57) and rearranging the equation yields:

$$e^{p} = C_0 z_d (s_\infty - s_0) + (C_1 - \frac{C_0}{\alpha})(s_\infty - s_0) - (s_\infty - s_0)(C_1 - \frac{C_0}{\alpha} + C_1 z_d) e^{-\alpha z_d} \qquad \textbf{(6.61)}$$

Differentiating Eq. (6.61) with respect to z_d, and then letting z_d approach infinity, Eq. (6.62) is obtained:.

$$C_0 = \lim_{z_d \to \infty} \left[\frac{1}{s_\infty - s_0} \frac{de_{ij}^{p}}{dz_d} \right] \qquad \textbf{(6.62)}$$

Following a similar procedure, J_1 in the hydrostatic kernel function is determined as:

$$J_1 = \lim_{z_h \to \infty} \left[\frac{1}{\sigma_\infty - \sigma_0} \frac{d\varepsilon_h^p}{dz_h} \right] \tag{6.63}$$

where:

σ_∞ = hydrostatic stress at $z_h = \infty$

σ_0 = confining pressure in triaxial test (at $z_h = 0$)

The failure and yield stresses and strain rates at failure determined from data reported by Zhang et al. (1986) are summarized in Table 6.2. The strain rate ($d\epsilon_h^p/dz_h$) at $z_h \to \infty$ was determined from the slope of the curve for hydrostatic strain versus hydrostatic intrinsic time at a large z_h value (Fig. 6.12) (the slope remained almost constant for $z_h > 0.3$). The strain rate (de_{ij}^p/dz_d) at $z_d \to \infty$ was determined in a similar fashion from a plot of deviatoric strain versus deviatoric intrinsic time. The hydrostatic stress σ_∞ was calculated as ($\sigma_0 + 0.408 s_\infty$) (Valanis and Peters 1991). From these data C_0 and J_1 were determined to be 2.94 kPa^{-1}, 0.154 kPa^{-1}, respectively.

Differentiating Eq. (6.61) with respect to z_d, and then letting z_d approach to zero yields:

$$\left. \frac{de^p}{dz_d} \right|_{z_d \to 0} = C_1(\alpha - 1)(s_\infty - s_0) \tag{6.64}$$

Another expression of the strain derivative may be obtained from Eq. (6.55):

$$\left. \frac{de^p}{dz_d} \right|_{z_d \to 0} = \sigma_0 + b s_0 \tag{6.65}$$

Table 6.2. Failure stresses and strain rates derived from triaxial test data (σ_0=48.3 kPa) for wheat at a moisture content of 8.1% w.b. and bulk density of 817 kg/m^3 (Zhang et al. 1986)

Deviatoric stress at failure (s_∞), kPa	57.8†
Hydrostatic stress at failure (σ_∞), kPa	71.9
Deviatoric stress at yield (s_0), kPa	33.4†
Deviatoric strain rate at failure (de_{ij}^p/dz_d)	71.6
Hydrostatic strain rate at failure ($d\epsilon_h^p/dz_h$)	3.62
Slope (α)	3164

† Reported by Xu et al. (1993)

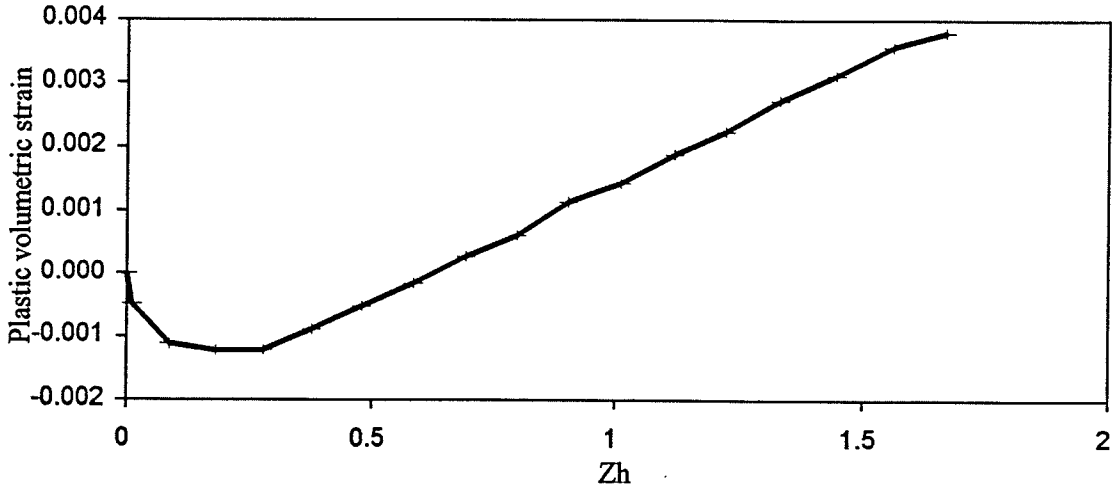

Figure 6.12 Variation of hydrostatic (volumetric) plastic strain with hydrostatic intrinsic time.

Equating Eqs. (6.64) and (6.65) yields:

$$C_1 = \frac{C_0 - b}{\alpha - 1} \tag{6.66}$$

The coefficient C_1 is calculated to be $8.0\text{x}10^{-4}$ using Eq. (6.66). Parameter Γ_0 was calculated to be -7 kPa^{-1} using Eqs. (6.12), (6.16), and (6.17) at $\epsilon_h^p=0$.

6.5 Verification of Stress-based Endochronic Theory

The model parameters listed in Table 6.1 were used to predict the stress-strain behaviour of wheat en masse under the axial compression with a constant confining pressure of 20.7 kPa. The integrations of Eqs.(6.9) and (6.12) were carried out numerically. Model predictions compared with the experimental data reported by Zhang et al. (1987) (Figs.6.13 and 6.14). The predicted deviatoric stresses closely followed the experimental data with an average relative difference of 4% and an average difference of 0.83 kPa. The average difference between predicted and measured volumetric strain is 1.08×10^{-3}. The relative difference could not be calculated for volumetric strains because measured strains had zero values. Predictions by the stress-based theory are consistent with those by the strain-based theory of Valanis and Peters (1991) (Figs. 6.13 and 6.14). It is interesting to note that predictions of volumetric strains averaged from stress theory and strain theory are in closer agreement with the experimental data than either theory alone (Fig. 6.14) because of the complementarity of the theories.

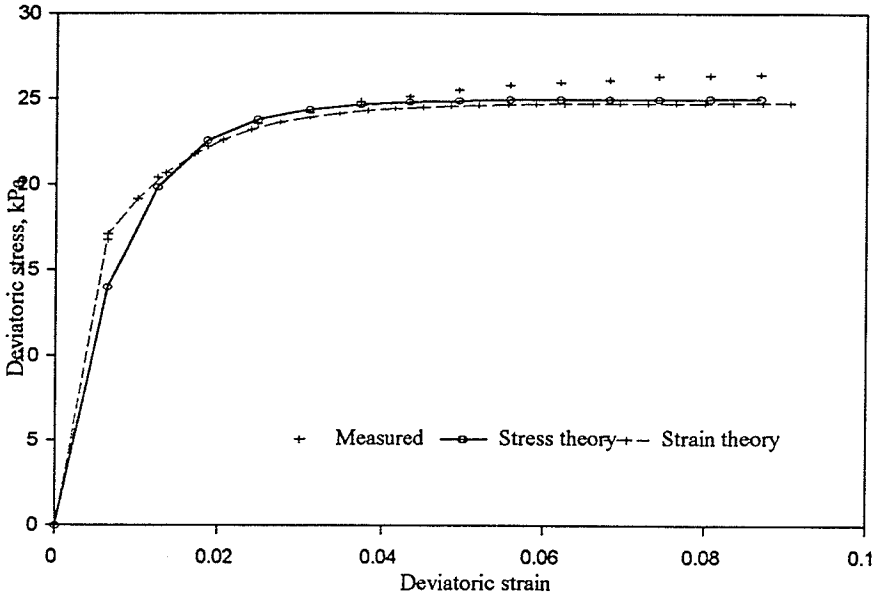

Figure 6.13 Comparison of predicted deviatoric stresses with data reported by Zhang (1987) for triaxial loading at a confining pressure of 20.7 kPa.

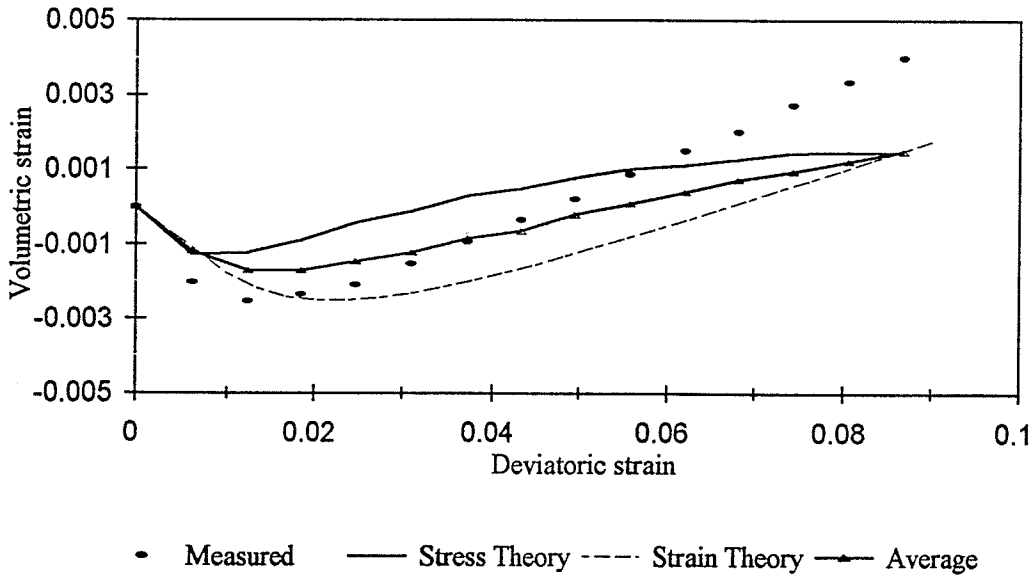

Figure 6.14 Comparison of predicted volumetric strains with data reported by Zhang et al. (1987) for triaxial loading at a confining pressure of 20.7 kPa.

7. ENDOCHRONIC FINITE ELEMENT ALGORITHM

7.1 Grain-Storage System

A finite element algorithm of strain-based endochronic theory has been developed by Xu (1992), in which the grain-storage system was assumed to consist of three components: (i) grain; (ii) grain-structure interface; (iii) structure (bin wall). In this study, the same system is used for model development. The constitutive laws for the structure and interface elements are the same as that in Xu (1992). In this Chapter, the focus is on formulating stress-based endochronic theory for the grain. Matrix expressions are given for an axisymmetric situation, because most on-farm storage grain bins are cylindrical and grain pressures are considered to be axisymmetric.

7.2 Bin Wall Element

The bin wall, assumed to be made of steel, was considered to be linearly elastic. Hooke's law was used to describe the bin wall behaviour (Zhang 1987, Xu 1992):

$$\{d\sigma\}=[D_w]\{d\varepsilon\} \tag{7.1}$$

where:

$[D_w]$ = the stress-strain matrix for the wall

$\{d\sigma\}$ = stress vector

$\{d\epsilon\}$ = strain vector

For an axisymmetric thin-walled bin, the bin wall may be treated as a membrane in which no shear stress develops. Therefore, the bin wall was discretized by a line element (Fig. 7.1), and $[D_w]$ was expressed as:

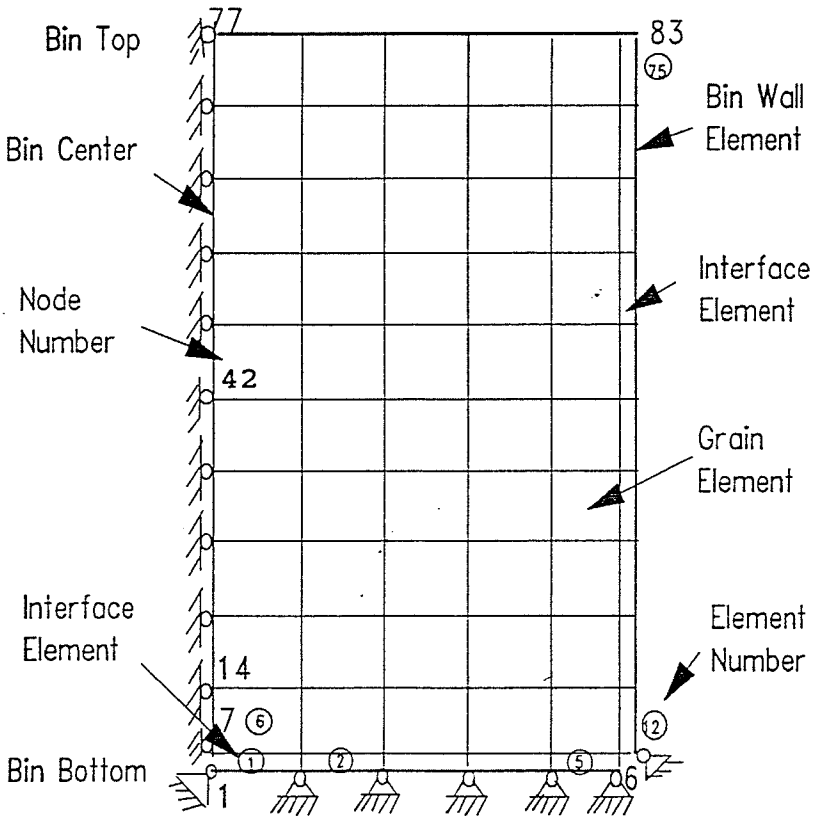

Figure 7.1 Discretization of grain bin system.

$$[D_w]=\frac{E_w}{1-\nu_w^2}\begin{bmatrix}1 & \nu_w\\ \nu_w & 1\end{bmatrix} \tag{7.2}$$

where:

E_w = elastic modulus of bin wall material

ν_w = Poisson's ratio of bin wall material

7.3 Interface Element

In finite element analysis, the contact surface between two materials has common nodes which undergo the same displacements. This implies that relative motions at the common nodes are not allowed (displacement must be continuous). On the contact surface between the grain and the wall, the grain is free to slide over the wall, thus creating a discontinuous displacement field from the grain to the wall. To model the relative motion and force transaction between the grain and bin wall, an interface element (Zhang et al. 1987, Xu 1992) should be used:

$$\{d\sigma\}=[D_i]\{d\varepsilon\} \tag{7.3}$$

where:

$\{d\sigma\} = [d\sigma_r\ d\sigma_z\ d\sigma_\theta\ d\sigma_{rz}]^T$

$\{d\epsilon\} = [d\epsilon_r\ d\epsilon_z\ d\epsilon_\theta\ d\epsilon_{rz}]^T$

$[D_i]$ = stress-strain matrix for the interface

For an axisymmetric body, $[D_i]$ is expressed as (Xu 1992):

$$[D_i] = \begin{bmatrix} d_1 & d_2 & d_2 & 0 \\ d_2 & d_1 & d_2 & 0 \\ d_2 & d_2 & d_1 & 0 \\ 0 & 0 & 0 & G_i \end{bmatrix} \quad \textbf{(7.4)}$$

where:

$d_1 = \lambda_p E_i(1-\nu_i)/[(1+\nu_i)(1-2\nu_i)]$

$d_2 = \lambda_p E_i\nu_i/[(1+\nu_i)(1-2\nu_i)]$

E_i = elastic modulus of interface in compression

ν_i = Poisson's ratio of interface

λ_p = participation factor (0.01 - 0.1)

G_i = shear modulus of interface.

E_i and ν_i can be expressed in terms of the initial elastic bulk modulus K_h and initial shear modulus G of the grain as described in the following section. The shear modulus (G_i) was determined from the frictional behaviour of grain on the wall (Xu 1992):

$$G_i = d\tau/d\gamma = 0.5(\mu\sigma_n - \tau)\sqrt{t/(N\gamma)} \quad \textbf{(7.5)}$$

where:

μ = friction coefficient between grain and bin

σ_n = normal stress

τ = shear stress

t = thickness of the interface element

N = displacement modulus

γ = shear strain (s/t)

s = relative displacement

7.4 Grain Element

The grain element was modelled by stress-based endochronic theory described in the previous Chapter. The constitutive equations are converted to the matrix forms in this section.

Using the definitions of deviatoric stress $dS_{ij}=d\sigma_{ij}-d\sigma_h\delta_{ij}$ and deviatoric strain $de_{ij}=d\epsilon_{ij}-\delta_{ij}d\epsilon_h/3$ (where δ is the Kronecker delta), and the relationships represented by Eqs. (3.10) and (3.11), the following constitutive equations were obtained:

$$d\sigma_{ij}=d\sigma_h\delta_{ij}+dS_{ij}$$

$$=K_h\delta_{ij}(d\varepsilon_h-d\varepsilon_h^p)+2G(de_{ij}-de_{ij}^p)$$

$$=(K_h\delta_{ij}d\varepsilon_h+2Gde_{ij})-(K_h\delta_{ij}d\varepsilon_h^p+2Gde_{ij}^p) \qquad \textbf{(7.6)}$$

which can be expressed in matrix form as:

$$\{d\sigma\}=[D_e]\{d\epsilon\}-\{dH\} \qquad \textbf{(7.7)}$$

where $\{d\sigma\}$ and $\{d\epsilon\}$ are engineering stress and strain vectors for axisymmetric conditions. $[D_e]$ is the initial elastic coefficient matrix given as:

$$[D_e] = \begin{bmatrix} D1 & D2 & D2 & 0 \\ D2 & D1 & D2 & 0 \\ D2 & D2 & D1 & 0 \\ 0 & 0 & 0 & G \end{bmatrix} \tag{7.8}$$

and

$$D1 = K_h + \frac{4}{3}G; \qquad D2 = K_h - \frac{2}{3}G \tag{7.9}$$

The "plastic" stress vector {dH} is given as:

$$\{dH\} = K_h d\epsilon_h^p \{I\} + 2G\{de^p\} \tag{7.10}$$

in which $\{I\}=[1\ 1\ 1\ 0]^T$.

A graphical interpretation of Eq.(7.7) was given in Xu (1992).

7.5 Calculation of Plastic Strains

To calculate the "plastic" stress vector {dH}, numerical calculation of plastic strains is necessary. By the property of convolution integral, an alternative expression of Eq.(6.9) may be written as:

$$e_{ij}^p = \int_0^{z_d} \frac{d\Phi_d(z_d - z')}{dz'} s_{ij} dz' \tag{7.11}$$

Substitution of Eq.(6.15) into Eq.(7.11) gives:

$$e_{ij}^{p} = \int_{0}^{z_d} (C_0 + C_1\beta_1 e^{-\beta_1(z_d - z')}) s_{ij} dz' \tag{7.12}$$

Assume that the domain of integration (0, z_d) was divided into n subregions. Then, the current plastic strain can be calculated from previous step using Eq.(7.12):

$$(e_{ij}^{p})_n = (e_{ij}^{p})_{n-1} + \int_{(z_d)_{n-1}}^{z_d} (C_0 + C_1\beta_1 e^{-\beta_1(z_d - z')}) s_{ij} dz' \tag{7.13}$$

Applying the first mean-value theorem to the above integral yields:

$$(de_{ij}^{p})_n = (e_{ij}^{p})_n - (e_{ij}^{p})_{n-1} \approx s_{ij}|_{z'=z_d} \int_{(z_d)_{n-1}}^{z_d} (C_0 + C_1\beta_1 e^{-\beta_1(z_d - z')}) dz' \tag{7.14}$$

i.e.,

$$(de_{ij}^{p})_n \approx s_{ij}|_{z'=z_d} (C_0 dz_d + C_1(1 - e^{-\beta_1 dz_d})) \tag{7.15}$$

where z_d is the current value of the deviatoric intrinsic time scale, and dz_d corresponds to the current incremental loading process.

Similarly, the hydrostatic plastic strain ($d\epsilon_h^p$) is obtained by using Eqs. (6.12), (6.16) and (6.17):

$$(d\varepsilon_h^p)_n = (dz_h)_n \left(\sigma_h|_{z'=z_h} J_1 + (e_{ij}^{p} ds_{ij})|_{z'=z_h} \frac{\Gamma_1}{2} \right) \tag{7.16}$$

Equation (7.16) shows that the plastic volumetric strain is caused by i) consolidation due to

hydrostatic stress, and ii) shearing-volumetric coupling.

Equations (7.15) and (7.16) imply that no history of previous values should be stored to obtain current values.

7.6 Endochronic Finite Element Algorithm

Following Xu (1992), express the constitutive relations for the wall, grain and interface in a general matrix form:

$$\{d\sigma\}=[D]\{d\epsilon\}-\{dH\} \tag{7.17}$$

where [D] is now the elastic coefficient matrix, and {dH} is the plastic stress vector which is equal to zero for the wall and interface.

Using the principle of virtual work, one may obtain (Xu 1992):

$$\int_v \{\delta d\varepsilon\}^T\{d\sigma\}dv=\int_v \{\delta du\}^T\{dX\}dv+\int_{S_\sigma} \{\delta du\}^T\{dT\}dS \tag{7.18}$$

where:

{T} = surface traction force

{X} = unit volume body force

The differential displacement vector {du} is related to the differential nodal displacement vector {dq} as follows:

$$\{du\}=[N]\{dq\} \tag{7.19}$$

where:

[N] = the matrix of shape (interpolation) functions

Strains are related to the nodal displacements as:

$$\{d\varepsilon\}=\frac{\partial\{du\}}{\partial\{x\}}=[B]\{dq\} \tag{7.20}$$

where:

[B] = ∂[N]/∂{x}, gradient matrix

By substituting Eqs. (7.19), (7.20) and (7.17) into Eq. (7.18) one obtains:

$$\begin{aligned}\{\delta dq\}^T[\int_v [B]^T[D][B]dv\{dq\}-\int_v [N]^T\{dX\}dv\\ -\int_{S_\sigma}[N]^T\{dT\}dS-\int_v [B]^T\{dH\}dv]=0\end{aligned} \tag{7.21}$$

The non-trivial solution of Eq.(7.21) gives:

$$[K]\{dq\}=\{dP\}+\{dP_z\} \tag{7.22}$$

where:

$$[K]=\int_v [B]^T[D][B]dv \tag{7.23}$$

$$\{dP\}=\int_v [N]^T\{dX\}dv+\int_{S_\sigma}[N]^T\{dT\}dS \tag{7.24}$$

$$\{dP_z\}=\int_v [B]^T\{dH\}dV \tag{7.25}$$

The stiffness matrix [K] remains constant during the iterative process, therefore, updating is

unnecessary. Comparing with linear elastic formulation, only the force vector is corrected by adding or subtracting the plastic force vector $\{dP_z\}$ during iterations.

7.7 Solution Technique

The solution technique developed by Xu (1992) for strain-based model was used with a slight modification to obtain solutions to Eq.(7.22). The method has been shown to yield a rapid convergence and to permit large load increments. The solution procedure can be summarized as follows:

1. Apply a load increment $\{dP\}$ and determine the corresponding increments of elastic stress $\{d\sigma'\}_1$ and strain $\{d\epsilon'\}_1$ using the relationship $[K]\{dq\}=\{dP\}$.

2. Update stresses and strains: $\{\sigma'\}_1 = \{ \sigma_0 \} + \{d\sigma'\}_1$ and $\{\epsilon'\}_1=\{\epsilon_0\}+\{d\epsilon'\}_1$.

3. Initiate dz_1 by taking the plastic strain as a fraction of the total strain, e.g., $\{d\epsilon^p\}_1=0.1\{d\epsilon'\}_1$.

4. Calculate $\{dH\}_1$ using dz_1, and update stresses: $\{\sigma'\}_2 = \{\sigma'\}_1 + \{dH\}_1$.

5. Compute the residual force vector: $\{R\} = \{dP\}-\{R_o\}$, where R is the unbalanced force vector, and R_o is the internal nodal force vector corresponding to the current state of stress.

6. Stop the iteration process if:

$$ERR=\frac{\|\{R\}\|}{\|\{dP\}\|}\leq TOL \qquad \textbf{(7.26)}$$

where $\|.\|$ is the norm of a vector and TOL is a prescribed small tolerance

7. Resolve $[K]\{dq\}=\{R\}$ to find $\{d\sigma'\}_2$ and $\{d\epsilon'\}_2$ and repeat Steps 2 to 6.

In theory, the smaller the tolerance, the greater the number of iterations, and the higher the

accuracy. However, an excessively small tolerance may accumulate the truncation errors. In this study, the tolerance was 1%. A Fortran program was written based on the above algorithm (Appendix). The elements used in the program are four-node quadrilateral elements as described by Zhang (1987). The program was developed for both stress-based and strain-based endochronic theories. The program flowchart of strain-based endochronic FEM (Xu 1992) was applicable to stress-based endochronic FEM as well. The graphical illustration of the iteration process, with the explanation of the solution principle, can be found in Xu (1992).

7.8 Validation of Finite Element Algorithm

The endochronic finite element model was validated using experimental data reported by Zhang (1987) for a model bin. The bin was made of 0.8 mm thick aluminum with a height of 1.2 m and a diameter of 0.9 m. The cylindrical bin wall was considered to be hinged at the rigid bin floor. The bin structure and external loads were assumed to be axisymmetric; therefore, only half of the bin was modelled. Because the bin is classified as a shallow bin, Rankine's theory was also used as a comparison.

The grain in the bin was Larned wheat with a bulk density of 817 kg/m^3, Poisson's ratio of 0.29, a moisture content of 8.1% d.b. and an internal friction angle of 25°. The endochronic model parameters shown in Table 5.1 were used in modelling.

The bin was divided into 10 equal layers in the vertical direction and 5 equal sections in the radial direction (Fig.7.1). There is a total of 75 elements in the system. The FORTRAN codes were executed on an IBM 3090 mainframe computer at the University of Manitoba. The average number of iterations for each load increment was about 4.

Comparison of model prediction with experimental data

The model predictions were compared with both experiment data and FEM prediction reported by Zhang (1987) or Rankine's theory (Table 7.1). Predictions of both microscopic and endochronic finite element models were within the 95% confidence interval of the measured data, whereas predictions of other FEM or Rankine's theory were not. The difference in percentage of measured mean were shown in Table 7.1. Rankine's theory does not consider friction between grain and the wall, therefore it predicts higher lateral pressure. At height of 12 cm (near bottom), the prediction by Rankine's theory was beyond the 95% confidence interval (Table 7.1). At height of 37.5 cm, all the models except Rankine's predict lower lateral pressure than measured mean. At the other two levels, predictions by endochronic finite element models or microscopic models were in good agreement with experiment data, their relative differences were within 5%. The average differences of three levels were within 6% for any models developed in this study. These comparisons show that the proposed endochronic finite element models can satisfactorily predict the static lateral pressures in grain storage bins.

Table 7.1. Comparison of static lateral pressures (kPa)

Height	Predictions			Zhang et al. (1987)		
(cm)	Stress-based	Strain-based	Microscopic	Mean (95%CI*)	FEM	Rankine
12.0	3.03 (4.1%)†	3.03 (4.1%)	2.95 (1.4%)	2.91(2.77, 3.04)	2.99(2.7%)	3.51(20.6%)
37.5	2.34 (9.6%)	2.32 (10.3%)	2.33 (10.0%)	2.59(2.29, 2.90)	2.13(18.1%)	2.68(3.5%)
63.0	1.61 (3.6%)	1.58 (5.4%)	1.67 (0.0%)	1.67(1.43, 1.9)	1.45(13.2%)	1.85(10.8%)

† Relative difference to mean measured values

* 95% Confidence Interval

8. SUMMARY AND CONCLUSIONS

In this study, theories of bin loads have been developed from both microscopic and macroscopic approaches. By studying the microstructure of granular media at the particle level, an analytical microscopic theory has been developed for predicting static loads for the first time. The new theory accounts for the contributions of particle deformations to load, and Janssen's equation was derived as a special case of the present theory with an assumption of rigid particles. The new theory has been extended for the analysis of hygroscopic and discharge loads. For hygroscopic loads, dynamic microstresses are calculated from moisture-induced volumetric expansion of grain kernels. For discharge loads, the overpressure factor is predicted from the dilatancy angle, the internal friction angle, and the structural angle of the stored grain. The theory relates lateral pressure during discharge to shear-induced dilatancy. This has brought our understanding of bin loads to the particle level. The theory has been validated against the experimental data for both model bins and a full-size bin.

A class of mechanical models has been constructed for modeling the shear-volumetric coupling behavior of granular materials at macroscopic level. Endochronic theories have been developed by using these mechanical models. The proposed endochronic theories have been verified against triaxial test data for wheat. A finite element algorithm has been developed for analysis of static loads in axisymmetric grain bin systems by using the stress-based endochronic theory for the stored grain. The endochronic finite element model was validated against the experimental data from Zhang (1987).

From the study, the following conclusions were drawn:

1. The microscopic theory provides alternative analytic equations for predicting static,

hygroscopic, and discharge loads using microscopic parameters.

2. Janssen's equation, recommended by most design standards and codes, is a special case of the microscopic theory, with the assumption of rigid particles.

3. The lateral to vertical pressure ratio (k value) is a function of stresses, depth, the structural angle of the particle assembly, and Poisson's ratio of particles (particle rigidity).

4. The behavior of granular media can be modeled by endochronic theories. For wheat at a confining pressure of 20.7 kPa, stress-based endochronic theory predicts deviatoric stresses with an average relative difference of 4% and a mean absolute difference of 0.8kPa. The average difference between predicted and measured volumetric strain is 1.08×10^{-3}.

5. Model parameters of endochronic theories can be evaluated from cylindrical triaxial tests.

6. The proposed FEM predicts static lateral pressures within 95% Confidence Intervals of measured data.

9. RECOMMENDATIONS FOR FURTHER WORK

In this study, the system of granular media in storage structure has been studied, microscopically and macroscopically. The theories have been validated against experimental data. These models provide rational way of calculating the static, hygroscopic, and discharge loads. The recommendations for further work are as follows:

1. Determine experimentally the maximum dilatancy angle for agricultural products.
2. Extend the microscopic model to include cohesive materials.
3. Investigate the complementarity of stress-based and strain-based endochronic theories.
4. Extend the finite element model to include the finite strain case and Newtonian time for dynamic analysis.

REFERENCES

ACI. 1983. Recommended practice for design and construction of concrete bins, silos, and bunkers for storage of granular materials. Revised 1983, and commentary. ACI 313R-77. American Concrete Institute, Detroit, MI, USA.

Airy, W. 1897. The pressure of grain. Proceedings of Institution of Civil Engineering, London, 131:347-358.

ASAE. 1995. ASAE Standards 1995. 42th Edition. American Society of Agricultural Engineers, St. Joseph, MI, USA.

Atewologun, A.O.; Riskowski, G.L. 1991. Experimental determination of Janssen's stress ratio by four methods for soybeans under static conditions. Transactions of the ASAE, 34(5):2193-2198.

Balendran, B. And Sia Nemat-Nasser. 1993. Viscoplastic flow of planar granular materials. Mechanics of Materials, 16:1-12

Bardet, J.P. 1990. A comprehensive review of strain localization in elastic soils. Computers and Geotechnics, 10:163-188.

Bideau, D. and A. Hansen. 1993. Disorder and granular media. North-Holland, Elsevier Science Publishers B.V., Sara Burgerhartstraat 25, P.O.Box 211, 1000 AE Amsterdam, The Netherlands.

Bjerrum, L., S. Kringstad and O. Kummeneje. 1961. The shear strength of fine sand. Proceedings of Fifth International Conference of Soil Mechanics and Foundations Engineering, London, England, 1:29-37.

Blight, G.E. 1986. Swelling pressure of wetted grain. Bulk Solids Handling 6(6):1135-1140.

Britton, M.G., Q. Zhang. 1989. State-of-the-art in the design of grain storage structures. ASAE Paper No. 89-4535, American Society of Agricultural Engineering, St. Joseph, MI, USA. 11pp.

Britton, M.G., Q. Zhang and K. McCullagh. 1993. Moisture induced vertical loads in model grain bin. ASAE Paper No. 93-4503, American Society of Agricultural Engineering, St. Joseph, MI, USA. 7pp.

CFBC. 1990. Canadian Farm Building Code. NRCC No. 30627. National Research Council of Canada, Ottawa, On. 28pp.

Chen, W.F. and E. Mizuno. 1990. Nonlinear analysis in soil mechanics. Developments in Geotechnical Engineering 53, Elsevier Science Publishers B.V.

Cowin, S.C. 1979. The pressure ratio in the theory of bin pressures. Journal of Applied Mechanics, Transaction of the ASME, 46:524-528.

Dafalias, Y.F. and E.P. Popov. 1975. A model of nonlinearly hardening materials for complex loadings. Acta Mechanics, 21:173-192.

Dale, A.C. and R.N. Robinson. 1954. Pressure in deep grain storage structures. Agricultural Engineering 35(8):570-573.

Darve, F., H. Dendani. and B. Chau. 1988. Different classes of constitutive equations and their characteristics. Proceedings of the international workshop on constitutive equations for granular non-cohesive soils, Case Western University, Cleveland, Ohio, 11-17.

Desai, C.S., M.M. Zaman, J.G. Lightner and H.J. Siriwardance. 1984. Thin-layer element for interfaces and joints. International Journal for Numerical and Analytical Methods in Geomechanics, 8:19-43.

DIN. 1987. Design loads for buildings - loads on silos. DIN 1055, Blatt 6, Deutsche Normen, Berlin.

Drucker, D.C. and W. Prager. 1952. Soil Mechanics and Plastic or Limit Design. Quarterly of Applied Mathematics, 10:157-175.

Fung, Y.C. 1965. Foundations of solid mechanics. Prentice-Hall, Inc., Englewood Cliffs, N.J.

Granik, V. T. and M. Ferrari. 1993. Microstructural mechanics of granular media. Mechanics of Materials 15:301-322.

Han, C. and A. Drescher. 1993. Shear bands in biaxial tests on dry coarse sand. Soils and Foundations, 33:118-132.

Horne, M.R. 1964. The behavior of an assembly of rotund, rigid, cohesionless particles. Proceeding of Royal Society, 278:62-90.

Janssen, H.A. 1895. Versuche über getreidedruck in silozellen. Zzeitschriff des Vereines Deutscher Ingenieure, 39: 1045-1049.

Jenike, A.W. 1980. Effect of solids flow properties and hopper configuration. Unit and Bulk Materials Handling. ASME. United Engineering Centre, 345 East 47th Street, New York.

Jenike, A.W. and J.R. Johanson. 1968. Bin loads. Journal of Structural Division, Proceedings of ASCE, 94(ST4):1011-1041.

Jenike, A.W. and J.R. Johanson. 1969. On the theory of bin loads. Journal of Engineering for Industry, Transaction of the ASME, 92:339-344.

Jacoben, M. 1992. Shear strength of uni-sized gravels under triaxial compression. Soils and Foundations, 32:148-152.

Kmita, J. 1991. An experimental analysis of internal silo loads. Bulk Solids Handling, 11:459-468.

Katona, M.G. and M.A. Mulert. 1984. A Viscoplastic Cap Model for Soils and Rock. Mechanics of Engineering Materials, Edited by C. S. Desai and R. H. Gallapher, Johon Wiley and Sons Ltd.

Ketchum, M.S. 1909. The design of walls, bins, and grain elevators, McGraw-Hill, New York, NY.

Lade, P.V. and J.M. Duncan. 1973. Cubical triaxial tests on cohesionless soil. Journal of Soil Mechanics, ASCE, 99:793-812.

Lade, P.V. and J.M. Duncan. 1975. Elastoplastic stress-strain theory for cohesionless soil. Journal of Geotechnical Engineering, ASCE, 101:1037-1053.

Lade, P.V. 1977. Elasto-plastic stress-strain theory for cohesionless soil with curved yield surfaces. International Journal of Solids and Structures, 13:1019-1035.

Lee, K.L. and H.B. Seed. 1967. Drained strength characteristics of sands. Journal of the soil mechanics and foundations division. Proceedings of the American Society of Civil Engineers, 93:117-141.

Mahmoud, M.H. 1979. Shallow flexible grain bins. Ph.D. Thesis, University of Windsor, On. Canada.

Manbeck, H.B., V.M. Puri, M.G. Britton. 1995. Structural loads in grain storages. In: Stored grain ecosystems, edited by D.S. Jayas, N.D.G. White and W.E. Muir, Marcel Dekker, Inc., NY, USA.

Mohsenin, N. N. 1986. Physical Properties of Plant and Animal Materials. Second Edition, Gordon and Breach Science Publisher, New York, NY, USA.

Momen, H. and J. Ghaboussi. 1982. Stress dilatancy and normalized work for sands. IUTAM Conference on deformation and failure of granular materials, 265-274.

Moroto, N. 1987. On deformation of granular materials in simple shear. Soils and Foundations, 27:77-85.

Mróz, Z. 1967. On the description of anisotropic hardening. Journal of the Mechanics and Physics of Solids, 15:163-175.

Negussey, D. and Y.P. Vaid. 1990. Stress dilatancy of sand at small stress ratio states. Soils and Foundations, 30:155-166.

Nemat-Nasser, S. 1980. On behaviour of granular materials in simple shear. Soils and Foundations, 20:59-73.

Nemat-Nasser, S. 1982. Fabric and its influence on mechanical behaviour of granular materials. Deformation and failure of granular materials edited by P.A. Vermeer and H.J.Luger, 37-42.

Oda, M. 1977. Co-ordination number and its relation to shear strength of granular materials. Soils and Foundations, 17:29-42.

Ooi, J.Y. and J.M. Rotter. 1990. Wall pressures in squat steel silos from simple finite element analysis. Computers & Structures, 37:361-374.

Ord, A., I. Vardoulakis and R. Kajewski. 1991. Shear band formation in Gasford sandstone. International Journal of Rock Mech. Min. Sci. & Geomech. Abstr., 28:397-409.

Peters, J.F. 1988. Internal variable model for frictional materials. Proceedings of the international workshop on constitutive equations for granular non-cohesive soils, Case Western University, Cleveland, Ohio, 551-569.

Prat, P.C. and Z.P. Bazant. 1991. Microplane model for triaxial deformation of saturated cohesive soils. Journal of Geotechnical Engineering, 117:891-912.

Puri, V.M. and H.B. Manbeck. 1991. Potential of finite element method in modelling load response of particulate materials. ASAE Paper 91-4076, American Society of Agricultural Engineers, St. Joseph, MI, USA.

Rankine, W.J.M. 1857. On the stability of loose earth. Phil. Trans. Royal Soc. London. 147pp.

Reimbert, M. and A. Reimbert. 1956. Silos traite theorique et practique. Edition Eyrolles, Paris.

Roberts, A.W. 1991. Recent developments and future directions. Bulk Solids Handling, 11:17-35.

Rotter, J.M. and Q. Zhang. 1989. Elastic buckling of imperfect cylindrical shells containing

granular solids. Research Report-University of sydney, School of Civil and Mining Engineering n R589 Feb 1989 34p.

Rowe, P.W. 1962. The stress-dilatancy relation for static equilibrium of an assembly of particles in contact. Proceeding of Royal Society, 269:500-527.

Rong, G. 1994. Discrete element modelling for flow of particulte materials in bins. Ph.D. thesis, University of Guelph, Ontario, Canada.

Schmidt, L.C. and Y.H. Wu. 1989. Prediction of dynamic wall pressures on silos. Bulk Solids Handling, 9:333-338.

Shield, R.T. 1955. On Coulomb's law of failure in soils. Journal of the Mechanics and Physics of Solids, 4:10-16.

Smith, D.L.O. and R.A. Lohnes. 1980. Grain silo overpressures induced by dilatancy upon unloading. ASAE Paper No. 80-3013, American Society of Agricultural Engineers, St. Joseph, MI, USA.

Smith, D.L.O. and R. A. Lohnes. 1983. Bulk strength and stress-strain behaviour of four agricultural grains. Journal of Powder & Bulk Solids Technology 7(4):1-7.

Subhash, G., S.Nema-Nasser, M.M.Mehrabadi and H.M.Shodja. 1991. Experimental investigation of fabric-stress relations in granular materials. Mechanics of materials, 11:87-106.

Theimer, O.F. 1969. Failures of reinforced concrete grain silos. Journal of Engineering for Industry, Transactions of the ASME, Series B, 91:460-477.

Thompson, S.A.; Galili, N.; Williams, R.A. 1995. Lateral pressures during filling of a full-scale grain bin. Transactions of ASAE, 38(3):919-926.

Tripodi, M.A., V.M. Puri, H.B. Manbeck and G.L. Messing. 1992. Constitutive models for cohesive particulate materials. Journal of Agricultural Research, 53:1-21.

Vardoulakis, I. 1980. Shear band inclination and shear modulus of sand in biaxial tests. International Journal for Numerical and Analytical Methods in Geomechanics, 4:103-119.

Valanis, K.C. 1971. A theory of viscoplasticity without a yield surface, part I: General theory. Archives of Mechanics, 23: 517-533.

Valanis, K.C. 1980. Fundamental consequences of a new intrinsic time measure, plasticity as a limit of the endochronic theory. Archives of Mechanics, 32: 171-191.

Valanis, K.C. 1984. Continuum foundations of endochronic plasticity. Transactions of the ASME, 106:367-375.

Valanis, K.C. and J. Fan. 1984. A numerical algorithm for endochronic plasticity and comparison with experiment. Computer & Structures, 19:717-724.

Valanis, K.C. and J.F. Peters. 1991. An endochronic plasticity theory with shear-volumetric coupling. International Journal for Numerical and Analytical Methods in Geomechanics, 15:87-102.

Watanabe, O. and S.N. Atluri. 1985. An new endochronic approach to computational elasto-plasticity: example of a cyclically loaded cracked plate. ASME, Journal of Applied Mechanics, 52: 857-864.

Watanabe, O. and S.N. Atluri. 1986. Internal time, general internal variable, and multi-yield-surface theories of plasticity and creep: a unification of concepts. International Journal of Plasticity, 2:37-57.

Wu, H.C. and T.P. Wang. 1983. Endochronic description of sand response to static loading. Journal of Engineering Mechanics, 109:970-989.

Wu, H.C. and M.R. Aboutorabi. 1988. Endochronic modelling of coupled volumetric-deviatoric behaviour of porous and granular materials. International Journal of Plasticity, 4:163-181.

Xu, S., Q. Zhang, M.G. Britton. 1991. Applicability of endochronic model to grain en masse. ASAE Paper 91-4516, American Society of Agricultural Engineers, St. Joseph, MI, USA.

Xu S. 1992. Endochronic finite element analysis of loads in grain storage bins. A thesis for the *Degree of Master of Science* in structure & environment, Department of Agricultural Engineering, University of Manitoba, Canada.

Xu, S., Q. Zhang and M.G. Britton. 1993a. Effect of grain dilatancy on dynamical loads in grain bins. ASAE paper: 93-4504, American Society of Agricultural Engineers, 2950 Niles Road, St. Joseph, Michigan, USA.

Xu, S., Q. Zhang and M.G. Britton. 1993b. An endochronic finite element model for predicting loads in grain storage structures. Transactions of the ASAE, 36: 1191-1199.

Zhang, Q. 1987. Finite element analysis of grain storage bin behaviour for static and thermal loads using elastoplastic constitutive equation. Ph.D. dissertation. The Pennsylvania State University, University Park, Pa, USA.

Zhang, Q. and M.G. Britton. 1995. Predicting hygroscopic loads in grain storage bins.

Transactions of the ASAE 38(4):1221-1226.

Zhang, Q., M.G. Britton and R. Jaremek. 1993. Dynamical loads during discharge for wheat, barley and conola in a smooth and corrugated-walled model bin. J. Agric. Engng Res., 56:111-119.

Zhang, Q., M.G. Britton and S. Xu. 1994b. Using dilatancy angle to predict dynamical loads during discharge in bulk solids storage structure. Proceedings of the 1994 Powder and Bulk Solids: 383-389.

Zhang, Q., M.G. Britton and S. Xu. 1995. Moisture induced loads in bulk solids storage structure. Proceedings of the 1995 Powder and Bulk Solids: 509-515.

Zhang, Q., S. Xu. and M.G. Britton. 1994a. Application of dilatancy theories in predicting dynamical loads in bulk solids storage structures. ASAE paper: 94-4512, American Society of Agricultural Engineers, 2950 Niles Road, St. Joseph, Michigan, USA.

Zhang, Q., V.M. Puri, H.B. Manbeck. 1989. Static and thermal loads in full size grain bins predicted by vectorized FEM on supercomputer. Transaction of the ASAE. 32:685-690.

Zhang, Q., V.M. Puri, H.B. Manbeck and M.C. Wang. 1987. A finite element model for predicting static and thermally induced bin wall pressures. Transactions of the ASAE 30:1797-1806.

APPENDIX LIST OF FINITE ELEMENT CODES

```
C   ------------------------------------------------------------------------------
C     A FORTRAN PROGRAM FOR FINITE ELEMENT ANALYSIS
C          OF GRAIN-BIN SYSTEMS
C     USING ENDOCHRONIC MODELS & INITIAL STRESS METHOD
C   ------------------------------------------------------------------------------
C
          IMPLICIT REAL*8(A-H,O-Z)
          INTEGER NEY,NEX,NE,NDF,KSTAGE
C.....( NC1, NC2, NC3 ) ARE USED TO DEFINE SIZES OF ARRAYS
C    NDF:          NUMBER OF DEGREE OF FREEDOM
C    NE:           NUMBER OF ELEMENT
C    A(NDF,NDF): STIFFNESS MATRIX
C    F(NDF):       FORCE VECTOR
C    DISP(NDF): DISPLACEMENT VECTOR
C    U(NDF):       DISPLACEMENT INCREMENT VECTOR
C    STE( ):       STRESS
C    STN( ):       STRAIN
C    STER( ):      STRESS INCREMENT
C    STNR( ):      STRAIN INCREMENT
C    STEE(4): ELEMENT STRESS
C    STNE(4): ELEMENT STRAIN
C    DZ(I):         INTRINSIC TIME FOR ELEMENT I
C    Q1(),Q2():BACK STRESS
C    HZ() :         "PLASTIC" STRESS VECTOR
C    XC(4,I):      X-COORDINATE FOR ELEMENT I
C    YC(4,I):      Y-COORDINATE FOR ELEMENT I
C    MODEL: 1 FOR STRESS-BASED THEORY; OTHERS FOR STRAIN-BASED
C
          PARAMETER(NC1=480,NC2=960,NC3=240)
          DIMENSION U(NC1),U1(NC1),DISP(NC1),F1(NC1),RZ(NC1),B(NC1,NC1)
          DIMENSION STEE(4),STNE(4),DEP(4),DSTE(4),F4(4)
          COMMON/CODE/KI,KO,MODEL
          COMMON/KMAT/A(NC1,NC1),F(NC1)
          COMMON/STREN/STE(NC2),STN(NC2),STER(NC2),STNR(NC2)
          COMMON/WALL/HBIN,RBIN,TBIN,EMW,PRW
          COMMON/INTF/EMIN,EMIH,PRI,CKW,CKB,CFW,CFB,THR,TBI,TWI
          COMMON/LOADS/DEN,DPS1,DPS2,CT,NDEP,NSCH1,NSCH2
          COMMON/GRID/KODE(NC3),ND(4,NC3),XC(4,NC3),YC(4,NC3),KWALL
          COMMON/CONST/PA,PI,NN2,NN4,NN8
          COMMON/ENDO/DZ(NC3),EVP(NC3),VP(NC3),Q1(NC2),Q2(NC2)
          COMMON/PARAM/EK,EG,GAMA,EKA,FID,AL1,A1,FI1,AE,CE
          COMMON/PARS/G1,C0,CC1,HJ1,B1
          COMMON/F/HZ(NC2),HS(NC2),HZ1(NC2),YA1(NC2),YA2(NC2)
C.... CONSTANTS
          KI=5
          KO=6
          NN2=2
          NN4=4
          NN8=8
```

```
      PA=10.13
      PI=3.14159
      TOLF=0.01D0
      NITZ=6
C
C        INPUT AND OUTPUT PARAMETERS
C        ---------------------------------------------
      READ(KI,*) MODEL
C..... CONTROLL PARAMETERS
      READ(KI,*) KOUT,NDEP,NSCH1,NSCH2,NITM,TOL
      READ(KI,*) NEX,NEY
C..... BIN PARAMETERS
      READ(KI,*) HBIN,RBIN,TBIN,EMW,PRW,CT
      WRITE(KO,3) HBIN,RBIN,TBIN,EMW,PRW,CT
      FORMAT(5X,'BIN PARAMETERS:',/10X,'HEIGHT=',T35,F15.4/10X,
     *'RADIUS=',T35,F15.4/10X,'WALL THICKNESS=',T35,F15.4/10X,
     *'ELASTIC MODULUS=',T35,E15.4/10X,'POISSON RATIO=',T35,F15.4/10X,
     *'COEFF OF CONTRACTION=',T35,E15.4//)
C..... INTERFACE PARAMETERS
      READ(KI,*) EMIN,EMIH,PRI,CKW,CKB,CFW,CFB,THR
      WRITE(KO,4) EMIN,EMIH,PRI,CKW,CKB,CFW,CFB,THR
4     FORMAT(5X,'INTERFACE PARAMETERS:',
     */10X,'ELASTIC MODULI=',T30,2E15.4/10X,
     *'POISSON RATIO=',T30,F15.4/10X,'DISP MOULI =',T30,2F15.4/10X,
     *'FRICTION COEFF=',T30,2F15.4/10X,
     *'RATIO OF WIDTH TO HEIGHT=',5X,F15.4//)
C..... SURCHARGE LOADS
      READ(KI,*) PS1,PS2
      WRITE(KO,9) PS1,PS2
      FORMAT(5X,'LOAD VALUES:',/10X,'SURCHARGES=',T35,2F15.4/10X,
     * //5X,50('*')//)
C..... GRAIN PARAMETERS (endochronic MODEL)
      READ(KI,*) EK,EG,GAMA,EKA,FID
      READ(KI,*) AL1,A1,FI1,AE,CE
      READ(KI,*) G1,C0,CC1,HJ1,B1
      WRITE(KO,16) G1,C0,CC1,HJ1,B1
16    FORMAT(2X,' ENDOCHRONIC MODEL PARAMETERS (STRESS-BASED):',//5X,
     *'COUPLING COEFF.:GAMA1',T35,F15.4/5X,
     *'KERNEL FUNCTION:C0,CC1,J1',T35,3E10.3/5X,
     *'BETA1: ',T35,E10.3,//5X,50('*')//)
      WRITE(KO,17) EK,EG,GAMA,EKA,FID,AL1,A1,FI1,AE,CE
17    FORMAT(2X,' ENDOCHRONIC MODEL PARAMETERS (STRAIN-BASED):',//5X,
     *'MODULI: K,G ',T35,2E15.4/5X,
     *'COUPLING COEFF.:GAMA,EKA',T35,2F15.4/5X,
     *'KERNEL FUNCTION:FID,AL1,A1',T35,3E10.3/5X,
     *'HARDENING FUNCTION:FI1,AE,CE ',T35,3E10.3/5X,//5X,50('*')//)
      READ(KI,*) DEN,ANG
C
C GRADING
      CALL MGRID(NEX,NEY,NE,NDF,NGF)
      NST=4*NE
C INITIALIZATION
```

```
      KSTAGE=0
      IF(NDEP.EQ.0) KSTAGE=1
      CALL INULV(DISP,NC1)
      CALL INULV(EVP,NC3)
      CALL INULV(VP,NC3)
      CALL INULV(STE,NC2)
      CALL INULV(STN,NC2)
      CALL NULVEC(Q1,NC2)
      CALL NULVEC(HZ,NC2)
      CALL NULVEC(DZ,NE)
C
C           LOADING LOOP STARTS HERE
C           ----------------------------------------
C
C.... INCREMENT OF LOAD
      IF(NSCH1.GT.0) DPS1=PS1/FLOAT(NSCH1)
      IF(NSCH2.GT.0) DPS2=PS2/FLOAT(NSCH2)
      NSCH=NSCH1+NSCH2
      NSCHE=NSCH+1
C.....SURCHARGE LOOP; INCREMENT = 1, NSCH1+MSCH2
      DO 200 KS=1,NSCHE
      IF(NDEP.GT.0) DEN=DEN/FLOAT(NDEP)
      KW=NDEP
      IF(KW.LE.0) KW=1
C.....LOADS LOOP; INCREMENT = 1, NDEP
      DO 100 KL=1,KW
      CALL NULVEC(YA1,NC2)
C
C           FORM AND SOLVE SYSTEM EQUATION
C           ------------------------------------------------------
      CALL NULVEC(HZ1,NC2)
      CALL FORCE(F,NE,NEX,NEY,NDF)
      ZNORM=0.0D0
      DO 166 I=1,NDF
166   ZNORM=ZNORM+F(I)*F(I)
      DO 43 M=1,NDF
      F1(M)=F(M)+F1(M)
43    CONTINUE
C
C        CALCULATE INITIAL ELASTIC RESPONCE
C        ----------------------------------
      CALL STIFF(NEX,NEY,NE,NDF)
      CALL MODIFY(NDF,NEY,NEX)
C --- CALCULATE NEW DISPLACEMENT VALUES
      CALL SOLVE(U,NDF)
C --- CALCULATE AND UPDATE STRESSES AND STRAINS
      CALL STRESS(NEY,NEX,NE,U)
      DO 75 I=1,NST
      STE(I)=STE(I)+STER(I)
      STN(I)=STN(I)+STNR(I)
75    CONTINUE
C.....ACCUMULATE DISPLACEMENTS
```

```
          DO 85 I=1,NDF
          DISP(I)=DISP(I)+U(I)
85      CONTINUE
C
C           ITERATION FOR UNBALANCED FORCES
C           ------------------------------------------------------
          DO 111 KF=1,6
          CALL INTRIN(NE,NST)
          DO 150 I=1,NST
          STE(I)=STE(I)+HZ(I)
          Q1(I)=Q2(I)
          YA1(I)=YA2(I)
150       CONTINUE
          WRITE(6,*)'HZ:',(HZ(I),I=1,NST)
C --- CALCULATE AND UPDATE STRESSES AND STRAINS
          CALL FMOD(NE,NDF,F1)
          CALL STIFF(NEX,NEY,NE,NDF)
          CALL MODIFY(NDF,NEY,NEX)
C**** CHECK IF THE SOLUTION IS REACHED ( ERR < TOLERENCE )
C.....CALCULATION OF NORMALS
          RNORM=0.0D0
          DO 66 I=1,NDF
66      RNORM=RNORM+F(I)*F(I)
          RATIO=RNORM/ZNORM
          WRITE(KO,330) KZ,RATIO,RNORM,ZNORM
330       FORMAT(1X,'ITERATION',I4,4X,'RESIDUAL',3E12.4)
C --- CALCULATE NEW DISPLACEMENT VALUES
          CALL SOLVE(U,NDF)
C --- CALCULATION AND UPDATE STRESSES AND STRAINS
          CALL STRESS(NEY,NEX,NE,U)
          DO 175 I=1,NST
          STE(I)=STE(I)+STER(I)
          STN(I)=STN(I)+STNR(I)
175       CONTINUE
C.....UPDATE INTRINSIC TIME COMPONENT
          DO 37 I=1,NE
          VP(I)=VP(I)+EVP(I)
37        CONTINUE
          IF(RATIO.LE.0.01) GOTO 95
111       CONTINUE
C END OF ITERATION
          WRITE(KO,94) RATIO
94        FORMAT(1X//5X,50('*')/10X, '**** WARNING ****',/5X,
         *'PLASTIC FORCE FAILED TO CONVERGE',/10X,'RATIO = ',E15.4///)
          CALL OUTPUT(NE,NEY,NEX,0,KOUT,DISP,TEMP)
          STOP
C
95        CALL TENCHK(NE,NEX,NEY)
C IF NO GRAIN/INTERFACE ELEMENTS ARE IN TENSION, CONTINUE
C.....UPDATE BACK STRESSES
          DO 550 I=1,NST
          Q1(I)=Q2(I)
```

```
550    CONTINUE
100    CONTINUE
C END OF INCREMENT OF LOADS
C
C            OUTPUT RESULTS
C            ------------------------
C STATIC PRESSURE WITHOUT SURCHARGE
         WRITE(6,*)'STE:'
         CALL WRT(NE,NST,STE)
         CALL OUTPUT(NE,NEY,NEX,KSTAGE,KOUT,DISP,TEMP)
         IF(NSCH.EQ.0) GOTO 210
110    IF(KSTAGE.GT.1) GOTO 210
200    CONTINUE
C END OF INCREMENT OF SURCHARGE
C STATIC PRESSURE WITH SURCHARGE
         CALL OUTPUT(NE,NEY,NEX,KSTAGE,KOUT,DISP,TEMP)
210    STOP
         END
C          ------------------------------------------------
C          SUBROUTINES FOR THE SYSTEM
C          ------------------------------------------------
         SUBROUTINE WRT(NE,NST,W)
         IMPLICIT REAL*8(A-H,O-Z)
         DIMENSION W(NST)
         DO 10 I=1,NE
         J1=4*I
         J0=J1-3
10     WRITE(6,111) I,(W(J),J=J0,J1,1)
111    FORMAT(1X,I5,4D15.6)
         RETURN
         END
C
C-------------------------------------------------AUTOMATIC GRIDING
         SUBROUTINE MGRID(NEX,NEY,NE,NDF,NGF)
C---------------------------------------MGRID(NEX,NEY,NE,NDF,NGF)
         PARAMETER(NC1=480,NC2=960,NC3=240)
         IMPLICIT REAL*8(A-H,O-Z)
         DIMENSION X(NC3),Y(NC3)
         COMMON/CODE/KI,KO,MODEL
         COMMON/GRID/KODE(NC3),ND(4,NC3),XC(4,NC3),YC(4,NC3),KWALL
         COMMON/WALL/HBIN,RBIN,TBIN,EMW,PRW
         COMMON/INTF/EMIN,EMIH,PRI,CKW,CKB,CFW,CFB,THR,TBI,TWI
         CALL NULMAT(XC,4,NE)
         CALL NULMAT(YC,4,NE)
         RTB=0.01D0
         WRITE(6,*)'RTB :',RTB
         XN=RBIN/FLOAT(NEX)
         YN=HBIN/FLOAT(NEY)
C TBI=THICKNESS OF INTERFACE(BOTTOM); TWI(WALL)
         TBI=RTB*XN
         TWI=RTB*YN
         NX1=NEX+1
```

```
      NX2=NEX+2
      NY1=NEY+1
      NE=NX2*NEY+NEX
      NGF=NX2*NY1+NX1
      NDF=2*NGF
      DO 1 I=1,4
      DO 1 J=1,NE
1     ND(I,J)=0
C KODE= -1/BOTTOM INTERFACE; 0/WALL 1/INTERFACE; 4/GRAIN
      DO 80 I=1,NX1
      KODE(I)=-1
      X(I)=XN*FLOAT(I-1)
80    Y(I)=0.0D0
      KODE(NX1)=4
      X(NX1)=X(NX1)-TWI
      DO 10 J=1,NY1
      Y1=(J-1)*YN
      IF(J.EQ.1)Y1=Y1+TBI
      I1=(J-1)*NX2+NX1
      DO 10 I=1,NX2
      II=I1+I
      Y(II)=Y1
      KODE(II)=4
      IF(I.EQ.NEX) KODE(II)=1
      IF(I.EQ.NX1) KODE(II)=0
10    CONTINUE
      DO 20 I=1,NX2
      X1=(I-1)*XN
      X11=X1
      DO 20 J=1,NY1
      JJ=(J-1)*NX2+I+NX1
      IF(I.EQ.NX1)X1=X11-TWI
      IF(I.EQ.NX2)X1=X11-XN
20    X(JJ)=X1
      DO 50 I=1,NE
      K=I
      IF(I.GT.NEX)K=I+1
      ND(1,I)=K
      ND(2,I)=K+1
      IF(KODE(I).EQ.0) ND(2,I)=NX2+K
      IF(KODE(I).EQ.0) GOTO 50
      IF(I.LE.NEX)K=I-1
      ND(3,I)=K+1+NX2
      ND(4,I)=K+NX2
50    CONTINUE
      DO 70 I=1,NE
      DO 70 J=1,4
      J1=ND(J,I)
      IF(J1.LE.0) GOTO 70
      XC(J,I)=X(J1)
      YC(J,I)=Y(J1)
70    CONTINUE
```

```
C DETERMINING ELEMENT TYPE FOR BIN WALL:
C KWALL = 0 / THIN WALL; 1 / THICK WALL
      DR=RBIN/FLOAT(NEX)
      RATIO=TBIN/DR
      KWALL=0
      IF(RATIO.GE.10.0D0) KWALL=1
      RETURN
      END
C
C-------------------- MODIFYING [K] {U} = {F} (ACCORDING TO BC'S)
      SUBROUTINE MODIFY(NDF,NEY,NEX)
C-----------------------------------------------MODIFY(NDF,NEY,NEX)
      PARAMETER(NC1=480,NC2=960,NC3=240)
      IMPLICIT REAL*8(A-H,O-Z)
      COMMON/KMAT/A(NC1,NC1),F(NC1)
      NC=NEX*2+3
      NM=NC+NEY+1
      DO 10 I=1,NM
      K=I
      IF(I.GT.NC)K=I+NC-1
      IF(I.GT.(NC+2))K=(I-NC-2)*(NEX+2)*2+2*NC+1
      CALL MZERO(NDF,K)
10    CONTINUE
      RETURN
      END
C
C------------------------------------ GLOBAL STIFFNESS MATRIX A
      SUBROUTINE STIFF(NEX,NEY,NE,NDF)
C-----------------------------------------------STIFF(NEX,NEY,NE,NDF)
      PARAMETER(NC1=480,NC2=960,NC3=240)
      IMPLICIT REAL*8(A-H,O-Z)
      DIMENSION ND2(8),CORD(4,2),WEIT(3),SAMP(3),DER(2,4),DERV(2,4),
     *DERW(2),DERVW(2),BE(4,8),BT(8,4),BTDB(8,8),FUN(4),
     *STEE(4),STNE(4), BEW(2,4),BTW(4,2),BTDBW(4,4),FUNW(2),
     *D(4,4),DB(4,8),DW(2,2),DBW(2,4)
      REAL*8 KE(8,8),JINV(2,2),JAC(2,2)
      COMMON/KMAT/A(NC1,NC1),F(NC1)
      COMMON/STREN/STE(NC2),STN(NC2),STER(NC2),STNR(NC2)
      COMMON/INTF/EMIN,EMIH,PRI,CKW,CKB,CFW,CFB,THR,TBI,TWI
      COMMON/WALL/HBIN,RBIN,TBIN,EMW,PRW
      COMMON/GRID/KODE(NC3),ND(4,NC3),XC(4,NC3),YC(4,NC3),KWALL
      COMMON/CONST/PA,PI,NN2,NN4,NN8
      COMMON/PARAM/EK,EG,GAMA,EKA,FID,AL1,A1,FI1,AE,CE
      COMMON/PARS/G1,C0,CC1,HJ1,B1
C
      NST=4*NE
      DO 10 I=1,NDF
      DO 10 J=1,NDF
10    A(I,J)=0.0D0
C GAUSSIAN POINTS AND WEIGHT
      CALL GAUSS(NGP,SAMP,WEIT)
C CALCULATION OF ELEMENT STIFFNESS MATRIX [K]e
```

```
C.... DO FOR EACH ELEMENT
          DO 100 I=1,NE
          CALL INULV(ND2,NN8)
          CALL NULMAT(KE,NN8,NN8)
          KOD=KODE(I)
          DO 15 J=1,4
          J1=4*(I-1)+J
          STEE(J)=-STE(J1)
          STNE(J)=-STN(J1)
          CORD(J,1)=XC(J,I)
          CORD(J,2)=YC(J,I)
          K1=2*ND(J,I)
          IF(K1.LE.0) GOTO 15
          ND2(2*J-1)=K1-1
          ND2(2*J)=K1
15      CONTINUE
C STRESS-STRAIN MATRIX
C... THIN WALL
          IF(KOD.EQ.0.AND.KWALL.EQ.0) CALL DMATW(DW,EMW,PRW)
 C THICK WALL
          IF(KOD.EQ.0.AND.KWALL.EQ.1) CALL DMATE(D,EMW,PRW)
C FLOOR INTERFACE
          IF(KOD.EQ.-1) CALL DMATI(D,STEE,STNE,KOD,EG,EK)
C WALL INTERFACE
          IF(KOD.EQ.1) CALL DMATI(D,STEE,STNE,KOD,EG,EK)
C GRAIN
          IF(KOD.GE.3) CALL DMATG(D,EG,EK)
C********** INTEGRATION OF [B]T[D][B] dv
          IF(KOD.NE.0.OR.KWALL.NE.0) GOTO 40
C.....1-D LINEAR ELEMENT (THIN WALL ELEMENT)
C     DO 35 J=1,NGP
C     C=WEIT(J)
C     X=SAMP(J)
          C=2.0
          X=0.0
          CALL SHPFW(FUNW,DERW,X)
          VJAC=DERW(1)*CORD(1,2)+DERW(2)*CORD(2,2)
          DERVW(1)=DERW(1)/VJAC
          DERVW(2)=DERW(2)/VJAC
          CALL NULMAT(BEW,NN2,NN4)
          CALL BWMAT(BEW,DERVW,FUNW,RBIN)
          CALL MATMUL(DBW,DW,NN2,NN2,BEW,NN2,NN4)
          CALL MATRAN(BTW,BEW,NN2,NN4)
          CALL MATMUL(BTDBW,BTW,NN4,NN2,DBW,NN2,NN4)
          COEF=DABS(VJAC)*C*2.0D0*PI*RBIN*TBIN
          DO 35 K1=1,NN4
          DO 35 K2=1,NN4
          KE(K1,K2)=KE(K1,K2)+BTDBW(K1,K2)*COEF
35      CONTINUE
          GOTO 65
40      CONTINUE
C.....2-D QUADRILATERAL ELEMENT
```

```
C     DO 60 J1=1,NGP
C     DO 60 J2=1,NGP
C     C1=WEIT(J1)
C     C2=WEIT(J2)
C     X=SAMP(J1)
C     Y=SAMP(J2)
            C1=2.0
            C2=2.0
            X=0.0
            Y=0.0
            CALL SHPFUN(FUN,DER,X,Y)
            CALL MATMUL(JAC,DER,NN2,NN4,CORD,NN4,NN2)
            CALL INVBY2(JAC,JINV,DETM)
            CALL MATMUL(DERV,JINV,NN2,NN2,DER,NN2,NN4)
            CALL BEMAT4(BE,EQR,DERV,FUN,CORD,NN4)
            CALL MATMUL(DB,D,NN4,NN4,BE,NN4,NN8)
            CALL MATRAN(BT,BE,NN4,NN8)
            CALL MATMUL(BTDB,BT,NN8,NN4,DB,NN4,NN8)
            COEF=DABS(DETM)*C1*C2*2.0D0*PI*EQR
            DO 60 K1=1,NN8
            DO 60 K2=1,NN8
            KE(K1,K2)=KE(K1,K2)+BTDB(K1,K2)*COEF
60        CONTINUE
C INSETRT ELEMENT STIFFNESS MATRIX  INTO GLOBAL MATRIX
65        DO 80 J1=1,NN8
            DO 80 J2=1,NN8
            IA=ND2(J1)
            JA=ND2(J2)
            IF(IA.LE.0.OR.JA.LE.0) GOTO 80
            A(IA,JA)=A(IA,JA)+KE(J1,J2)
80       CONTINUE
246      FORMAT(1X,8E10.4)
100      CONTINUE
            RETURN
            END
C
C------------------------------ CALCULATION OF STRESS AND STRAIN
            SUBROUTINE STRESS(NEY,NEX,NE,U)
C-----------------------------------------STRESS(NEY,NEX,NE,U)
            PARAMETER(NC1=480,NC2=960,NC3=240)
            IMPLICIT REAL*8(A-H,O-Z)
            INTEGER NN4,NN8
            DIMENSION U(NC1)
            DIMENSION ND2(8),D(4,4),BE(4,8),DSN(4),DSS(4),DSNT(4),
           * CORD(4,2),WEIT(3),SAMP(3),DER(2,4),DERV(2,4),
           * FUN(4),DEF(8),STEE(4),STNE(4),DW(2,2),BEW(2,4),FUNW(2),
           * DERW(2),DERVW(2),DSNW(2),DSSW(2),DEFW(4)
            REAL*8 JAC(2,2),JINV(2,2)
            COMMON/CODE/KI,KO,MODEL
            COMMON/STREN/STE(NC2),STN(NC2),STER(NC2),STNR(NC2)
            COMMON/WALL/HBIN,RBIN,TBIN,EMW,PRW
            COMMON/INTF/EMIN,EMIH,PRI,CKW,CKB,CFW,CFB,THR,TBI,TWI
```

```
      COMMON/GRID/KODE(NC3),ND(4,NC3),XC(4,NC3),YC(4,NC3),KWALL
      COMMON/CONST/PA,PI,NN2,NN4,NN8
      COMMON/PARAM/EK,EG,GAMA,EKA,FID,AL1,A1,FI1,AE,CE
      COMMON/PARS/G1,C0,CC1,HJ1,B1
      NST=4*NE
      CALL NULVEC(STER,NST)
      CALL NULVEC(STNR,NST)
C GAUSSIAN POINTS AND WEIGHT
      CALL GAUSS(NGP,SAMP,WEIT)
C
      DO 100 I=1,NE
      CALL INULV(ND2,NN8)
      KOD=KODE(I)
      DO 5 J=1,4
      J1=(I-1)*4+J
      STEE(J)=-STE(J1)
      STNE(J)=-STN(J1)
      CORD(J,1)=XC(J,I)
      CORD(J,2)=YC(J,I)
      K1=2*ND(J,I)
      IF(K1.LE.0) GOTO 5
      ND2(2*J-1)=K1-1
      ND2(2*J)=K1
5     CONTINUE
      IF(KOD.NE.0.OR.KWALL.NE.0) GOTO 10
C***************** GRADIENT MATRIX FOR 1-D THIN WALL ELEMENTS
C     C=WEIT(2)
      X=SAMP(2)
      CALL SHPFW(FUNW,DERW,X)
      VJAC=DERW(1)*CORD(1,2)+DERW(2)*CORD(2,2)
      DERVW(1)=DERW(1)/VJAC
      DERVW(2)=DERW(2)/VJAC
      CALL NULMAT(BEW,NN2,NN4)
      CALL BWMAT(BEW,DERVW,FUNW,RBIN)
C.....STRAINS AND STRESSES FOR 1-D ELEMENTS
      DO 6  J=1,NN4
      JJ=ND2(J)
      IF(JJ.LE.0) GOTO 6
      DEFW(J)=U(JJ)
6     CONTINUE
      CALL MVMUL(DSNW,BEW,NN2,NN4,DEFW,NN4)
      CALL DMATW(DW,EMW,PRW)
      CALL MVMUL(DSSW,DW,NN2,NN2,DSNW,NN2)
      CALL NULVEC(DSN,NN4)
      CALL NULVEC(DSS,NN4)
      DO 8 J=1,NN2
      DSN(J)=DSNW(J)
      DSS(J)=DSSW(J)
8     CONTINUE
      GOTO 90
C************************* GRADIENT MATRIX FOR 2-D ELEMENTS
10    J1=2
```

```
          J2=2
          X=SAMP(J1)
          Y=SAMP(J2)
          CALL SHPFUN(FUN,DER,X,Y)
          CALL MATMUL(JAC,DER,NN2,NN4,CORD,NN4,NN2)
          CALL INVBY2(JAC,JINV,DETM)
          CALL MATMUL(DERV,JINV,NN2,NN2,DER,NN2,NN4)
          CALL NULMAT(BE,NN4,NN8)
          CALL BEMAT4(BE,EQR,DERV,FUN,CORD,NN4)
          DO 15 J=1,NN8
          JJ=ND2(J)
          DEF(J)=U(JJ)
15      CONTINUE
          CALL MVMUL(DSN,BE,NN4,NN8,DEF,NN8)
          DSN(3)=0.5D0*DSN(3)
C.....STRESS-STRAIN MATRICES
30      IF(KOD.GE.3) CALL DMATG(D,EG,EK)
          IF(KOD.EQ.-1) CALL DMATI(D,STEE,STNE,KOD,EG,EK)
          IF(KOD.EQ.1) CALL DMATI(D,STEE,STNE,KOD,EG,EK)
          CALL MVMUL(DSS,D,NN4,NN4,DSN,NN4)
C ....STRESS INCREMENT IS 'DSS'
90      DO 80 J=1,NN4
          J1=(I-1)*4+J
          STER(J1)=DSS(J)
          STNR(J1)=DSN(J)
80      CONTINUE
100     CONTINUE
          RETURN
          END
C
C---------------------------------------- GLOBAL FORCE VECTOR
          SUBROUTINE FORCE(F1,NE,NEX,NEY,NDF)
C---------------------------------------FORCE(F1,NE,NEX,NEY,NDF)
          PARAMETER(NC1=480,NC2=960,NC3=240)
          IMPLICIT REAL*8(A-H,O-Z)
          DIMENSION ND2(8),F1(NDF),CORD(4,2),FE(8)
          COMMON/WALL/HBIN,RBIN,TBIN,EMW,PRW
          COMMON/INTF/EMIN,EMIH,PRI,CKW,CKB,CFW,CFB,THR,TBI,TWI
          COMMON/LOADS/DEN,DPS1,DPS2,CT,NDEP,NSCH1,NSCH2
          COMMON/GRID/KODE(NC3),ND(4,NC3),XC(4,NC3),YC(4,NC3),KWALL
          COMMON/CONST/PA,PI,NN2,NN4,NN8
C
          CALL NULVEC(F1,NDF)
          DO 20 I=1,NE
          KOD=KODE(I)
          IF(KOD.LT.3) GOTO 20
          CALL INULV(ND2,NN8)
          DO 50 J=1,4
          CORD(J,1)=XC(J,I)
          CORD(J,2)=YC(J,I)
          K1=2*ND(J,I)
          IF(K1.LE.0) GOTO 50
```

```
          ND2(2*J-1)=K1-1
          ND2(2*J)=K1
 50     CONTINUE
          CALL WEIGHT(FE,I,CORD,NEY,NEX)
 C    IF(KSTAGE.EQ.1.AND.KS.LE.NSCH1) CALL SCHG1(FE,CORD)
 C     CALL SCHG2(FE,I,CORD,NEX,NEY)
 C.....INSERT ELEMENT FORCE VECTOR INTO GLOBAL VECTOR
          DO 30 J=1,NN8
          JJ=ND2(J)
          IF(JJ.LE.0) GOTO 30
          F1(JJ)=F1(JJ)+FE(J)
 30     CONTINUE
 20     CONTINUE
          RETURN
          END
 C
 C------------------------------ GLOBAL "PLASTIC" FORCE VECTOR
          SUBROUTINE FMOD(NE,NDF,F1)
 C-------------------------------------------------FMOD(NE,NDF,F1)
          PARAMETER(NC1=480,NC2=960,NC3=240)
          IMPLICIT REAL*8(A-H,O-Z)
          DIMENSION ND2(8),CORD(4,2),WEIT(3),SAMP(3),DER(2,4),DERV(2,4),
         * BE(4,8),FUN(4),DSTE(4),STEE(4),DEP(4),F4(4),FZ8(8),BTF(8),
         * BEW(2,4),FUNW(2),DERW(2),DERVW(2),F1(NC1)
          REAL*8 JINV(2,2),JAC(2,2)
          COMMON/ENDO/DZ(NC3),EVP(NC3),VP(NC3),Q1(NC2),Q2(NC2)
          COMMON/F/HZ(NC2),HS(NC2),HZ1(NC2),YA1(NC2),YA2(NC2)
          COMMON/PARAM/EK,EG,GAMA,EKA,FID,AL1,A1,FI1,AE,CE
          COMMON/PARS/G1,C0,CC1,HJ1,B1
          COMMON/KMAT/A(NC1,NC1),F(NC1)
          COMMON/STREN/STE(NC2),STN(NC2),STER(NC2),STNR(NC2)
          COMMON/GRID/KODE(NC3),ND(4,NC3),XC(4,NC3),YC(4,NC3),KWALL
          COMMON/WALL/HBIN,RBIN,TBIN,EMW,PRW
          COMMON/CONST/PA,PI,NN2,NN4,NN8
 C
          CALL NULVEC(F,NDF)
          CALL GAUSS(NGP,SAMP,WEIT)
          DO 100 I=1,NE
          KOD=KODE(I)
          CALL NULVEC(FZ8,NN8)
          CALL NULVEC(F4,4)
          CALL INULV(ND2,NN8)
          DO 15 J=1,4
          J1=4*(I-1)+J
          STEE(J)=STE(J1)
          CORD(J,1)=XC(J,I)
          CORD(J,2)=YC(J,I)
          K1=2*ND(J,I)
          IF(K1.LE.0) GOTO 15
          ND2(2*J-1)=K1-1
          ND2(2*J)=K1
 15     CONTINUE
```

```
          CALL SHIFT(STE,F4,I,1)
          IF(KOD.NE.0) GOTO 40
C.....1-D LINEAR ELEMENT (THIN WALL ELEMENT)
C     DO 606 J=1,NGP
C     C=WEIT(J)
C     X=SAMP(J)
          C=2.0
          X=0.0
          CALL SHPFW(FUNW,DERW,X)
          VJAC=DERW(1)*CORD(1,2)+DERW(2)*CORD(2,2)
          DERVW(1)=DERW(1)/VJAC
          DERVW(2)=DERW(2)/VJAC
          CALL NULMAT(BEW,NN2,NN4)
          CALL BWMAT(BEW,DERVW,FUNW,RBIN)
          CALL NULVEC(BTF,NN8)
          DO 6 K1=1,NN4
          DO 6 K2=1,NN2
          BTF(K1)=BTF(K1)+BEW(K2,K1)*F4(K2)
6       CONTINUE
          COEF=DABS(VJAC)*C*2.0D0*PI*RBIN*TBIN
          DO 606 K1=1,NN4
          FZ8(K1)=FZ8(K1)+BTF(K1)*COEF
606     CONTINUE
          GOTO 65
40      CONTINUE
C.....2-D QUADRILATERAL ELEMENT
C     DO 60 J1=1,NGP
C     DO 60 J2=1,NGP
C     C1=WEIT(J1)
C     C2=WEIT(J2)
C     X=SAMP(J1)
C     Y=SAMP(J2)
          C1=2.0
          C2=2.0
          X=0.0
          Y=0.0
          CALL SHPFUN(FUN,DER,X,Y)
          CALL MATMUL(JAC,DER,NN2,NN4,CORD,NN4,NN2)
          CALL INVBY2(JAC,JINV,DETM)
          CALL MATMUL(DERV,JINV,NN2,NN2,DER,NN2,NN4)
          CALL BEMAT4(BE,EQR,DERV,FUN,CORD,NN4)
          CALL NULVEC(BTF,NN8)
          DO 61 K1=1,NN8
          DO 61 K2=1,NN4
          BTF(K1)=BTF(K1)+BE(K2,K1)*F4(K2)
61      CONTINUE
          COEF=DABS(DETM)*C1*C2*2.0D0*PI*EQR
          DO 60 K1=1,NN8
          FZ8(K1)=FZ8(K1)+BTF(K1)*COEF
60      CONTINUE
C******* INSERT ELEMENT FORCE VECTOR INTO GLOBAL VECTOR
65      DO 80 J2=1,NN8
```

```
          JA=ND2(J2)
          IF(JA.LE.0) GOTO 80
          F(JA)=F(JA)+FZ8(J2)
80      CONTINUE
100     CONTINUE
          DO 200 J=1,NDF
          F(J)=F1(J)-F(J)
C     WRITE(6,*)'F:',(F(I),I=1,NDF)
          RETURN
          END
C
C-----------------------------------------INTRINSIC TIME DZ(NE)
          SUBROUTINE INTRIN(NE,NST)
C-------------------------------------------------INTRIN(NE,NST)
          PARAMETER(NC1=480,NC2=960,NC3=240)
          IMPLICIT REAL*8(A-H,O-Z)
          COMMON/GRID/KODE(NC3),ND(4,NC3),XC(4,NC3),YC(4,NC3),KWALL
          COMMON/STREN/STE(NC2),STN(NC2),STER(NC2),STNR(NC2)
          COMMON/F/HZ(NC2),HS(NC2),HZ1(NC2),YA1(NC2),YA2(NC2)
          COMMON/ENDO/DZ(NC3),EVP(NC3),VP(NC3),Q1(NC2),Q2(NC2)
          COMMON/PARAM/EK,EG,GAMA,EKA,FID,AL1,A1,FI1,AE,CE
          COMMON/PARS/G1,C0,CC1,HJ1,B1
          DIMENSION STEE(4),STNE(4),SR(4),Q(4),S(4)
          CALL NULVEC(DZ,NE)
          CALL NULVEC(HZ,NST)
          CALL NULVEC(Q2,NST)
          DO 100 I=1,NE
          KOD=KODE(I)
          IF(KOD.LT.3) GOTO 100
          CALL SHIFT(STN,SR,I,1)
          VSTN=SR(1)+SR(2)+SR(4)
          CALL SHIFT(HZ1,STNE,I,1)
          CALL SHIFT(STE,STEE,I,1)
          DO 33 J=1,4
          STNE(J)=-STNE(J)
33       STEE(J)=-STEE(J)
          If(MODEL.EQ.1) GOTO 44
          Z1=0.0D0
          CALL YLD(I,STEE,VSTN,Z1,F1)
          IF(F1.LE.0.01D0) ZR=0.0D0
          IF(F1.GT.0.01D0) CALL MULLR(I,STEE,VSTN,Z1,F1,ZR)
          DZ(I)=ZR
44       CALL DHZ(I,STEE,Q)
          CALL SHIFT(HZ,Q,I,0)
100      CONTINUE
          RETURN
          END
C
C           ---------------------------------------------------
C           SUBROUTINES FOR THE ELEMENTS
C           ---------------------------------------------------
C
```

```
C------------------------ANY GRAIN/INTERFACE ELEMENTS = TENSION ?
      SUBROUTINE TENCHK(NE,NEX,NEY)
C-----------------------------------------------TENCHK(NE,NEX,NEY)
      PARAMETER(NC1=480,NC2=960,NC3=240)
      IMPLICIT REAL*8(A-H,O-Z)
      COMMON/CODE/KI,KO,MODEL
      COMMON/GRID/KODE(NC3),ND(4,NC3),XC(4,NC3),YC(4,NC3),KWALL
      COMMON/STREN/STE(NC2),STN(NC2),STER(NC2),STNR(NC2)
      DO 100 I=1,NE
      KOD=KODE(I)
      IF(KOD.EQ.0) GOTO 100
      CALL NUMB(I1,I2,I3,I4,I)
      S1=STE(I1)
      S2=STE(I2)
      S3=STE(I3)
C
      IF(KOD.GE.2) GOTO 10
      IF(S1.LE.0.0D0.AND.S2.LE.0.0D0) GOTO 100
      WRITE(KO,101) I
101   FORMAT(1X/5X,'****** WARNING ******',/5X,
     *'INTERFACE ELEMENT NO.',3X,I3,3X, 'IN TENSION')
      GOTO 90
10    IF(S1.LE.0.0D0.AND.S2.LE.0.0D0) GOTO 100
      WRITE(KO,102) I
102   FORMAT(1X/5X,'****** WARNING ******',/3X,
     *'GRAIN ELEMENT NO.',3X,I3,3X, 'IN TENSION')
90    IF(S1.GT.0.0D0) STE(I1)=-0.1D0
      IF(S2.GT.0.0D0) STE(I2)=-0.1D0
      IF(STE(I4).GT.0.0D0) STE(I4)=-0.1D0
100   CONTINUE
      RETURN
      END
C
C------------------------------- SURCHARGE PRESSURE (CENTER)
      SUBROUTINE SCHG1(FE,CORD)
C-----------------------------------------------SCHG1(FE,CORD)
      IMPLICIT REAL*8(A-H,O-Z)
      DIMENSION FE(8),CORD(4,2)
      COMMON/LOADS/DEN,DPS1,DPS2,CT,NDEP,NSCH1,NSCH2
      COMMON/CONST/PA,PI,NN2,NN4,NN8
      CALL NULVEC(FE,NN8)
      IF(CORD(1,1).NE.0.0D0) RETURN
      WL=0.5D0*(CORD(4,2)-CORD(1,2))
      RAVG=5.0D0
C THIS SHOULD BE THE RADIUS OF THE PRESSURE DEVICE IN CM
      A=2.0D0*PI*RAVG*WL
      PF=DPS1*A/2.0D0
      FE(1)=PF
      FE(7)=PF
      RETURN
      END
C
```

```
C---------------------------------------------- BODY FORCES
SUBROUTINE WEIGHT(FE,I,CORD,NEY,NEX)
C---------------------------------WEIGHT(FE,I,CORD,NEY,NEX)
      IMPLICIT REAL*8(A-H,O-Z)
      DIMENSION FE(8),CORD(4,2)
      COMMON/WALL/HBIN,RBIN,TBIN,EMW,PRW
      COMMON/LOADS/DEN,DPS1,DPS2,CT,NDEP,NSCH1,NSCH2
      COMMON/CONST/PA,PI,NN2,NN4,NN8
      CALL NULVEC(FE,NN8)
      A=(CORD(2,1)-CORD(1,1))*(CORD(3,2)-CORD(2,2))
      PRES=DEN*A*PI/6.0D0
      FE(2)=PRES*(2.0D0*CORD(1,1)+CORD(2,1))
      FE(4)=PRES*(CORD(1,1)+2.0D0*CORD(2,1))
      FE(6)=FE(4)
      FE(8)=FE(2)
      RETURN
      END
C
C---------------------------------------- SURCHARGE PRESSURE (TOP)
      SUBROUTINE SCHG2(FE,I,CORD,NEX,NEY)
C----------------------------------------SCHG2(FE,I,CORD,NEX,NEY)
      IMPLICIT REAL*8(A-H,O-Z)
      DIMENSION FE(8),CORD(4,2)
      COMMON/WALL/HBIN,RBIN,TBIN,EMW,PRW
      COMMON/LOADS/DEN,DPS1,DPS2,CT,NDEP,NSCH1,NSCH2
      COMMON/CONST/PA,PI,NN2,NN4,NN8
      CALL NULVEC(FE,NN8)
      A=PI*RBIN*RBIN
      PRES=DPS2/A*PI/3.0D0*(CORD(3,1)-CORD(4,1))
      FE(6)=PRES*(2.D0*CORD(3,1)+CORD(4,1))
      FE(8)=PRES*(CORD(3,1)+2.D0*CORD(4,1))
      RETURN
      END
C
C-----------------------------------PSEUDO FORCE VECTOR {EP}
      SUBROUTINE DHZ(I,STEE,F4)
C-----------------------------------------------DHZ(I,STEE,F4)
      IMPLICIT REAL*8(A-H,O-Z)
      PARAMETER(NC1=480,NC2=960,NC3=240)
      DIMENSION Q(4),STEE(4),S(4),F4(4),SQ(4)
      COMMON/CODE/KI,KO,MODEL
      COMMON/STREN/STE(NC2),STN(NC2),STER(NC2),STNR(NC2)
      COMMON/F/HZ(NC2),HS(NC2),HZ1(NC2),YA1(NC2),YA2(NC2)
      COMMON/ENDO/DZ(NC3),EVP(NC3),VP(NC3),Q1(NC2),Q2(NC2)
      COMMON/PARAM/EK,EG,GAMA,EKA,FID,AL1,A1,FI1,AE,CE
      COMMON/PARS/G1,C0,CC1,HJ1,B1
      CALL NULVEC(F4,4)
      CALL NULVEC(S,4)
      CALL NULVEC(Q,4)
      CALL NULVEC(SQ,4)
      CALL DS(S,STEE,SH)
      Z1=DZ(I)
```

```
      IF(SH.EQ.0.0D0) WRITE(6,*)'WARNING:ZERO HYDROSTATIC STRESS'
      IF(SH.EQ.0.0D0) RETURN
C FH: Hydrostatic Hardening function
      FH=(1.0D0-FI1)*AE*DEXP(CE*(1.D0-DEXP(-DBLE(VP(I)))))+FI1*SH
      IF(MODEL.EQ.1) GOTO 300
      CALL SHIFT(Q2,Q,I,1)
      DO 220 J=1,4
220   SQ(J)=S(J)-Q(J)
      SQ2=S(1)*SQ(1)+S(2)*SQ(2)+S(4)*SQ(4)+2.D0*S(3)*SQ(3)
      DZG=Z1*2.D0*EG/FID/SH
      DZK=Z1*EK/FH/EKA*(SH-GAMA/FID/SH*SQ2)
      DO 23 J=1,4
23    F4(J)=DZG*SQ(J)+DZK
      F4(3)=(F4(3)-DZK)*0.5D0
      RETURN
300   CALL SHIFT(STNR,F4,I,1)
      CALL DS(Q,F4,SHD)
      Z0=Q(1)*Q(1)+Q(2)*Q(2)+Q(4)*Q(4)+2.D0*Q(3)*Q(3)+SHD*SHD*EKA*EKA
      Z0=0.1*DSQRT(Z0)
      CALL SHIFT(STER,F4,I,1)
      CALL DS(SQ,F4,SHD)
      CALL SHIFT(STN,F4,I,1)
      CALL DS(Q,F4,SHD)
      SQ2=Q(1)*SQ(1)+Q(2)*SQ(2)+Q(4)*SQ(4)+2.D0*Q(3)*SQ(3)
      BZ1=DABS(B1*Z0/SH)
      IF(BZ1.LE.1.0D-7) BZ1=1.0D-6
      DZG=2.D0*EG*(C0*Z0/SH+CC1*(1.0-DEXP(-BZ1)))
      DZK=Z0*EK/FH/EKA*(SH*HJ1+G1/2.0D0*SQ2)
      WRITE(6,*) 'Z0,DZG,DZK:',Z0,DZG,DZK
      DO 24 J=1,4
24    F4(J)=DZG*S(J)+DZK
      F4(3)=(F4(3)-DZK)*0.5D0
      RETURN
      END
C
C------------------------------------------- TIME ZONE F=0
      SUBROUTINE YLD(I,STEE,VSTN,Z1,F1)
C-------------------------------------YLD(I,STEE,VSTN,Z1,F1)
      IMPLICIT REAL*8(A-H,O-Z)
      PARAMETER(NC1=480,NC2=960,NC3=240)
      DIMENSION Q(4),STEE(4),S(4),F4(4),DSH(4),SQ(4),QI(4)
      COMMON/CODE/KI,KO,MODEL
      COMMON/STREN/STE(NC2),STN(NC2),STER(NC2),STNR(NC2)
      COMMON/F/HZ(NC2),HS(NC2),HZ1(NC2),YA1(NC2),YA2(NC2)
      COMMON/ENDO/DZ(NC3),EVP(NC3),VP(NC3),Q1(NC2),Q2(NC2)
      COMMON/PARAM/EK,EG,GAMA,EKA,FID,AL1,A1,FI1,AE,CE
      COMMON/PARS/G1,C0,CC1,HJ1,B1
      CALL NULVEC(F4,4)
      CALL NULVEC(S,4)
      CALL NULVEC(Q,4)
      CALL NULVEC(QI,4)
      CALL NULVEC(SQ,4)
```

```
          CALL NULVEC(DSH,4)
          K=0
          VPI=VP(I)+VSTN
C  Fd=SH
          DO 5 J=1,4
5       DSH(J)=STEE(J)
30      CALL DS(S,DSH,SH)
          K=K+1
          IF(SH.EQ.0.0D0) WRITE(6,*)'WARNING:ZERO HYDROSTATIC STRESS'
          IF(SH.EQ.0.0) RETURN
          CALL SHIFT(Q1,Q,I,1)
C FH: Hydrostatic Hardening function
          DEVI=CE*(1.D0-0.84D0*DEXP(VPI))
          FH=(1.0D0-FI1)*AE*DEXP(DEVI)+FI1*SH
          IF(FH.LT.SH) FH=SH
          IF(MODEL.EQ.1) GOTO 300
          ALZ=DBLE(AL1*Z1/SH)
          EALZ=DEXP(-ALZ)
C
C              1              -a1*dZd
C  S(Zi)-Q(Zi) = ----- [ S(Zi)-Q(Zi-1)e      ]
C             1+a
C
          A=A1/AL1*(1.0D0-EALZ)/FID+YA1(I)
          YA2(I)=A
          DO 20 II=1,4
          QI(II)=(Q(II)*EALZ+S(II)*A)/(1.0D0+A)
20      SQ(II)=(S(II)-Q(II)*EALZ)/(1.0D0+A)
C SQ2: S(ij)Q(ij)
          SQ2=S(1)*SQ(1)+S(2)*SQ(2)+S(4)*SQ(4)+2.D0*S(3)*SQ(3)
          IF(K.GT.1) GOTO 99
          DZG=Z1*2.D0*EG/FID/SH
          DZK=Z1*EK/FH/EKA*(SH-GAMA/FID/SH*SQ2)
          EVP(I)=-DZK/EK
          DO 23 J=1,4
          F4(J)=DZG*SQ(J)+DZK
23      DSH(J)=STEE(J)-F4(J)
          F4(3)=DZG*SQ(3)*0.5D0
          DSH(3)=STEE(3)-F4(3)
          IF(K.LE.1) CALL SHIFT(HZ,F4,I,0)
          IF(K.LE.1) CALL SHIFT(Q2,QI,I,0)
          IF(K.LE.1) GOTO 30
          QQ=SQ(1)*SQ(1)+SQ(2)*SQ(2)+SQ(4)*SQ(4)+2.D0*SQ(3)*SQ(3)
          DEVP=(SH-GAMA/FID/SH*SQ2)/FH
          F1=QQ/((FID*SH)**2)+DEVP*DEVP-1.0D0
          RETURN
300     CALL SHIFT(STN,F4,I,1)
          CALL DS(SQ,F4,SHD)
          CALL SHIFT(STNR,F4,I,1)
          CALL DS(Q,F4,SHD)
          Z0=Q(1)*Q(1)+Q(2)*Q(2)+Q(4)*Q(4)+2.D0*Q(3)*Q(3)+SHD*SHD*EKA*EKA
          Z0=DSQRT(Z0)
```

```
          IF(Z1.GE.Z0) Z1=Z0
          IF(Z1.LE.1.0D-10) Z1=1.0D-10
          CALL SHIFT(STER,F4,I,1)
          CALL DS(Q,F4,SHD)
          SQ2=Q(1)*SQ(1)+Q(2)*SQ(2)+Q(4)*SQ(4)+2.D0*Q(3)*SQ(3)
C     IF(Z1.LE.1.0D-8) Z1=1.0D-8
          BZ1=DABS(B1*Z1/SH)
C     DZG=C0/2.0D0+C1/Z1/BZ1*(1.0D0-DEXP(-BZ1))
          DZG=C0/SH+CC1*(1.0D0-DEXP(-BZ1))/Z1
          DZK=(SH*HJ1+G1/2.0D0*SQ2)/FH
          QQ=S(1)*S(1)+S(2)*S(2)+S(4)*S(4)+2.D0*S(3)*S(3)
          F1=QQ*DZG*DZG+DZK*DZK-1.0D0
          WRITE(6,*) 'Z1, Z0:',Z1,Z0,'DZG,DZK,F1:',DZG,DZK,F1
          WRITE(6,*) 'C1,B1,C0,QQ:',CC1,B1,C0,QQ
          RETURN
          END
C
C------------------------------DEVIATORIC STRESS
          SUBROUTINE DS(S,STEE,SH)
C------------------------------DS(S,STEE,SH)
          IMPLICIT REAL*8(A-H,O-Z)
          DIMENSION STEE(4),S(4)
          SH=(STEE(1)+STEE(2)+STEE(4))/3.0D0
          DO 10 II=1,4
10        S(II)=STEE(II)-SH
          S(3)=STEE(3)
          RETURN
          END
C
C-----------------------------------------------MULLER'S METHOD
          SUBROUTINE MULLR(I,STEE,VSTN,Z1,F1,ZR)
C----------------------------------MULLR(I,STEE,VSTN,Z1,F1,ZR)
          IMPLICIT REAL*8(A-H,O-Z)
          DIMENSION STEE(4)
          DATA NLIM,ZTOL,FTOL/10,1.0E-6,1.0E-2/
C INITIAL VALUES
          FC=F1
          Z2=1.0D-9
          Z3=1.0D-8
          CALL YLD(I,STEE,VSTN,Z2,F2)
          IF(F2.LE.0.1D0) THEN
          ZR=Z2
          RETURN
          END IF
          CALL YLD(I,STEE,VSTN,Z3,F3)
          IF(F3.LE.0.1D0) THEN
          ZR=Z3
          RETURN
          END IF
C ITERATIONS
          DO 20 J=1,NLIM
          H1=Z2-Z1
```

```
            H2=Z3-Z2
            G=H1/H2
            A=(F3*G-F2*(1.0D0+G)+F1)/(H1*(H1+F2))
            B=(F3-F2-A*H2*H2)/H2
            C=F2
            BAC=B*B-4.0D0*A*C
            IF(BAC.LT.0.0D0) THEN
            WRITE(6,*)' B*B - 4*A*C < 0'
            ZR=0.0D0
            RETURN
            END IF
            DISC=DSQRT(BAC)
            IF(B.LT.0.0D0) DISC=-DISC
C ROOT OF A*V**2 + B*V + C = 0
            DELX=-2.0D0*C/(B+DISC)
C UPDATE ZR
            ZR=Z2+DELX
            CALL YLD(I,STEE,VSTN,ZR,FR)
C STOPPING CRITERIA
            FCR=FR/FC
            IF((ABS(FCR).LE.FTOL).OR.(FR.LE.0.1D0)) THEN
            IC=2
            RETURN
            END IF
C SELECT 3 POINTS FOR THE NEXT ITERATION(IN ASCENDING ORDER).
C   DELX > 0, CHOOSE Z2,Z3,XR
C   DELX < 0, CHOOSE Z1,Z2,XR
            IF(DELX.GE.0.0D0) THEN
            Z1=Z2
            F1=F2
            IF(DELX.GT.H2) THEN
            Z2=Z3
            F2=F3
            Z3=ZR
            F3=FR
            ELSE
            Z2=ZR
            F2=FR
            END IF
            ELSE
            Z3=Z2
            F3=F2
            IF(ABS(DELX).GT.H1) THEN
            Z2=Z1
            F2=F1
            Z1=ZR
            F1=FR
            ELSE
            Z2=ZR
            F2=FR
            END IF
            END IF
```

```
20      CONTINUE
C
        IC=-1
        WRITE(6,200)NLIM,ZR,FR
        RETURN
200     FORMAT(/' TOL NOT MET AFTER ',I4,' ITERATIONS  Z =',
       * E12.5,' F = ', E12.5)
202     FORMAT(/' Z TOL MET IN ',I4,'  ITERATIONS  Z =',
       * E12.5,' F = ', E12.5)
203     FORMAT(/' F TOL MET IN ',I4,'  ITERATIONS  Z =',
       * E12.5,' F = ', E12.5)
        END
C
C       ---------------------------------------------------------------
C       SUBROUTINES FOR PROPERTY MATRICES [D]
C       ---------------------------------------------------------------
C
C PROPERTY MATRICES [D]
C---------------------------------- [D] FOR INTERFACE (BOTTOM)
        SUBROUTINE DMATI(D,STEE,STNE,KOD,EG,EK)
C ----------------------------------DMATI(D,STEE,STNE,KOD,EG,EK)
        IMPLICIT REAL*8(A-H,O-Z)
        REAL*8 D(4,4),STEE(4),STNE(4)
        COMMON/INTF/EMIN,EMIH,PRI,CKW,CKB,CFW,CFB,THR,TBI,TWI
        N=4
        CALL NULMAT(D,N,N)
        EC=0.01D0
        IF(K.EQ.0)WRITE(6,*)'PARTICIPATION FACTOR:',EC
        EEG=EG*EC
        EEK=EK*EC
        CALL DMATG(D,EEG,EEK)
        ES=ABS(STNE(3))
        IF(ES.LT.1.0E-5) ES=1.0D-5
        IF(KOD.EQ.-1) THEN
        SN=0.29D0*ABS(STEE(2))
        TINT=TBI
        CL=0.044D0
        GC=5.0D0
        ELSE
        SN=0.19D0*ABS(STEE(1))
        TINT=TWI
        CL=0.02D0
        GC=1.5D0
        END IF
        G=0.5D0*(SN-ABS(STEE(3)))*SQRT(TINT/ES/CL)
        IF(G.GT.GC) G=GC
        IF(G.LT.0.01D0) G=0.01D0
        D(3,3)=G
        IF(K.EQ.0)WRITE(6,*)'TINT:',TINT
        K=1
        RETURN
        END
```

```
C
C------------------------- ELASTIC (HOOKE LAW FOR AXISYMETRIC) [D]
      SUBROUTINE DMATE(D,EM,PR)
C-------------------------------------------------------DMATE(D,EM,PR)
      IMPLICIT REAL*8(A-H,O-Z)
      REAL*8 D(4,4)
      N=4
      CALL NULMAT(D,N,N)
      C1=EM*(1.0D0-PR)/((1.0D0+PR)*(1.0D0-2.0D0*PR))
      C2=PR/(1.0D0-PR)*C1
      C3=0.5D0*(1.0D0-2.0D0*PR)/(1.0D0-PR)*C1
      D(1,1)=C1
      D(1,2)=C2
      D(1,4)=C2
      D(2,1)=C2
      D(2,2)=C1
      D(2,4)=C2
      D(3,3)=C3
      D(4,1)=C2
      D(4,2)=C2
      D(4,4)=C1
      RETURN
      END
C
C-------------------------------------------------[D] FOR GRAIN
      SUBROUTINE DMATG(D,EG,EK)
C-------------------------------------------------DMATE(D,EG,EK)
      IMPLICIT REAL*8(A-H,O-Z)
      REAL*8 D(4,4)
      N=4
      CALL NULMAT(D,N,N)
      C1=EK+4.0D0/3.0D0*EG
      C2=EK-2.0D0/3.0D0*EG
      D(1,1)=C1
      D(1,2)=C2
      D(1,4)=C2
      D(2,1)=C2
      D(2,2)=C1
      D(2,4)=C2
      D(3,3)=EG
      D(4,1)=C2
      D(4,2)=C2
      D(4,4)=C1
      RETURN
      END
C
C-------------------------------------[D] (ELASTIC) FOR 1-D WALL
      SUBROUTINE DMATW(D,EM,PR)
C-------------------------------------------------DMATW(D,EM,PR)
      IMPLICIT REAL*8(A-H,O-Z)
      DIMENSION D(2,2)
      C=EM/(1.0D0-PR*PR)
```

```
      D(1,1)=C
      D(1,2)=PR*C
      D(2,1)=PR*C
      D(2,2)=C
      RETURN
      END
C
C       ------------------------------------------------
C       SUBROUTINES FOR FEM FUNCTIONS
C       ------------------------------------------------
C
C SHAPE FUNCTION:  FUN(4)=[N]; DER(2,4)=[N']
C
C------------------------------------------------- [N] FOR 2-D
      SUBROUTINE SHPFUN(FUN,DER,X,Y)
C-----------------------------------------------SHPFUN(FUN,DER,X,Y)
      IMPLICIT REAL*8(A-H,O-Z)
      INTEGER I,J
      REAL*8 DER(2,4),FUN(4)
      X1=0.25D0*(1.0D0-X)
      X2=0.25D0*(1.0D0+X)
      Y1=0.25D0*(1.0D0-Y)
      Y2=0.25D0*(1.0D0+Y)
      FUN(1)=4.0D0*Y1*X1
      FUN(2)=4.0D0*Y1*X2
      FUN(3)=4.0D0*Y2*X2
      FUN(4)=4.0D0*Y2*X1
      DER(1,1)=-Y1
      DER(1,2)=Y1
      DER(1,3)=Y2
      DER(1,4)=-Y2
      DER(2,1)=-X1
      DER(2,2)=-X2
      DER(2,3)=X2
      DER(2,4)=X1
      RETURN
      END
C
C------------------------------------------- [N] FOR 1-D WALL
      SUBROUTINE SHPFW(FUN,DER,X)
C-----------------------------------------------SHPFW(FUN,DER,X)
      IMPLICIT REAL*8(A-H,O-Z)
      DIMENSION FUN(2),DER(2)
      FUN(1)=0.5D0*(1.0D0-X)
      FUN(2)=0.5D0*(1.0D0+X)
      DER(1)=-0.5D0
      DER(2)=0.5D0
      RETURN
      END
C
C GRADIENT MATRIX [B]          BE(4,8)=[N'] ( DERV(2,4) )
C
```

```
C------------------------------------ [B] FOR LINEAR QUADRALATERAL
      SUBROUTINE BEMAT4(BE,SUM,DERV,FUN,CORD,NN4)
C---------------------------------BEMAT4(BE,SUM,DERV,FUN,CORD,NN4)
      IMPLICIT REAL*8(A-H,O-Z)
      INTEGER NN4
      REAL*8 DERV(2,4),FUN(4),CORD(4,2),BE(4,8)
      NN8=8
      CALL NULMAT(BE,NN4,NN8)
      SUM=0.0D0
      DO 5 I=1,NN4
      SUM=SUM+FUN(I)*CORD(I,1)
5     CONTINUE
      DO 10 I=1,NN4
      I2=2*I
      I1=I2-1
      BE(1,I1)=DERV(1,I)
      BE(2,I2)=DERV(2,I)
      BE(3,I1)=DERV(2,I)
      BE(3,I2)=DERV(1,I)
      BE(4,I1)=FUN(I)/SUM
10    CONTINUE
      RETURN
      END
C
C------------------------------------- [B] FOR 1-D WALL
      SUBROUTINE BWMAT(BE,DERV,FUN,R)
C-------------------------------------BWMAT(BE,DERV,FUN,R)
      IMPLICIT REAL*8(A-H,O-Z)
      REAL*8 DERV(2),FUN(2),BE(2,4)
      NN2=2
      NN4=4
      CALL NULMAT(BE,NN2,NN4)
      BE(1,1)=FUN(1)/R
      BE(1,3)=FUN(2)/R
      BE(2,2)=DERV(1)
      BE(2,4)=DERV(2)
      RETURN
      END
C
C      ---------------------------------------------------------------
C      SUBROUTINES FOR MATHEMATIC CACULATIONS
C      ---------------------------------------------------------------
C
C------------------------ GAUSSIAN POINTS SAMP(3),WEIGHT WEIT(3)
      SUBROUTINE GAUSS(NGP,SAMP,WEIT)
C-----------------------------------------GAUSS(NGP,SAMP,WEIT)
      IMPLICIT REAL*8(A-H,O-Z)
      DIMENSION SAMP(3),WEIT(3)
      NGP=3
      SAMP(1)=0.2D0*SQRT(15.0D0)
      SAMP(2)=0.0D0
      SAMP(3)=-SAMP(1)
```

```
      WEIT(1)=5.0D0/9.0D0
      WEIT(2)=8.0D0/9.0D0
      WEIT(3)=WEIT(1)
      RETURN
      END
C
C-------------------------------MATP(M1,N2)=MAT1(M1,M2)*MAT2(N1,N2)
      SUBROUTINE MATMUL(MATP,MAT1,M1,M2,MAT2,N1,N2)
C-------------------------------MATMUL(MATP,MAT1,M1,M2,MAT2,N1,N2)
      IMPLICIT REAL*8(A-H,O-Z)
      REAL*8 MAT1(M1,M2),MAT2(N1,N2),MATP(M1,N2)
      COMMON/CODE/KI,KO,MODEL
      IF(M2.EQ.N1) GOTO 15
      WRITE(KO,1)
1     FORMAT(1X//5X,'MATRIX MULTIPLICATION CAN NOT BE PERFORMED',//)
15    L=M2
        DO 5 I=1,M1
        DO 5 J=1,N2
        SUM=0.0D0
        DO 10 K=1,L
        SUM=SUM+MAT1(I,K)*MAT2(K,J)
10    CONTINUE
        MATP(I,J)=SUM
5     CONTINUE
        RETURN
        END
C
C------------------------------------------- MAT(M,N)=0.0D0
      SUBROUTINE NULMAT(MAT,M,N)
      C-------------------------------------------NULMAT(MAT,M,N)
      IMPLICIT REAL*8(A-H,O-Z)
      INTEGER M,N
      REAL*8 MAT(M,N)
      DO 5 I=1,M
      DO 5 J=1,N
      MAT(I,J)=0.0D0
5     CONTINUE
      RETURN
      END
C
C------------------------------------------------- VEC(N)=0.0D0
      SUBROUTINE NULVEC(VEC,N)
C-------------------------------------------------NULVEC(VEC,N)
      IMPLICIT REAL*8(A-H,O-Z)
      INTEGER N
      DIMENSION VEC(N)
      DO 5 I=1,N
      VEC(I)=0.0D0
5     CONTINUE
      RETURN
      END
C
```

```
C-----------------------------------------------------IVEC(N)=0.0
      SUBROUTINE INULV(IVEC,N)
C-----------------------------------------------------INULV(IVEC,N)
      INTEGER N,IVEC(1)
      DO 5 I=1,N
      IVEC(I)=0.0
5     CONTINUE
      RETURN
      END
C
C-------------------------------------------INVM(2,2)=1/MAT(2,2)
      SUBROUTINE INVBY2(MAT,INVM,DET)
C-------------------------------------------INVBY2(MAT,INVM,DET)
      IMPLICIT REAL*8(A-H,O-Z)
      REAL*8 MAT(2,2),INVM(2,2)
      DET=MAT(2,2)*MAT(1,1)-MAT(1,2)*MAT(2,1)
      INVM(1,1)=MAT(2,2)
      INVM(2,2)=MAT(1,1)
      INVM(1,2)=-MAT(1,2)
      INVM(2,1)=-MAT(2,1)
      DO 5 I=1,2
      DO 5 J=1,2
      INVM(I,J)=INVM(I,J)/DET
5     CONTINUE
      RETURN
      END
C-----------------------------------------PVEC(M)=MAT(M,N)*VEC(N)
      SUBROUTINE MVMUL(PVEC,MAT,M,N,VEC,NV)
C-----------------------------------------MVMUL(PVEC,MAT,M,N,VEC,NV)
      IMPLICIT REAL*8(A-H,O-Z)
      REAL*8 MAT(M,N),VEC(N),PVEC(M)
      INTEGER M,N
      COMMON/CODE/KI,KO,MODEL
      IF(N.EQ.NV) GOTO 20
      WRITE(KO,1)
1     FORMAT(1X///5X,'MATRIX-VECTOR MULT CAN NOT BE PERFORMED',//)
20    DO 5 I=1,M
      SUM=0.0D0
      DO 10 J=1,N
      SUM=SUM+MAT(I,J)*VEC(J)
10    CONTINUE
      PVEC(I)=SUM
5     CONTINUE
      RETURN
      END
C
C-------------------------------------------MTRAN(N,M) = MAT(M,N)
      SUBROUTINE MATRAN(MTRAN,MAT,M,N)
C-------------------------------------------MATRAN(MTRAN,MAT,M,N)
      IMPLICIT REAL*8(A-H,O-Z)
      INTEGER M,N
      REAL*8 MAT(M,N),MTRAN(N,M)
```

```
      DO 5 I=1,M
      DO 5 J=1,N
      MTRAN(J,I)=MAT(I,J)
5     CONTINUE
      RETURN
      END
C
C---------------------------------------CONST = V1(I) * V2(I)
      SUBROUTINE VVMUL(CONST,V1,V2,N)
C---------------------------------------VVMUL(CONST,V1,V2,N)
      IMPLICIT REAL*8(A-H,O-Z)
      REAL*8 V1(1),V2(1)
      CONST=0.0D0
      DO 10 I=1,N
      CONST=CONST+V1(I)*V2(I)
10    CONTINUE
      RETURN
      END
C
C---------------------------------------- MAT(M,N)=V1(M)*V2(N)
      SUBROUTINE VVMMUL(MAT,V1,M,V2,N)
C----------------------------------------VVMMUL(MAT,V1,M,V2,N)
      IMPLICIT REAL*8(A-H,O-Z)
      REAL*8 MAT(M,N),V1(M),V2(N)
      DO 10 I=1,M
      DO 10 J=1,N
      MAT(I,J)=V1(I)*V2(J)
10    CONTINUE
      RETURN
      END
C
C---------------------------------------- PVEC(N)=VEC(M)*MAT(M,N)
      SUBROUTINE VMMUL(PVEC,VEC,MV,MAT,M,N)
C---------------------------------------VMMUL(PVEC,VEC,MV,MAT,M,N)
      IMPLICIT REAL*8(A-H,O-Z)
      REAL*8 VEC(MV),MAT(M,N),PVEC(N)
      DO 5 I=1,N
      SUM=0.0D0
      DO 10 J=1,M
      SUM=SUM+VEC(J)*MAT(J,I)
10    CONTINUE
      PVEC(I)=SUM
5     CONTINUE
      RETURN
      END
C
C---------------------------------------
      SUBROUTINE NUMB(I1,I2,I3,I4,I)
C-----------------------------------------------NUMB(I1,I2,I3,I4,I)
      IMPLICIT REAL*8(A-H,O-Z)
      I1=4*(I-1)+1
      I2=I1+1
```

```
          I3=I1+2
          I4=I1+3
          RETURN
          END
C
C-----------------------------------------
          SUBROUTINE SHIFT(FT,FT4,IN,NCT)
C-------------------------------------------------SHIFT(FT,FT4,IN,NCT)
          PARAMETER(NC1=480,NC2=960,NC3=240)
          IMPLICIT REAL*8(A-H,O-Z)
          DIMENSION FT(1),FT4(4)
          CALL NUMB(I1,I2,I3,I4,IN)
          IF (NCT) 1,2,1
2       FT(I1)=FT4(1)
          FT(I2)=FT4(2)
          FT(I3)=FT4(3)
          FT(I4)=FT4(4)
          RETURN
1       FT4(1)=FT(I1)
          FT4(2)=FT(I2)
          FT4(3)=FT(I3)
          FT4(4)=FT(I4)
          RETURN
          END
C                         I,J=1,NDF EXCEPT NDM
C------------------------------------------------ A(I,J)=0
          SUBROUTINE MZERO(NDF,NDM)
C-------------------------------------------------MZERO(NDF,NDM)
          PARAMETER(NC1=480,NC2=960,NC3=240)
          IMPLICIT REAL*8(A-H,O-Z)
          COMMON/KMAT/A(NC1,NC1),F(NC1)
          DO 5 I=1,NDF
          IF(I.EQ.NDM) GOTO 5
          A(NDM,I)=0.0D0
          A(I,NDM)=0.0D0
5       CONTINUE
          F(NDM)=0.0D0
          RETURN
          END
C                     BY PARTIAL PIVOTING ELININATION
C------------------------------------------ SOLVE [K] {U} = {F}
          SUBROUTINE SOLVE(X,N)
C-----------------------------------------------------------SOLVE(X,N)
          PARAMETER(NC1=480,NC2=960,NC3=240)
          IMPLICIT REAL*8(A-H,O-Z)
          DIMENSION X(1)
          COMMON/KMAT/A(NC1,NC1),F(NC1)
          COMMON/CODE/KI,KO
          N1=N-1
C ELIMINATION
300     DO 5 I=1,N1
C..... PIVOTING
```

```
          NMAX=I
          I1=I+1
          DO 10 J=I1,N
          IF(DABS(A(NMAX,I)).LT.DABS(A(J,I))) NMAX=J
10      CONTINUE
C ..... CHECK FOR ILL CONDITION
          IF(DABS(A(NMAX,I)).GT.1.0E-6) GOTO 20
          WRITE(6,3) NMAX,I,A(NMMAX,I)
          WRITE(KO,3) NMAX,I,A(NMMAX,I)
3       FORMAT(1X//5X,50('*')/10X,'ILL CONDITION AT COLLUMN',2I5,E10.3)
C ..... INTERCHANGE
20      IF(NMAX.EQ.I) GOTO 30
          DO 25 J=1,N
          C=A(I,J)
          A(I,J)=A(NMAX,J)
          A(NMAX,J)=C
25      CONTINUE
          C=F(I)
          F(I)=F(NMAX)
          F(NMAX)=C
C ..... ELIMINATION
30      DO 40 J=I1,N
          IF(DABS(A(J,I)).EQ.0.0) GOTO 40
          C=A(J,I)/A(I,I)
          DO 45 L=I1,N
          A(J,L)=A(J,L)-C*A(I,L)
45      CONTINUE
          F(J)=F(J)-C*F(I)
40      CONTINUE
5       CONTINUE
C BACKSUBSTITUTION
          IF(DABS(A(N,N)).GT.1.0E-6) GOTO 70
          WRITE(KO,3) N
          STOP
70      X(N)=F(N)/A(N,N)
          DO 50 I=1,N1
          II=N-I
          SUM=0.0D0
          DO 55 J=1,I
          JJ=N-J+1
          SUM=SUM+A(II,JJ)*X(JJ)
55      CONTINUE
          X(II)=(F(II)-SUM)/A(II,II)
50      CONTINUE
          RETURN
          END
C               -------------------------
C               OUTPUT RESULTS
C               -------------------------
C
          SUBROUTINE OUTPUT(NE,NEY,NEX,KSTAGE,KOUT,DISP,TEMP)
C
```

```
      PARAMETER(NC1=480,NC2=960,NC3=240)
      IMPLICIT REAL*8(A-H,O-Z)
      REAL*8 DISP(1)
      DIMENSION ND2(8),STEE(4),STNE(4),CORD(4,2),DEF(8)
      CHARACTER TP1*4,TP2*9,TP3*5,TP4*9,TIPE*9
      COMMON/CODE/KI,KO
      COMMON/STREN/STE(NC2),STN(NC2),STER(NC2),STNR(NC2)
      COMMON/WALL/HBIN,RBIN,TBIN,EMW,PRW
      COMMON/INTF/EMIN,EMIH,PRI,CKW,CKB,CFW,CFB,THR,TBI,TWI
      COMMON/LOADS/DEN,DPS1,DPS2,CT,NDEP,NSCH1,NSCH2
      COMMON/GRID/KODE(NC3),ND(4,NC3),XC(4,NC3),YC(4,NC3),KWALL
      COMMON/CONST/PA,PI,NN2,NN4,NN8
      TP1='WALL'
      TP2='INTERFACE'
      TP3='GRAIN'
      TP4='PLATE'
      NEXI=NEX+1
      IF(KSTAGE.EQ.0) WRITE(KO,103)
103   FORMAT(1X/////10X,30('+')//20X,'RESULT OUTPUT',//10X,
     *30('+')///)
      IF(KSTAGE.EQ.0) WRITE(KO,3)
      IF(KSTAGE.EQ.1) WRITE(KO,4)
      IF(KSTAGE.EQ.2) WRITE(KO,6) TEMP
3     FORMAT(1X//1X,70('*')////5X,'STATIC PRESSURE WITHOUT SURCHARGE',
     */1X,40('-')//)
4     FORMAT(1X//1X,70('*')////5X,'STATIC PRESSURE WITH SURCHARGE',
     */1X,40('-')//)
6     FORMAT(1X//1X,70('*')////5X,'THERMAL PRESSURE',/1X,70('-')//1X,
     *'TEMPERATURE=',F10.4///)
C..... OUTPUT STRESSES ON WALL ONLY
      IF(KOUT.EQ.1) GOTO 100
      WRITE(KO,7)
7     FORMAT(25X,'*****WALL PRESSURE*****',
     *//1X,T19,'HEIGHT',T31,'LATERAL',T55,'VERTICAL'//)
      DO 5 I=1,NE
      KOD=KODE(I)
      IF((KOD.GE.3).AND.(KK.EQ.0)) THEN
      J1=(I-1)*4+2
      PV=-STE(J1)
      KK=1
      END IF
      IF(KOD.EQ.1) THEN
      DO 15 J=1,4
      CORD(J,1)=XC(J,I)
      CORD(J,2)=YC(J,I)
15    CONTINUE
      J1=(I-1)*4+1
      PL=-STE(J1)
      HL=0.5D0*(CORD(1,2)+CORD(4,2))
      WRITE(KO,9) HL,PL,PV
9     FORMAT(1X,T10,F15.4,T30,E15.4,T50,E15.4)
      KK=0
```

```
        END IF
5       CONTINUE
        IF(KOUT.NE.2) RETURN
100     WRITE(KO,102)
102     FORMAT(1X/5X,'*****OUTPUT FOR EACH ELEMENT*****',/)
        DO 105 I=1,NE
        CALL INULV(ND2,NN8)
        KOD=KODE(I)
        DO 115 J=1,4
        J1=(I-1)*4+J
        STEE(J)=-STE(J1)
        STNE(J)=-STN(J1)
        CORD(J,1)=XC(J,I)
        CORD(J,2)=YC(J,I)
        K1=2*ND(J,I)
        IF(K1.LE.0) GOTO 115
        ND2(2*J-1)=K1-1
        ND2(2*J)=K1
115     CONTINUE
        CALL NULVEC(DEF,NN8)
        DO 110 J=1,8
        JJ=ND2(J)
        IF(JJ.LE.0) GOTO 110
        DEF(J)=DISP(JJ)
110     CONTINUE
C
        YF=0.0
C     IF(KOD.GE.3.OR.KOD.EQ.1) YF=FPF(STEE)
        IF(KOD.GE.3) YF=ABS((STEE(1)-STEE(2))/(STEE(1)+STEE(2)))
        IF(KOD.EQ.0) TIPE=TP1
        IF(KOD.EQ.1.OR.KOD.EQ.-1) TIPE=TP2
        IF(KOD.EQ.-2) TIPE=TP4
        IF(KOD.GE.3.OR.KOD.EQ.-3) TIPE=TP3
        WRITE(KO,106) I,TIPE,YF,(ND(J,I),J=1,4),(CORD(J,1),J=1,NN4),
       *(CORD(J,2),J=1,NN4),(DEF(J),J=1,8,2),(DEF(J),J=2,8,2),STEE,STNE
        FORMAT(1X//2X,'ELEMENT NO:',5X,I3,10X,'TYPE:',3X,A9,F10.2/5X,
       * 'NODE NO:',T15,4I15/5X,'X-COORD:',T15,4F15.4/5X,
       * 'Y-COORD:',T15,4F15.4/5X,'H-DISP:',T15,4E15.4/5X,
       * 'V-DISP:',T15,4E15.4/5X,'STRESS:',T15,4E15.4/5X,
       * 'STRAIN:',T15,4E15.4)
C     WRITE(KO,111) I,STEE
C111  FORMAT(3X,I5,4E15.4)
105     CONTINUE
        RETURN
        END
```